Master Thesis
TVVR 10/5007

Climate warming effects on hydropower demand and pricing in California

Adaptability of California's high-elevation hydropower system to climate change considering simultaneously warming effects on energy supply and demand

Marion Guégan

Division of Water Resources Engineering
Department of Building and Environmental Technology
Lund University

Avdelningen för Teknisk Vattenresurslära
ISRN LUTVDG/TVVR-10/5007
ISSN-1101-9824

Climate warming effects on hydropower demand and pricing in California

Adaptability of California's high-elevation hydropower system to climate change considering simultaneously warming effects on energy supply and demand

Author: Marion Guégan

Supervisors: Cintia Bertacchi Uvo
Division of Water Resources Engineering
Lund University
Kaveh Madani
Water Science and Policy Center
University of California, Riverside

Examiner: Rolf Larsson
Division of Water Resources Engineering
Lund University

Abstract

While only about 30% of California's usable water storage capacity lies at higher elevations, high-elevation hydropower units generate on average 74% of California's in-state hydroelectricity. In general, high-elevation plants have small man-made reservoirs and rely mainly on snowpack. Their low built-in storage capacity is a concern with regard to climate warming. Snowmelt is expected to shift to earlier in the year and the system might not be able to store sufficient water for release in high-demanding periods. Previous studies have tried to explore the climate warming effects on California's high-elevation hydropower system by focusing on the supply side (exploring the effects of hydrological changes on generation and revenues), ignoring the warming effects on hydropower demand and pricing. This study extends the previous work by simultaneous consideration of climate change effects on high-elevation hydropower supply and demand in California. Artificial Neural Network (ANN) models are developed as long-term price forecasting tools to estimate the impact of climate warming on energy prices. California's Energy-Based Hydropower Optimization Model (EBHOM) is then applied to estimate the adaptability of California's high elevation hydropower system to climate warming considering the warming effects on hydropower supply and demand. The model is run for dry and wet warming scenarios, representing a range of hydrological changes under climate change. EBHOM's results relative to energy generation, energy spills, reservoir energy storage, and average shadow prices of energy generation and storage capacity expansion are examined and discussed. The modeling results are compared with previous studies to underline the importance of consideration of climate change effects on hydroelectricity demand and pricing in exploring the effects of climate change on California's hydropower system.

Keywords: Hydropower, Climate Change, Electricity Generation, Demand and Pricing, Artificial Neural Network, California, High-elevation Hydropower Systems.

Acknowledgements

I would like to gratefully acknowledge the supervision of Prof. Cintia Uvo Bertacchi and Dr. Kaveh Madani, initiator of this research project. Their constant encouragements and precious advices have been greatly appreciated and improved the quality of this research work. I specially thank Kaveh for his great support and availability all along the thesis, no matter time or day of the week.

I would also like to thank Juan Martin Bravo for his guidance and help on the Artificial Neural Network model he developed during his Doctoral Thesis.

Finally, I am grateful to all my friends, most importantly to Ivar, and my office mates Jacopo, Davide and Ashenafi for their love and support.

Table of Contents

Table of Figures

Table of Tables

1 Introduction

Hydropower facilities in California generated on average 37,000GWh or 15% of the annual in-state generation between 1983 and 2001, ranging annually between 9% and 30% depending on hydrological conditions (McKinney et al., 2003). When precipitation runoff is plentiful, hydroelectric generation is prioritized while other power plants, mostly gas-fired facilities, may be shut down temporarily (McKinney et al., 2003). Hydroelectricity's very low cost, near-zero emissions and load following capacity are some of the reasons for its great popularity (McKinney et al., 2003; Pew Center on Global Climate Change, 2009). The state of California has the second largest hydropower system in the US behind the state of Washington, with a total hydroelectric capacity over 14,000 MW representing 25% of California's electricity generation capacity (McKinney et al., 2003). California also relies on hydroelectricity imports from the Pacific Northwest including the states of Oregon and Washington, and Canada (Aspen Environmental Group and Cubed, 2005).

California's statewide average temperatures are expected to rise between 3°F and 10.5°F by 2100 (CCCC, 2006, Cayan et al. 2008). This temperature increase is expected to decrease the state's snowpack reserve at high elevations and shift the runoff from snowmelt to an earlier period of the year than today (CCCC, 2006). Variations in the annual runoff pattern may significantly alter hydropower generation depending on the system's storage and generation capacities. California's state is currently encouraging active research on the adaptability of hydropower systems to climate change (e.g. Aspen Environmental Group & Cubed, 2005; Tanaka et al., 2006; Medellin-Azuara et al., 2008; Vicuna et al., 2008; Vicuna et al., 2009; Madani and Lund, in press). Besides affecting the availability of water for electricity generation, higher temperatures will likely increase demand for cooling in warm periods (CCCC, 2006; Franco and Sanstad, 2006; Aroonruengsawat and Auffhammer, 2009).

Rising energy demand coupled with reduced hydroelectricity generation could lead to substantial impact on the electricity market. A rise in hydroelectricity prices is foreseeable and electricity distributors will probably also have to shift to more expensive, less environmentally friendly energy sources to replace the lost hydropower generation (Union of Concerned Scientists, 2006). To the best of the author, no study has addressed the impact of climate change on electricity prices in California by considering simultaneously changes in supply and demand of hydroelectricity.

California's Electricity Supply Industry (ESI) is a deregulated competitive market supervised by the state. It relies on long-term contracts regulated by the state to avoid market manipulations as it happened during the California crisis of 2000-2001 (CBO, 2001). The California Power Exchange (CalPX) operates the day-ahead market and sets the price that the generators will sell electricity based on a bidding process. California Independent System Operator (CalISO) then operates the region's power grid and wholesale electric markets and deals with real-time imbalance energy, ancillary services and transmission usage.

The specificity of the electricity market compared to other commodities is that it requires a well coordinated balance between generation and consumption since storage of electricity remains limited and expensive (Amjady and Hemmati, 2006). Therefore, accurate short-term price forecasting is crucial information for producers and retailers to develop their bidding strategy in a day-ahead electricity market; and has prompted many research works (e.g. Zhao et al., 2007; Zarezadeh et al., 2008; Amjady and Keynia, 2010a). However this is not an easy task as price of electricity is a nonlinear, time variant and volatile signal owning multiple periodicity, high frequency components and significant outliers, i.e., unusual prices (especially in periods of high demand) due to unexpected events in the electricity markets (Amjady and Hemmati, 2006). The application of Artificial Neural Network (ANN) models has provided a good ability to forecast normal electricity prices (Zhao et al., 2007). ANNs provide an appealing solution for relating non-linear input and output variables in complex systems (ASCE, 2000; Dawson and Wilby, 2001).

The present research addresses the impacts of climate warming on California's high-elevation hydropower system considering simultaneously the impact of climate change on the supply, demand and pricing sides. The main contribution of this work is the development of a long-term price forecast model using Artificial Neural Networks. The novel price representation is based on the estimation of a relationship between temperature, electricity demand, time of the year and electricity price allowing the estimation of climate warming scenarios impacts on electricity prices. A novel method of Madani and Lund (2009) for hydropower operation optimization based on profit maximization was finally used to estimate statewide high-elevation hydropower system adaptability to climate change.

The present report is organized as follows: Section 2 describes California's hydropower system; Section 3 describes historical electricity demand and pricing trends in California; Section 0 is a literature review of climate change effects on hydropower supply and demand; Section 5 defines the methodology of this research work; Section 6 details the ANN models developed and the estimated effects of climate warming scenarios on electricity prices; Section 7 presents the results from the hydropower optimization model simulations under climate warming scenarios; Section 8 discusses the limitations of the study and future direction; and finally Section 9 concludes the research.

2 California and Hydropower

Climate across the California region can be very different due to the great differences in altitude and in latitude of the state. According to Kauffman (2003), five major climate types can be observed in close proximity in California; namely Desert, Cool Interior, Highland, Steppe and Mediterranean. As the objective of this research is to study the impacts of statewide climate change on California's high-elevation hydropower system, only major trends of temperature and precipitation distribution will be presented. Much of California has warm dry summers and cool wet winters (Zhu et al., 2005). In terms of electricity demands this corresponds to high demands in summer for air cooling (Figure 1) and in winter for heating whereas the lowest demands occur in spring and autumn when neither great heating nor cooling is required. Precipitation in California is very uneven throughout the year with around 75% of the annual average of 584mm occurring between November and March (Zhu et al., 2005) and falls as snow in the Sierra Nevada mountain range (Moser et al., 2009). This results in spatially uneven runoff with more than 70% of California's average annual runoff occurring in northern California (Madani and Lund, 2009).

California's hydroelectric system generated 15% on average of the annual in-state generation between 1983 and 2001 (McKinney et al., 2003). In-state hydropower is generated by four types of hydropower systems: high-head low-storage hydropower plants, low-head multipurpose dams, pumped-storage plants, and run-of-the-river units (Pew Center on Global Climate Change, 2009). The distribution of California's hydropower system is displayed in Figure 2.

While only about 30% of the state's usable water storage capacity lies at higher elevations, high-elevation hydropower units generate on average 74% of California's in-state hydroelectricity (Madani and Lund, 2009). 156 high-elevation hydropower plants, above 1,000 feet (or 305 meters), have been identified by Madani and Lund (2009). Most of them are located in Northern California (Aspen Environmental Group and Cubed, 2005). Hydroelectric generation is generally their only purpose and only little amounts of water are necessary to produce substantial quantities of electricity with vertical drops of water of hundreds of feet (Pew Center on Global Climate Change, 2009). They have been designed to take advantage of the snowpack acting as a natural reservoir and their man-made reservoir is usually small (Madani and Lund, in press). Their limited storage capacity may make them sensitive to future snowpack volume and runoff timing variations (Madani and Lund, in press).

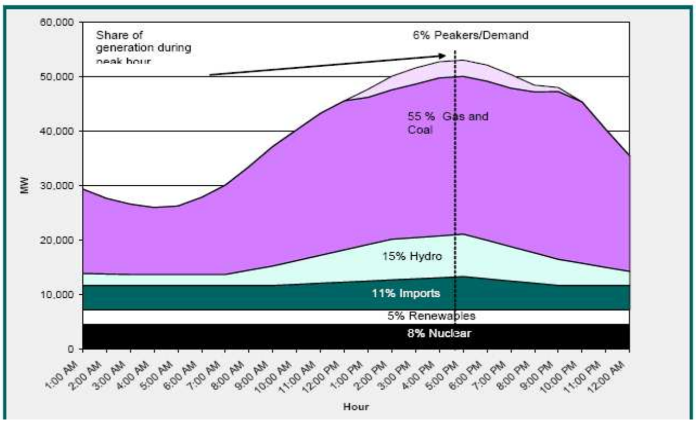

Figure 1 - Electricity supply and demand profile for a typical hot summer day (Source: Mc Kinney et al., 2003)

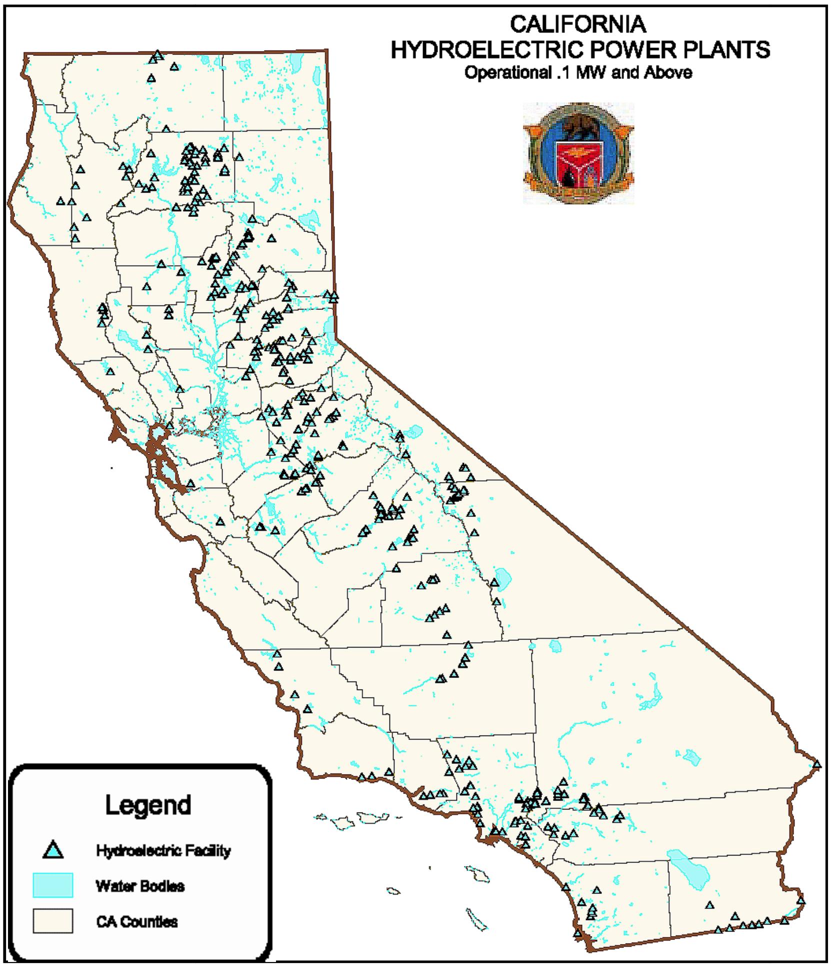

Figure 2 - Hydroelectric power plants distribution in California (capacity > 1MW) (Source: California Energy Comission, http://www.energy.ca.gov/hydroelectric/hydro_power_plants.html)

3 Electricity demand and pricing in California

The disparities between the trends in electricity demand in California and the US have been of great interest to the scientific community (e.g. Kandel et al., 2008; Horowitz, 2007; Rosenfeld, 2006). California's aggregate electricity consumption per capita (ECP) remained almost flat since 1976 while it increased by around 50% nationwide as seen in Figure 3. On a sector-by-sector basis, the main difference comes from the industrial and residential sectors. Between 1973 and 2005, California's residential per capita electricity consumption increased slowly (by 14%) compared to the US where it increased by 60% (Kandel et al, 2008). California's residential ECP slow increase is among others related to: its mild climate compared to other states resulting in less heating and less cooling demand in winter and summer respectively (Kandel et al., 2008); the high concentration of urban areas where there are many multi-family units (Kandel et al., 2008); the higher than US average energy prices (see Figure 4) encouraging consumers to save energy (Kandel et al., 2008); and probably the aggressive energy efficiency programs launched around 1976 (Horowitz, 2007). Between 1973 and 2005, California's industrial sector reduced its ECP by 39%, partly because there has been a structural change in California's economic structure since the late 1990s which has bartered energy-intensive manufacturing for less-energy intensive services (Tanton, 2008).

While California's ECP remained roughly flat, its aggregate electricity consumption increased by 65% between 1980 and 2008, as did imports of electricity with for example an increase by 60% in coal-based electricity imports from 1983 to 2005 (Tanton, 2008).

The electricity peak demand in California has also been increasing since the 1960s but the growth rate slowed down after the initialization of energy efficiency programs in 1976 (Rosenfeld, 2006). California electricity peak demand reached 55GW in 2004 (Rosenfeld, 2006).

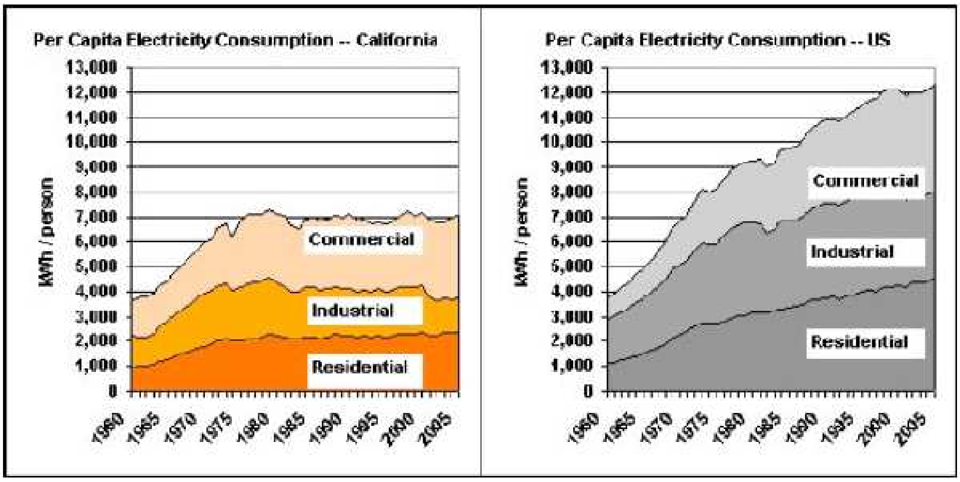

Figure 3 - California and US per capita electricity use by sector, 1960-2008. (Kandel et al., 2008)

US average nominal retail electricity prices have increased significantly since the 1970s as shown in Figure 4, as a result of the 1970s fuel crisis (Bloom Energy, 2010). On average, prices in California are higher than in the rest of the nation. The second energy crisis experienced by California in 2001 led to a retail price jump by 30% between 1999 and 2002, and prices have not decreased significantly since then (Figure 4). In 2006, California's state had the second highest retail sales in the US according to Kandel et al. (2008). A linear regression of the average retail prices for the period 1960-2005 corresponds to an annual growth rate of about 0.25cents/KWh. If a similar linear increase is assumed up to the end of the 21st century, this would lead to an increase of 25 cents/KWh by 2100, corresponding to an increase of more than 100% compared to average retail prices of 2005.

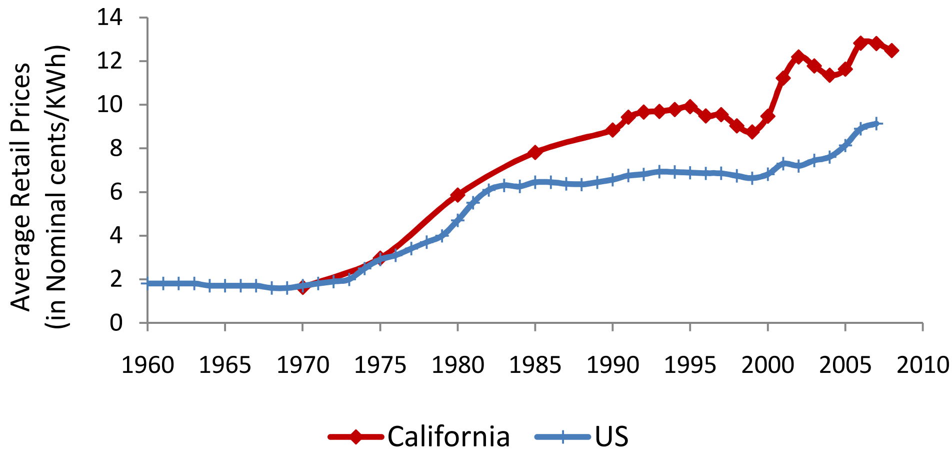

Figure 4 - Average Retail Price of Electricity to Ultimate Consumer in Nominal Dollars, for US and California, 1960-2008. (Source: EIA, data compiled from AER: Table 8.10; SEDS – California: Table 5.3 & California Electricity Profile: Table 8)

4 California and Climate Change

4.1 Climate Change scenarios for California

The scientific community agrees on the fact that the surface temperature is expected to increase worldwide, whereas the future hyetograph pattern is still uncertain (CCCC, 2006; Cayan et al., 2008). Cayan et al. (2008) focused their study on changes in climate at the surface, mostly related to temperature and precipitation, and addressed plausible pathways for the California region. The climate change scenarios are produced by combining Global Climate Models (GCMs) to Green House Gas (GHG) emission scenarios as defined in the IPCC Fourth Assessment released in 2007. They addressed namely the three following GCMs: the Parallel Climate Model (PCM) from the National Center for Atmospheric Research (NCAR) and U.S. Department of Energy, the CM2.1 from the National Oceanic and Atmospheric Administration (NOAA) Geophysical Fluids Dynamics Laboratory (GFDL) and the Hadley Center model (HADCM2). Three probable sets of projections of GHG emissions for California are the B1 (low emissions), A2 (medium-high emissions) and A1fi (high emissions) storylines (Figure 5) (Cayan et al., 2008).

The magnitude of projected temperature rise over the twenty-first century varies depending on the model sensitivity and the emission scenarios as illustrated in Figure 6. By 2100, temperature increases are estimated to range between 1.5°C and 4.5°C (2.8°F -8.0°F), under the lower emission scenario B1 in the less responsive GCM PCM and under the higher emission scenario A2 in GFDL respectively (Cayan et al., 2008). Generally, warming is expected to be greater in summer than the rest of the year for all scenarios except PCM B1 (Cayan et al., 2008). Warming should affect both wet and dry days with about the same degree (Cayan et al., 2006). In their work, Cayan et al. (2008) present different plausible temperatures increases for two regions in California: Northern California region (NOCAL) and Southern California region (SOCAL).

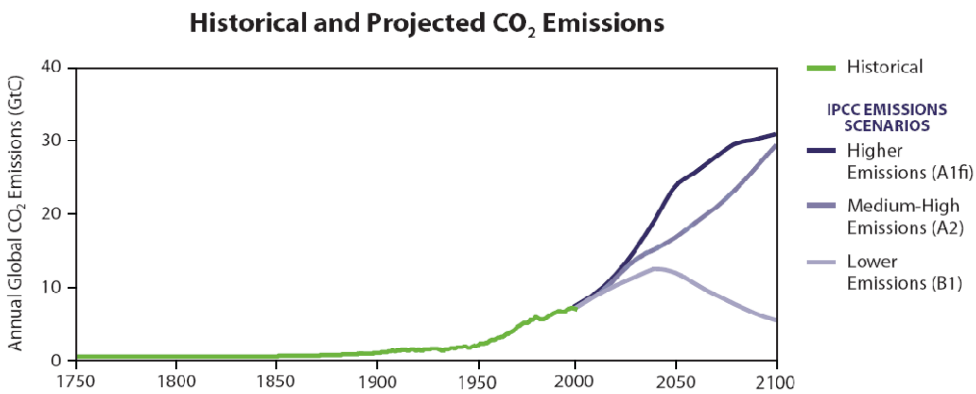

Figure 5 - Historical and projected CO2 emissions - scenarios B1, A2 and A1fi (Source: CCCC, 2006)

Climate warming is likely to affect hydropower operation simultaneously on the supply/generation, demand and pricing sides. To the best of the author, these issues have always been addressed independently. The following sections review recent research conducted in California on climate warming impacts on the supply side (e.g. Madani and Lund, 2009; in press; Vicuna et al., 2008; 2009) and then on the demand side (e.g. Franco and Sanstad, 2006; Aroonruengsawat and Auffhammer, 2009).

Previous works assessing climate change impacts in California have commonly used a range of plausible scenarios from an earlier work of Cayan et al. (2006) or directly based on the former IPCC Third Assessment. (eg. Medellín-Azuara et al., 2008; Vicuna et al., 2008; Aroonruengsawat and Auffhammer, 2009; Madani and Lund, in press).

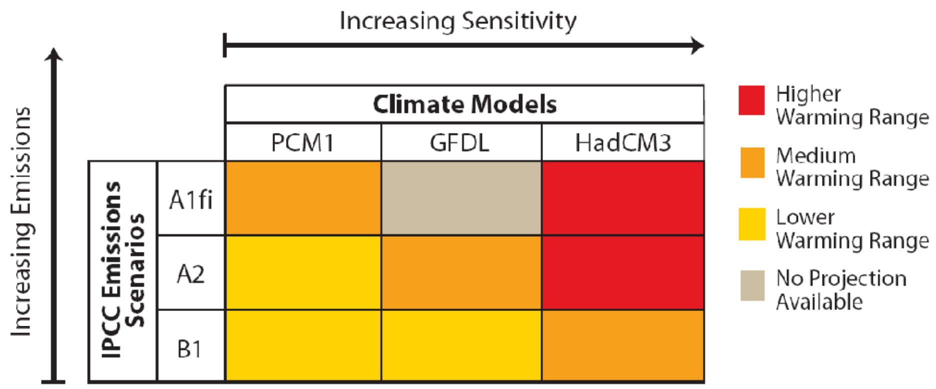

Figure 6 - Warming ranges for 3 plausible GCMs coupled with 3 GHGs for California (Source: CCCC, 2006)

4.2 Impacts on the supply side

Climate change will impact hydrological conditions. California's 21st century hydrology is expected to be altered in the following manner: part of the winter precipitation falling as snow nowadays will turn to rain; higher temperatures will lead to a shift of the snowmelt peak flow; a reduction of the peak flow's intensity and increased winter runoff (Moser et al., 2009).

Hydrological changes are a big concern for California's hydropower system which may face water shortages in summer when the demand is the highest (Moser et al., 2009). This issue should be less problematic for low-elevation multipurpose hydropower systems (less than 1,000 feet) benefitting from large man-made reservoirs, than for high-elevation units with small man-made reservoirs (Tanaka et al., 2006). Relying mainly on natural snowpack reserves, high-elevation hydropower systems have a limited flexibility in operation. If their storage capacity cannot accommodate to hydrological changes, high-elevation hydropower systems may be vulnerable to climate change (Madani and Lund, in press).

According to Madani and Lund (in press), most studies assessing the impacts of climate change on hydropower generation in California have focused on large-scale low-elevation systems (e.g. Tanaka et al., 2006) or on a few individual high-elevation hydropower units (e.g. Vicuna et al, 2008; 2009). High-elevation systems are nonetheless generating on average 74% of California's in-state hydroelectricity (Madani and Lund, 2009) which has prompted recent research on the impacts of climate change on high-elevation hydropower systems (e.g. Vicuna et al., 2008; Madani and Lund, 2009; in press).

Vicuna et al. (2008) studied the impact of four climate change scenarios on high-elevation hydropower system in the Upper American River using a linear programming model optimizing the system for revenue maximization, restricted to operational and physical constraints. The model ran under historical conditions replicated expected patterns of operation with reservoir refilling in spring and electricity generated in priority when it is the most valuable. For the two drier scenarios, both power generation and energy revenue decrease but generation more than revenue, showing the ability of the system to store water when prices are low for a later release when energy is more valuable (July-September) (Vicuna et al., 2008). For the wetter scenarios, the increase in generation outpaces the increase in revenue and the generation pattern is similar to the hydrograph. For all scenarios, the occurrence of spillage increased, caused by the inconvenient hydrograph.

The energy price representation considered by Vicuna et al. (2008) distinguishes two constant on-peak and off-peak monthly prices; capturing some effects of non-constant energy prices. If fixed monthly prices were used, a model based on revenue maximization would suggest no generation in months with low energy prices to allow maximum generation in month where energy is valuable (Madani and Lund, 2007). Madani and Lund (2009) formulated a new approach where the price representation is derived from the distribution of hourly real time prices for each month. This allows capturing the hourly variability in energy prices – on a monthly basis – of the overall energy market which is responding mostly to on-peak and off-peak variability in energy demands (Madani and Lund, 2009). The energy price used is a function of the percent time turbines are in operation, assuming they operate in hours when the energy market offers higher prices (Madani and Lund, 2009).

Madani and Lund (2009) also introduced a novel approach to model the behavior of a large number of high-elevation hydropower systems, the Energy-Based Hydropower Optimization Model (EBHOM). To the best of the author, EBHOM is the only one of its kind, allowing modeling an entire region's high elevation hydropower system in a relatively straight forward manner, without the need to develop traditional streamflow and reservoir volume-based models for each plant in the system. EBHOM was tested against the traditional hydropower optimization model developed by Vicuna et al. (2008) on the Upper American River system (Madani et al., 2008). Both models predicted the same changes in generation and revenue with respect to the historical case. Even if the EBHOM is very simplified compared to traditional optimization models, it produces reasonable results and is a step forward towards modeling global trends including "the effects of climate change and energy prices on system-wide generation and hydropower revenues" (Madani and Lund, in press).

Madani and Lund (in press) applied EBHOM to estimate the impacts of climate warming on California's high elevation hydropower system for the three following scenarios: warming-only, dry warming (GFDL-A2) and wet warming (PCM-A2). Warming-only and dry warming scenarios reduce both generation and revenue while the wetter scenario has the opposite effect. Current storage and generation capacities are able to cope with some of the supply loss of the dry warming scenario. Compared with the base historical scenario, the decrease of runoff by 20% led to revenue losses of only 14%. Contrarily, the increase by 10% of annual runoff compared to the base case, led to an increase of only 6% in generation and 2% in revenues for the wet case scenario. Spills increased for all scenarios except the dry one.

The above mentioned studies have only considered that climate warming will change hydrologic conditions and alter hydropower water supply. Potential changes in electricity demand and prices have not been accounted for. These could be the result of various climatic, economic, technologic, policy or market reasons (Madani and Lund, in press). Environmental constraints haven't been addressed either.

4.3 Impacts on the demand side

On the demand side, climate warming is expected to increase the need for cooling in summer and attenuate the need for heating in winter (CCCC, 2006).

Franco and Sanstad (2006) examined the statewide correlation between daily average quantities: mean daily temperatures and base loads; and extreme quantities: maximum daily temperatures and peak loads. A nonlinear convex relationship between average daily temperature and demand, and a linear relationship between summer peak load and maximum temperatures were determined. They developed climate change scenarios for the 21st century and examined demand responsiveness (considering the relationships between demand and temperature invariant in the future). Relative to the base period 1961-1990, electricity demand increased in the range 3.1–20.3% and peak load increased in the range 4.1–19.3% by 2100. It is noteworthy that even a small increase in demand would result in a high increase in energy expenditures (Franco and Sanstad, 2006). Aroonruengsawat and Auffhammer (2009) used a unique panel of household electricity billing data from California's three largest investor-owned companies. They did not estimate demand as a function of statewide temperature but divided California in 16 climate zones. They projected an increase in aggregate demand ranging from 18% to 55% by 2100 assuming a constant population. This represents an average annual growth rate of aggregate electricity demand ranging between 0.17% and 0.44%. In reality these growth rates accelerate with time.

Aroonruengsawat and Auffhammer (2009) coupled climate warming to economical future scenarios. They developed two scenarios considering electricity price increases based on the projected impacts of AB 32 compliance combined with natural gas price increases: a discrete 30% increase by 2020 remaining to the same level until the end of the century and two successive increases of 30% by 2020 and 20% by 2040. By 2100, the total change in demand ranges between +4% and +39% and between -7% and +24% for the low and high price increase scenarios respectively. Higher prices result in a decreased demand compared to the base case where no price increase was considered. Aroonruengsawat and Auffhammer (2009) also considered population increase scenarios. Combined to a low forcing climate warming scenario, a low projection of 0.18% population growth rate per year (equivalent to a population increase by 18% by 2100) predicts an increase of 65-70% in residential electricity demand by 2100. This increase is much higher than the 20% increase predicted for the climate warming only scenario. The worst case they predicted coupled a high forcing scenario with a high growth rate (+1.47% per year) and suggested an increase in demand up to 478%. Their conclusion is that demographic trends have substantial impacts on future energy demands and might outweigh the impact of climate change on energy demand.

5 Method

The overall method used in this work is shortly described hereafter and schematized in a flowchart in Figure 7. Further details on the models selected and the choices and assumptions made are given in the following sections.

An ANN was developed to map the relationship between a set of inputs and the hourly electricity prices. The inputs include notably temperature, demand and deterministic components (season, day of the week, hour, etc.). An ANN model was chosen for this purpose as it is a powerful machine learning tool providing an appealing solution for relating input and output variables in complex systems (Dawson and Wilby, 2001). ANNs are capable of extracting information from systems even with little prior physical knowledge about the systems (Zhang et al., 1998). The ANN architecture chosen is a multilayer feed-forward model using the Shuffle Complex Evolution (SCE-UA) global-search optimization method developed by Duan et al. (1992).

The performance of ANNs is reliant on the quantity and quality of the calibration data (Kingston et al., 2005). Before calibration of the model, a preliminary statistical analysis of the collected data was performed to get an overview of existing trends, potential problems and allow an adequate data preprocessing.

Once the ANN was trained, simulations with perturbed input data were run to account for the chosen climate warming scenarios. Scenarios were chosen from the work of Cayan et al. (2008) based on the IPCC Fourth Assessment. The outputs of the trained ANN are predicted hourly prices. The price representation chosen for the next modeling steps is based on the work of Madani and Lund (2009) capturing the hourly variability of energy prices.

Climate warming effect on California's high elevation hydropower system was estimated using the energy-based hydropower optimization model EBHOM developed by Madani and Lund (2009). Price frequency and revenue curves (integration over the price frequency curves) were drawn and used as inputs to the hydropower optimization model EBHOM together with the historic monthly generation data and seasonal runoff distributions. The results obtained from EBHOM are monthly optimized generation, revenue and end-of-month storage data for the statewide high-elevation hydropower system, considering climate change effects on the demand, supply and pricing sides.

Previous findings from Madani and Lund (in press), assessing climate change impacts on the supply side only, were finally compared to the results from this research.

The following sections review the method in details. Section 6 includes a description of existing ANN models, followed by data collection and analysis, ANN model selection, set up and calibration. It includes the application of the trained ANN model to estimate future price scenarios. Section 7 presents EBHOM model and its results.

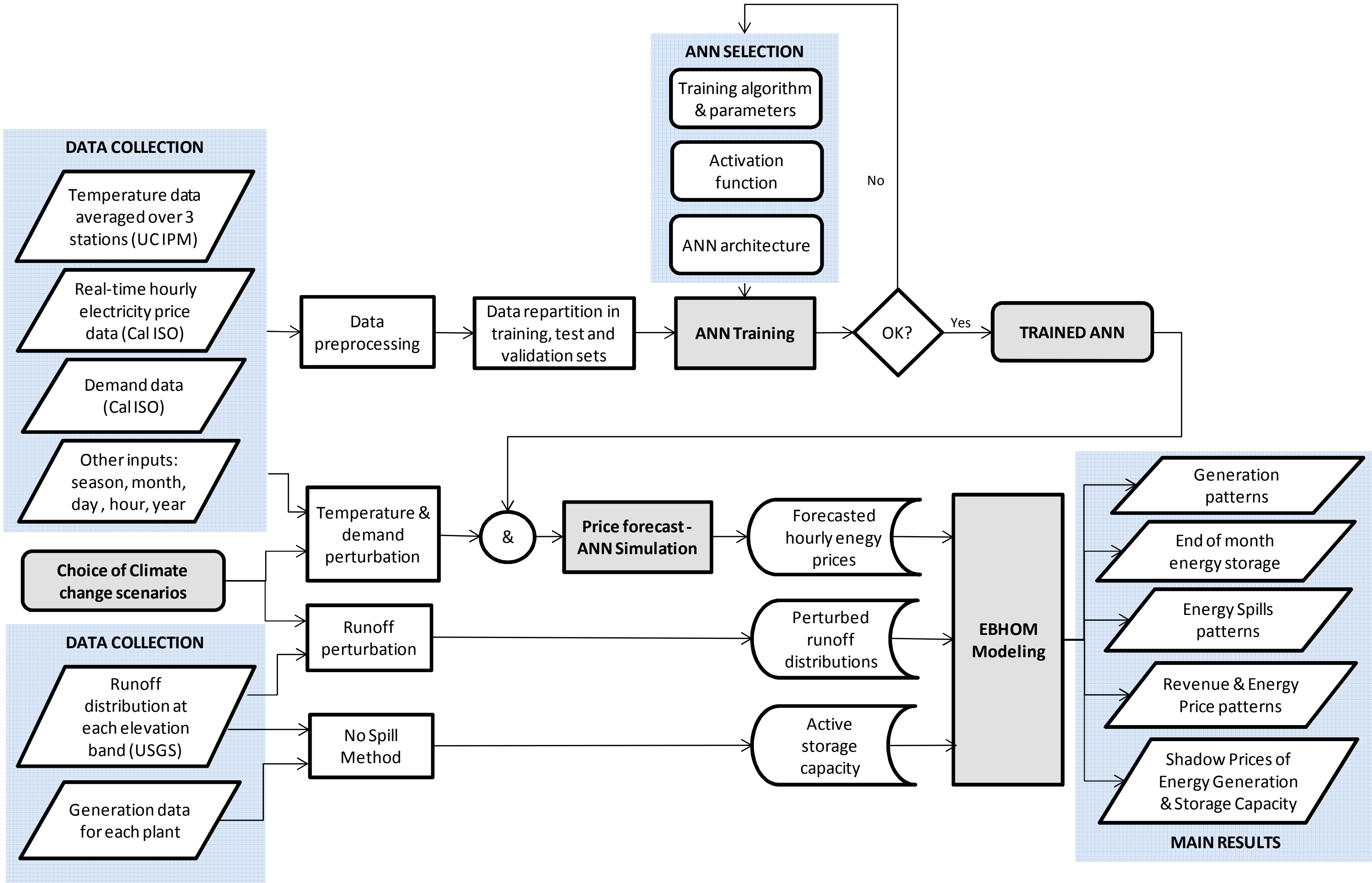

Figure 7 - Flow chart of the project's methodology (to read from left to right)

6 Artificial Neural Network

6.1 Background and motivation: ANNs to model electricity prices

Artificial Neural Networks (ANNs) are networks of interconnected neurons that were developed in an attempt to reproduce the powerful human brain's architecture (Hsieh and Tang, 1998). ANNs are powerful machine learning models that have been successfully developed for different purposes namely for nonlinear modeling (e.g. Kingston et al., 2005) and classification (e.g. Olsson et al., 2004). They provide an appealing solution for relating input and output variables in complex systems (Dawson and Wilby, 2001) and have been widely applied in different fields namely hydrological modeling (e.g. Dawson and Wilby, 2001; Kingston et al. 2005; Olsson et al., 2004), electricity load forecasting (e.g. Azadeh et al., 2006; Ortiz-Arroyo et al., 2005; Hippert and Taylor, 2010) and electricity price short-term forecasting (e.g. Ranjbar et al., 2006; Zarezadeh et al., 2008; Gao et al., 2000).

In recent years there has been active research to develop accurate short-term price forecasting tools for the energy market (e.g. Zhao et al., 2007; Lu et al., 2005; Amjady and Keynia, 2010a; Yamin et al., 2004; Zarezadeh et al., 2008). Electricity price is a nonlinear, time variant and volatile signal owning multiple periodicity, high frequency components and significant outliers, i.e., unusual prices (especially in periods of high demand) due to unexpected events in the electricity markets (Amjady and Hemmati, 2006). California's ESI turned into a competitive deregulated market in the 1990s (CBO, 2001). The deregulation of energy market created competition among electricity producers and retailers who need price forecasts to develop their bidding strategy in the electricity market (Lu et al., 2005; Amjady and Hemmati, 2006). Optimal decisions are now highly dependent on market electricity price (Amjady and Keynia, 2010a). For instance, electricity generation scheduling is based on profit maximization in the new structures whereas it was based on cost minimization – to satisfy the electricity demand and all operating constraints – in the earlier regulated environment (Zarezadeh et al., 2008).

Dealing with short-term price forecasting, ANNs have shown a good ability to forecast normal electricity prices (Zhao et al., 2007). One of the main advantage of ANNs over traditional methods such as regression and time series or regressive integrated moving average (ARIMA) is that they are more adapted to long-term patterns as they can cope with high non linear behavior of the target signal (Amjady and Hemmati, 2006). However, one main problem encountered in most studies is the inability of the models to deal with price spikes in the electricity market (e.g. Zhao et al., 2007; Lu et al., 2005; Amjady and Keynia, 2010a; Yamin et al., 2004). Generally, price spikes are abnormal market clearing prices that include namely *abnormal high prices* which are prices much higher than normal prices (Zhao et al., 2005). Price spikes are highly erratic and are caused by a number of complex factors and unexpected events such as transmission network contingencies, transmission or congestion and generation contingencies (Zhao et al., 2007). According to Lu et al. (2005), almost all the existing techniques require filtering out the price spike signals in order to forecast normal prices with rather high accuracy.

To the best of the author, research on ANNs has exclusively focused on short-term price forecasting following the needs from the market. No ANN model for long-term electricity price forecasting accounting for climate change scenarios has been developed, and neither for estimating impacts of future climate on any other variable.

6.2 Background on ANN model types

A typical ANN consists of a number of neurons (also called nodes) that are organized in a specific arrangement (ASCE, 2000). One way of classifying neural networks is by the direction of information flow and processing: feedforward and recurrent networks (ASCE, 2000). In a feedforward network (Figure 8), information flows unidirectionally from an input layer towards an output layer. In between the input and output layers there can be one or several hidden layers processing information before it reaches the output layer. In this case neurons are only connected between different layers, but not to other neurons belonging to the same layer. In a recurrent network information flows in both directions – inputs toward outputs and vice versa – and also nodes belonging to the same layer can be interconnected. Recurrent networks allow modeling dynamic systems by making feedback possible in the network but it is also possible to treat explicitly dynamic systems with feed-forward networks by including lagged inputs (Maier and Dandy, 2000). Feed-forward networks namely multilayer perceptron (MLP) models are commonly used for prediction and forecasting applications in hydrological problems (ASCE, 2000; Kingston et al., 2005) and in short-term electricity price forecasting (e.g. Ranjbar et al., 2006; Zarezadeh et al., 2008). Feed-forward networks have in general a faster processing speed than recurrent networks (Maier and Dandy, 2000) and Hornik et al. (1989) showed that with a single hidden layer they can approximate any non linear function, given that sufficient degrees of freedom (i.e. hidden neurons) are provided.

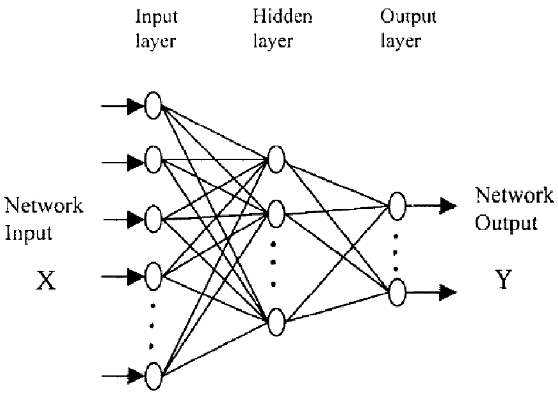

Figure 8 - Schematic diagram of a feedforward three-layer ANN (Source: ASCE, 2000)

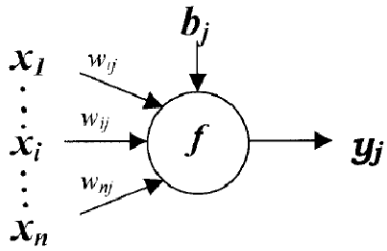

Figure 9 - Schematic diagram of a neuron "j" (Source: ASCE, 2000)

A schematic diagram of a j^th^ neuron is displayed in Figure 9. This neuron transforms an input vector $X = (x_1, \ldots, x_i, \ldots, x_n)$ into a single output y_j. Neuron 'j' is characterized by a set of weights represented by a vector $W_j = (w_{1j}, \ldots, w_{ij}, \ldots, w_{nj})$, a bias b_j and an activation function f. The inputs to the neuron can be causal variables i.e. the inputs to the system if the neuron is in the input layer, or they can be outputs from neurons belonging to previous layers. The activation function determines the response of the neuron as follows: $y_j = f\left(X * W_j + b_j\right)$. Sigmoid functions, namely logistic sigmoid ('logsig') or hyperbolic tangent ('tanh' or 'tansig'), are commonly used in the hidden layers (ASCE, 2000). They return a non-linear output response which makes them a useful tool to map nonlinear processes and are usually combined to a linear activation function in the output layer (ASCE, 2000).

In order to obtain a model representing reality as accurately as possible, the model has to be trained and optimized. Training, or calibrating, an ANN model is the process of adjusting its parameters (weights) to minimize a predefined error function (Kingston et al, 2005). A data sample is presented to the model and the error is calculated by comparing the simulated and the observed target intensities. Local or global search optimization algorithms may be used to train the ANN (Maier and Dandy, 2000). Local search methods scan the error surface in a single direction whereas global search methods scan simultaneously the error surface in different directions (Kingston et al., 2005). Back-propagation algorithm is among the most widely applied methods to train an ANN in hydrological modeling (Maier and Dandy, 2000) and in electricity price short-term forecasting (e.g. Ranjbar et al., 2006; Zarezadeh et al., 2008). Radial basis function method and conjugate gradient method are examples of other local search algorithms (ASCE, 2000). One of the major drawbacks of local-type search optimization methods is that they are not designed to handle the presence of multilocal optima (Duan et al., 1992). It is therefore not guaranteed that the user will obtain the global optimum as the ANN may get stuck in one of the local minima of the error surface (Kingston et al., 2005). Global search methods have the ability to escape local minima in the error surface and shall, in principle, find the optimal weight configurations (Maier and Dandy, 2000). Genetic algorithms and Shuffle Complex Evolution algorithms are examples of global search methods that have been applied in the hydrological field (Kingston et al., 2005). The reader is referred to Maier and Dandy (2000), ASCE (2000) and Duan et al. (1992) for a more exhaustive review of training methods.

During the training phase, the ANN has to be adjusted in order to minimize the error function. The optimal ANN architecture is commonly determined through a trial-and-error procedure by trying out different number of hidden layers and nodes (ASCE, 2000; Maier and Dandy, 2000). Increasing the size of the ANN increases the number of free parameters (weights). An ANN should contain enough parameters to improve its capacity to map a complex relationship between the inputs and outputs (Dawson and Wilby, 2001). However, increasing the size of the network over a certain threshold may produce the opposite effect if the ANN starts overfitting the data, annihilating its ability to generalize trends (Dawson and Wilby, 2001). This phenomenon appears when the ANN performs well during the training period but produces poor results if a new data sample is presented to the ANN; the ANN fitted the training data so well that it fitted to the noise contained in the sample (Hsieh and Tang, 1998). Cross-validation procedure also referred to as cross-training is commonly used to prevent overfitting to occur (Maier and Dandy, 2000). It consists of dividing the data sample into three sets – usually called the training, validation and test sets – and then using them independently to check when the ANN is optimized. The ANN is considered to be optimized when the training set minimizes the error function and the error starts increasing over the validation set (ASCE, 2000). It has also been suggested in literature that if the number of training samples exceed a specific threshold, defined by a ratio between the number of training samples and the number of connection weights, overfitting will not arise. These ratios can vary consistently in literature (Maier and Dandy, 2000), but it should be interpreted as follows: the higher the number of training samples, the lower the probability of overfitting the data.

6.3 ANN model set up

The method used to design the ANN was inspired from the protocol for implementing ANN Rainfall-Runoff model defined by Dawson and Wilby (2001) and modeling suggestions from Maier and Dandy (2000). The modeling process steps will be explicitly detailed as far as possible so that the validity of the model and results can be assessed. The procedure was the following:

1. Selection of the adequate predictors and predictands & Data collection
2. Data preprocessing
3. ANN Selection: choice of an appropriate network type and training algorithm
4. Network training: choice of the architecture and training set
5. Evaluation of ANN performance

6.3.1 Data collection - Predictors and predictand selection

Hourly prices were selected as the only predictand. Real-time hourly energy prices for 2005-2008 were collected from the California ISO Open Access Same-time Information System (OASIS) website (http://oasishis.caiso.com/). In April 2009 a new market design was implemented. Instead to look at three main price zones, Cal ISO started using Locational Marginal Pricing that produces prices at 3,000 different pricing nodes around the California grid. Therefore the data sets from after April 2009 are considerably different from the previous system so data could not be gathered easily for 2009. Cal ISO serves more than 30 million consumers with electricity so these hourly prices are considered as representative for California's energy market.

Electricity price is driven by many factors in a competitive energy market (Ranjbar et al., 2006). Research works applying ANNs to short-term price forecasting have chosen among others the following predictors: historical hourly prices, system loads, lagged hourly prices and day of the week as they are often easily accessible (e.g. Ranjbar et al., 2006; Zarezadeh et al., 2008). Gao et al. (2000) also considered fuel costs, power import/export data and other weather variables. In the present research the following inputs were chosen: temperature, demand, season, month, day of the week, hour, lagged hourly temperatures for the three previous hours, a 'degree-day' temperature input. The season is expected to account for the annual price variability, the hour for the daily periodicity and the day of the week for the weekly periodicity, i.e. to distinguish workdays from weekends.

Hourly temperature data for the period 2005-2008 were extracted from the website of University of California Statewide Integrated Pest Management Program (UC IPM) (http://www.ipm.ucdavis.edu/WEATHER/wxretrieve.html). These data were available for several Pest stations across California but not further north nor further south than the Fresno and Colusa Counties respectively. It was decided to extract hourly data from three different Pest stations and to define their average as the representative temperature for the state of California.

Hourly electricity load data were also collected from CalISO OASIS website (http://oasishis.caiso.com/) for 2005-2008. Demand was also estimated using temperature data based on the work of Franco and Sanstad (2006). Using daily demand of electricity from 2004 for the area services by the Cal ISO, they found out that there is a high correlation between the daily demand and the average daily temperature measured in four locations of California. They approximated the relationship by the U-shaped third degree polynomial plotted in Figure 10. The polynomial reached its minimum daily demand for $T_{min} = 53{,}5°F$. Estimating hourly demands through this function implies that the hourly demand follows the same pattern as the mean daily demand. This seems to be a reasonable assumption for this work since we are interested in the big picture over California and that temperatures are also flattened. However this remains a limitation to map properly hourly prices that contain many peaks which might result from periods of peak demand.

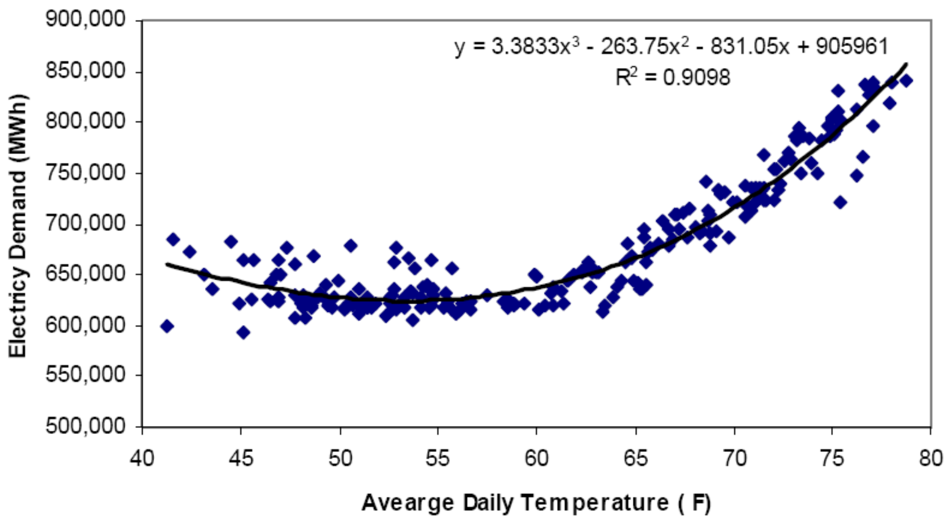

Figure 10 - Electricity demand in the CalISO area as function of average daily temperatures, 2004 (Source: Franco and Sanstad, 2006)

6.3.2 Data analysis and preprocessing

6.3.2.1 Data analysis

ANNs are reliant on the quantity and quality of the calibration data (Kingston et al., 2005). A preliminary analysis of the data was performed to get a better understanding of the varying nature of hourly prices and to check if there aren't any major abnormal trends. Temporary irregularities in the energy market or extreme weather conditions may for instance lead to substantial variations in the energy prices while being the result of single events, hedging the generalization capacity of ANNs.

The main statistical characteristics of the set are given in Table 1. The data set has a mean of 57$/MWh and a standard deviation of around 37$/MWh. Around 80% of the data are in the range 25-90 but the hourly prices are highly volatile with prices up to 400$/MWh which is 7 times the average price.

Table 1 - Dataset statistical characteristics before preprocessing

Prices in $/MWh				Price Percentiles in $/MWh				
Average	**Standard Deviation**	**Minimum**	**Maximum**	**10th**	**25th**	**50th**	**75th**	**90th**
56.77	36.52	0.00	399.99	24.23	37.78	50.85	67.18	89.91

The hourly price time-series for 2005-2008 is plotted in Figure 11 where two 'abnormal' trends are noticed (circled in the figure) with exceptionally high prices. Figure 12 is plot of monthly average prices in each year. The same two periods of higher than normal prices can be observed. The first one happened in 2005, where prices have started increasing in July, reached a maximum average value of 80$/MWh in October and have only dropped to normal levels in January 2006. The second period of higher than normal prices happened in the first half of 2008 and peaked to a monthly average value of more than 100$/MWh in June 2008. A specific investigation of these two periods was conducted in the next paragraphs.

In 2005, national natural gas prices increased substantially over levels seen in 2004 (California ISO, 2006) resulting in increasing production costs for electricity. This steady rise began in January and later on prices peaked immediately after Hurricanes Katrina and Rita hit the US Gulf Coast (California ISO, 2006). The most destructive wave of the hurricanes occurred the last week of August in southeast Louisiana and caused severe destruction along the Gulf coast from central Florida to Texas. In particular, national gas production and transportation infrastructures in the Gulf of Mexico Region were destructed (California ISO, 2006). After this event, Western markets – which have not been directly affected by the hurricanes –started trading gas at a discount of approximately $2/mmBtu (million British thermal units) to national prices (Department of Market Monitoring – California ISO, 2006). In December 2005, a cold snap coupled with limitations to the Gulf Coast transportation and production infrastructure resulted in a second peak, with California prices reaching their highest levels since December 2000 (California ISO, 2006).

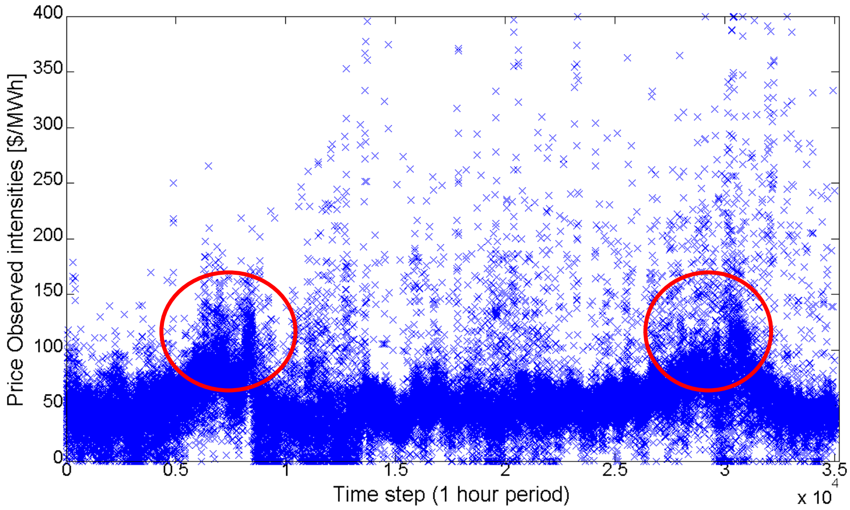

Figure 11 - Real-time hourly prices observed for the time series 2005-2008

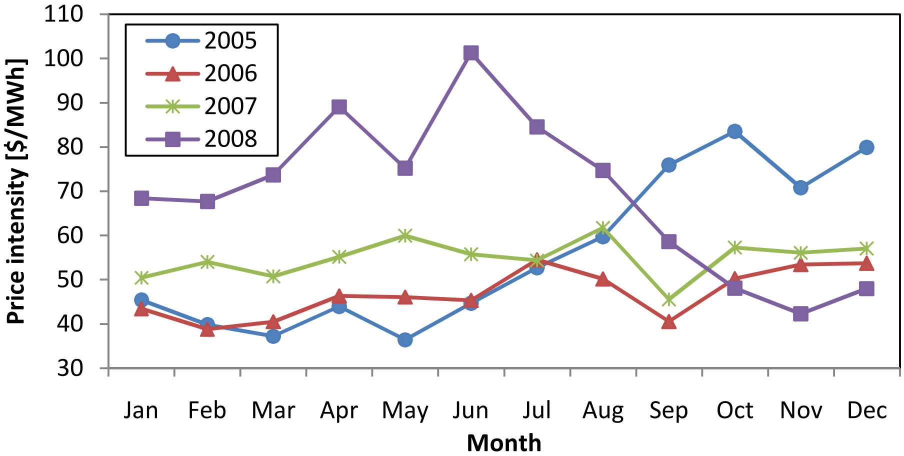

Figure 12 - Average Hourly Prices per month for each year 2005-2008

The climatic conditions of 2008 were investigated as extreme temperatures can lead to an increase in electricity demand, and drought conditions to a reduction in generation from hydropower units. According to NOAA (2009) summer and fall 2008 were warmer than average in California as it experienced its 6th warmest summer and 3rd warmest fall on record whereas temperatures in winter were slightly below normal. California experienced its driest spring (March-May) on record and also received below normal precipitation in summer and fall 2008 (NOAA, 2009). At the same time, the snowpack was referred to as among the healthiest in more than a decade in some parts of Western US with most locations near to above average (NOAA, 2009). From these facts, it is hard to assess if there was a shortage of supply as the abundant snowpack runoff may have compensated for the drought. However, the 2008 Annual Report from California ISO (2009) states that "monthly average hydroelectric production in 2008 was below 2007 levels for most months and well below the monthly production levels for 2005 and 2006". Furthermore, the same report from California ISO (2009) explains that the primary driver of the high electricity prices in 2008 was the spike in worldwide fossil fuel costs. Natural gas, which is the primary fuel for California's energy supply, reached its highest level since Hurricanes Katrina and Rita impacted much natural gas infrastructure in 2005. These high natural gas prices, coincident with low hydroelectric production in California in the first half of that year, resulted in high production costs of electric power in 2008 and the need for additional imports from the Pacific Northwest and Southwest (California ISO, 2009). The senior vice president and chief customer officer of Pacific Gas & Electric also declared that "The combination of skyrocketing natural gas prices, increased electricity demand and lower supplies of hydroelectric power are having a significant impact on the cost of electricity" (PG&E, 2008).

As the main focus of this paper is to investigate the relation between prices and climate, prices have been plotted against temperature in Figure 13. The top graph is a plot of the raw hourly data while the bottom one shows the average price corresponding to each degree Fahrenheit. From the top graph, no obvious conclusion can be drawn regarding the relationship between the real-time prices and the temperature. This strengthens the need for a powerful modeling tool able to represent highly non linear relationships. The bottom plot in Figure 13 shows that prices tend to increase for both low (>30°F) and high (>90°F) temperatures but more significantly for high ones. This corresponds to the great need for cooling in the long warm periods in California. In-between average temperatures are around the mean of the entire set which is 57°F. Year 2008 presents higher prices than other years for most temperatures above 50°F. This phenomenon has been discussed earlier.

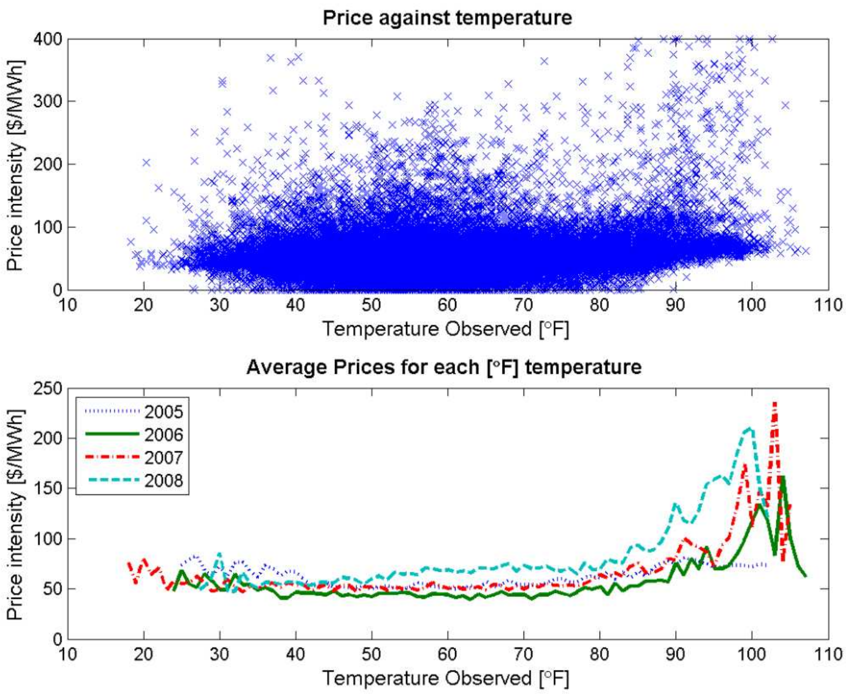

Figure 13 - Hourly prices against temperature (top) and Average hourly prices per temperature (bottom)

It is well-known that the hour of the day has a significant influence on the demand and therefore on the price too. Figure 14 showing the average prices per hour in each season was plotted to check this affirmation. From Figure 14 one can see that the main difference between seasons occur between 12PM and 20PM. The high cooling demand in summer increases the price, peaking at 17PM, while the 'no' or little heating demand in winter decreases the price.

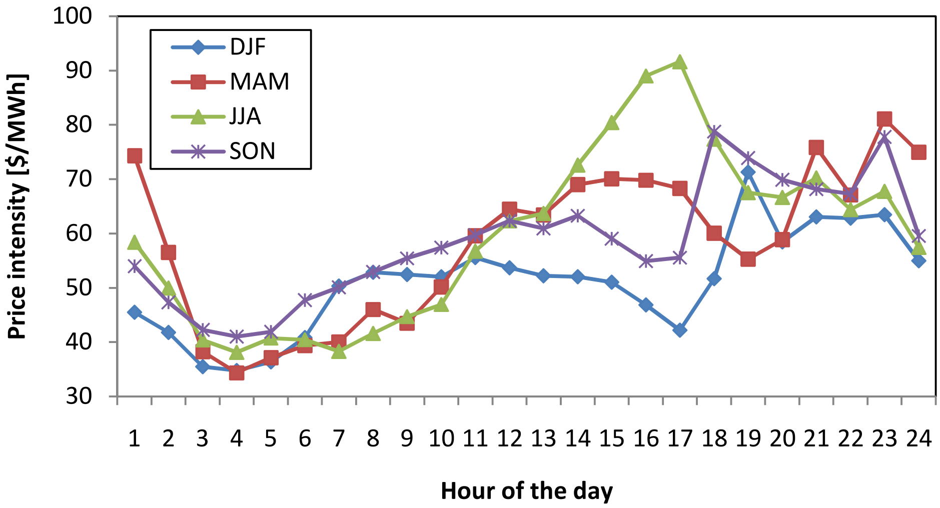

Figure 14 - Hourly average prices in each season

6.3.2.2 Data preprocessing

From the results of the data analysis, it was chosen to exclude the period September to December 2005 from the input data to the ANN as they partly result form an extreme event (Hurricane Katrina) and would most probably hedge the training of the neural network. The price increase in 2008 was the result of a combination of several factors. It was decided to keep 2008's data to keep a great quantity of data and because soaring prices of fossil fuels together with dry periods are most likely to occur again in the future. However, an additional neuron in the input layer was introduced to account for this specific phenomenon. This input is equal to 1 for the period January-June 2008 and 0 otherwise.

The statistical characteristics of the preprocessed data set are given in Table 2. Negative price intensities have been set to zero and the overall zero-depth probability is 1.30%.

Table 2 - Dataset statistical characteristics after preprocessing

Prices in $/MWh				Price Percentiles in $/MWh				
Average	Standard Deviation	Minimum	Maximum	10th	25th	50th	75th	90th
54.87	36.54	0.00	399.99	23.88	36.88	49.13	64.14	84.28

The last stage of the data preprocessing was the standardization of the hourly prices and temperatures, by subtracting the mean value of the set and dividing it by the standard deviation. Standardized temperature data ranged between -2.72 and 3.05 and standardized price data between -1.50 and -9.44. The output data i.e. the hourly prices were then scaled between 0.1 and 0.9 to avoid squashing when using the log sigmoid function in the hidden layer (and similarly between -0.9 and 0.9 when using the hyperbolic tangent activation function).

6.3.3 ANN Selection

A multilayer feed-forward ANN was coupled with the global-search algorithm developed by Duan et al. (1992) called the “Shuffle Complex Evolution” (SCE-UA). A single hidden layer with a sigmoid activation function was chosen. The choice of the sigmoid function (tansig or logsig) and the number of hidden neurons were based on a sensitivity analysis detailed in section 6.4.1. The activation function in the output layer is linear. Cross-validation was used as the stopping criteria to prevent overfitting the training dataset. The model was developed in FORTRAN by Juan Martin Bravo in application to river discharge analysis and was modified for our case study.

The general idea of SCE-UA algorithm is to generate a population of random points from the feasible space of parameters that will evolve towards an optimal solution, i.e. the global minimum of the error surface. The steps are the followings. First the population is divided into several communities (called complex) that evolve independently. Within each community, only the part of the population with the best probability of converging towards a global solution is kept and stored in a ‘sub-complex’ using the Complex Evolution Algorithm (CCE) (Duan et al., 1992). The points stored in the sub-complex will become parents by generating offsprings towards an improvement direction. Each sub-complex will generate offsprings in different directions toward an optimum, based on its own ‘knowledge’ of the error surface. The population is mixed regularly in order to share the knowledge between the communities and to ensure survivability. Finally a set of optimum parameters will eventually be found after several iterations of the procedure. None of the information from the sample is ignored as each member of a community is a potential parent with the ability to participate to the reproduction process. The evolution process also ensures that the communities don’t get trap into unpromising regions. The SCE-UA method has good convergence properties over a broad range of problems and it should have a high probability of finding the global optimum (Duan et al., 1992).

The flowchart of SCE-UA algorithm and further description of the algorithm’s steps can be found in the publications from the authors, Duan et al. (1992, 1994).

Duan et al. (1994) established some guidelines on how to choose the algorithmic parameters in the SCE-UA model. The parameters were initialized to the recommended values (n is the number of parameters to optimize):

- Number of points in complex: $m = 2n + 1$
- Number of points in each sub-complex: $q = n + 1$
- Number of consecutive offspring generated by each sub-complex: $\alpha = 1$
- Number of evolution steps taken by each complex: $\beta = m = 2n + 1$

Finally the number of complex is problem dependant and was chosen based on sensitivity analysis detailed in section 6.4.1.

6.3.4 Network training

Cross-validation procedure was chosen to prevent overtraining. The data set was partitioned into three sets referred to as calibration, test and validation in the following proportions: 50%, 25% and 25% respectively. Data was split randomly between the sets but a control was performed to ensure a good distribution among the different sets by checking that extreme (or close to extreme) values of price and temperature were within the training set and that means and standard deviations of all sets were similar. The training set should be representative of the entire population and include all ranges of intensities because of the inability of ANNs to extrapolate (Maier and Dandy, 2000).

6.3.5 Evaluation of ANN performance

The results of the ANN modeling were assessed in terms of: correlation with the determination coefficient R^2, root mean square error (RMSE), the ANN's output price patterns and the frequency distribution of prices. As the dataset is large, it is important to assess the quality of the developed model not only based on R^2 value. Furthermore, it is important to keep in mind that in this research, the final desired output from the ANN model is to draw revenue curves for each month (for several climate change scenarios) that will serve as inputs to the EBHOM model. These revenue curves are nothing else than the integration over the price frequency curves for each month (Madani and Lund, 2009), so the frequency distribution of prices was directly assessed in terms of revenue curves.

6.4 ANN Calibration

ANN training was performed through a trial and error process. Firstly a sensitivity analysis was performed to determine the best network architecture and the training algorithm parameters; it also includes an assessment of the choice of some inputs. Several dataset breakdowns were then considered based on both deterministic and stochastic approaches. Finally, a comparison of the different ANN models developed was performed to select the ANN model to be used a long-term price forecasting tool.

6.4.1 Sensitivity analysis

An ANN is a black-box model which has to be calibrated to determine the optimal architecture and parameters. The sensitivity analysis carried out includes assessment of the following parameters:

- Number of complexes for the SCE-UA optimization algorithm
- Number of hidden nodes
- Activation function: logsig or tansig
- Relevancy of the input selection

6.4.1.1 Number of complex and hidden neurons

The optimal numbers of complex and hidden nodes were determined in the same way. The first models developed used only one complex and hidden neuron and were then independently increased to 2, 4 and 8 in the next models. Higher values have also been tried out, but the time required running such models over the entire dataset exceeded 48 hours, which was considered excessive. Time is a limiting factor in the ANN models improvements. A single hidden layer was chosen as it should be enough to model any non-linear relationship (e.g. Hornik et al., 1989). Table 3 shows R^2 values for the different models tried out to estimate the adequate number of complex and hidden neurons. Correlation in terms of R^2 value improves with increasing complexes and hidden neurons so they were both set to 8 for the next modeling steps.

Table 3 - Calibration results used to select the adequate number of complex and hidden neurons

Run	Number Complex	Hidden neurons	Activation function	R^2_{train}	R^2_{valid}	R^2_{test}
1	1	4	logsig	0.26	0.23	0.24
2	8	4	logsig	0.27	0.23	0.25
3	1	8	logsig	0.27	0.23	0.26
4	8	8	logsig	0.29	0.25	0.24
5	8	1	logsig	0.20	0.18	0.19
6	8	2	logsig	0.22	0.19	0.21
7	8	4	logsig	0.27	0.23	0.25
8	**8**	**8**	**logsig**	**0.29**	**0.25**	**0.24**

6.4.1.2 Logsig vs. Tansig activation function

A sigmoid-type activation function - usually logistic sigmoid (logsig) or hyperbolic tangent (tansig) – is commonly used in the hidden layer (Maier and Dandy, 2000). A comparison of ANNs with identical architectures and these two activation functions (cf. Table 4) led to the choice of tansig for the following reasons:

- correlations are similar for both ANNs;
- the average price returned by the ANN using tansig function is closer to the average of historical prices. It also returns higher maximum price values;
- tansig function was used in earlier research works applying ANNs to short-term electricity price forecasting (e.g. Ranjbar et al., 2006; Zarezadeh et al., 2008; Gao et al., 2000).

Table 4 - Results used to select the adequate activation function in the hidden layer

Run	Activation function	$R^2{}_{sim}$	Average Price ($/MWh)	Maximum Price ($/MWh)
Historic	-	-	54.87	399.99
9	Logsig	0.25	54.96	177.59
10	Tansig	0.25	54.93	217.39

6.4.1.3 Assessment of the selected inputs

First, an ANN model using solely temperature as input was tried out and then additional inputs were included (season, month, day, hour, temperatures in 3 earlier hours and load). The correlation improves significantly when more predictors are considered (cf. Table 5, R^2_{sim} jumps from 0.08 to 0.23) because temperature only cannot represent accurately the high volatility of electricity prices. Among the other predictors, none were assessed during the sensitivity analysis, except the load input. ANN models should be able to determine single-handedly which inputs are critical, but it might increase processing speed if the inputs selected *a priori* have little importance (Maier and Dandy, 2000).

Table 5 - Results used to assess the adequacy of the selected predictors

Run	Number Complex	Hidden neurons	Input neurons	Activation function	R^2_{train}	R^2_{valid}	R^2_{test}	R^2_{sim}	RMSE
11	8	2	**1**	logsig	0.09	0.07	0.08	0.08	0.070
12	8	2	**8**	logsig	0.25	0.21	0.23	0.23	0.065
13	16	4	**1**	logsig	0.09	0.07	0.09	0.09	0.070

To estimate the impact of climate change simultaneously on electricity demand and prices, two approaches were imagined. Developing two ANNs in series, the first one modeling demand using temperature and the other predictors, and the second ANN estimating prices based on the output demand from the first ANN; or building a single ANN considering that demand is a linear function of temperature previously estimated by Franco and Sanstad (2006). A model using this demand function was compared to a model using historical hourly demand to estimate if results are improved by using historical hourly demand data gathered from CalISO (http://oasishis.caiso.com/). Using historical hourly demand data improved the R^2

correlation by only 0.03 (see Table 6) which was not considered as a significant improvement. In terms of revenue curves, it is hard to assess which model is more accurate. Depending on the month, it is a different model that fits historical revenues better as illustrated with June and October months on Figure 15.

Finally, the demand function as temperature estimated by Franco and Sanstad (2006) was chosen; nearly no accuracy was gained by using directly hourly demand data from CalISO, training two ANNs in series may be time consuming, and there will also be uncertainty in the estimation of demand from the first ANN model.

Table 6 - Results used to choose the demand input to the ANN between historical demand and the demand function defined by Franco and Sanstad (2006)

Run	Demand specification	R^2_{train}	R^2_{valid}	R^2_{test}	R^2_{sim}	RMSE
14	Demand = f (T)	0.30	0.24	0.27	0.28	0.140
15	Real demand	0.33	0.29	0.31	0.31	0.136

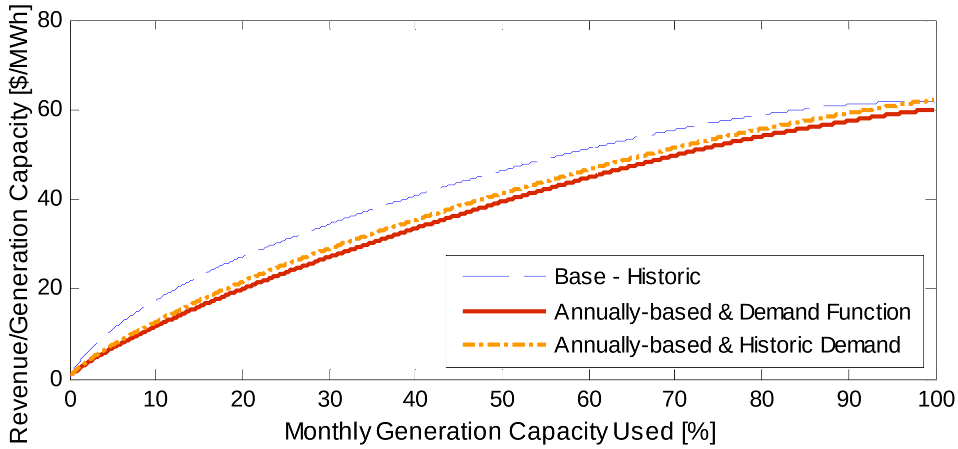

a) June

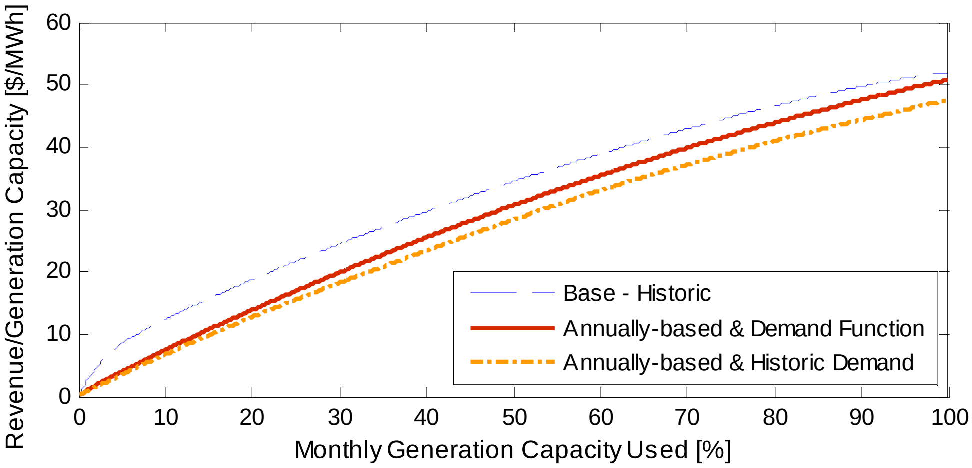

b) October

Figure 15 – Revenue curve comparison between two Annually-based ANN models fed with historical hourly demand data or with demand as a function of temperature estimated by Franco and Sanstad (2006) for June (a) and October (b)

6.4.2 Comparison of ANNs developed for different dataset breakdowns

Generally in a competitive energy market, hourly electricity price series contain multiple seasonalities such as, weekly and daily periodicities (Amjady and Hemmati, 2006). It is very hard for a single ANN to map correctly the input/output relationship of such a signal in all time periods (Amjady and Keynia, 2010b). In previous research, datasets have sometimes been partitioned along: periods of warm/cool days (e.g. Ranjbar et al. 2006), public holidays (e.g. Amjady and Keynia. 2010b), workdays/weekends (e.g. Gao et al., 2000) or stochastic components (e.g. Zhao et al., 2007). As part of the ANN calibration procedure, different data breakdowns have also been tried out in this work. A summary of the experiments and results obtained during training is given in Table 8; the results from the earlier sensitivity analysis detailed in 6.4.1 are not included. In the present section, common results to all experiments are first presented, then each experiment is discussed and compared to the others and finally two ANNs are elected for estimating future price representation.

6.4.2.1 General comments on the ANNs results

General observations and comments can be drawn from the application of an ANN to model electricity prices for the selected inputs in this research. The results from the calibration of the ANN model over the entire dataset are used here for illustrative purposes (cf. Figures 16-18) and apply to all the other ANN models developed during calibration. Figure 16 shows the frequency of historical prices and ANN output prices, Figure 17 the historical and ANN output prices against temperature and Figure 18 the hourly price time series for 2006 and 2008.

The ANN returns essentially prices in the range 25-100$/MWh; lower and higher prices are poorly modeled and no prices higher than 300$/MWh are returned (cf. Figure 16). The frequency of prices belonging to the range 25-100$/MWh is very similar to the historical price frequency as highlighted in Figure 16. This pattern is interesting as it reflects the ability of the ANN to reproduce the historical price frequency where most data are available; around 80% of the data belong to the range 25-100$/MWh. The ANN cannot however model the very high prices because they are too rare. ANNs learn better on the (frequent) average data than on the (rare) extreme intensities (Olsson et al., 2004).

Price intensities start increasing significantly when temperatures exceed 80°F (Figure 17) and the highest price intensities are returned by the ANN in summer (Figure 18). This result was expected as it corresponds to the high air conditioning demand during summer in California. High prices (over 100$/MWh) observed for middle range temperatures (40-80°F) are not modeled (cf. Figure 17). The inputs selected in this research are presumably not driving these high prices so this result seems reasonable. These high prices can be considered as price spikes which are highly erratic in competitive energy markets and difficult to model using ANNs (Zhao et al., 2007) as discussed earlier in Section 6.1.

From Figure 18, one can see that there is a sudden price drop observed in the middle of the year 2008. This was expected as a binary input was added to account for the specific conditions in the first half of 2008 (explained in Section 6.3.2.2).

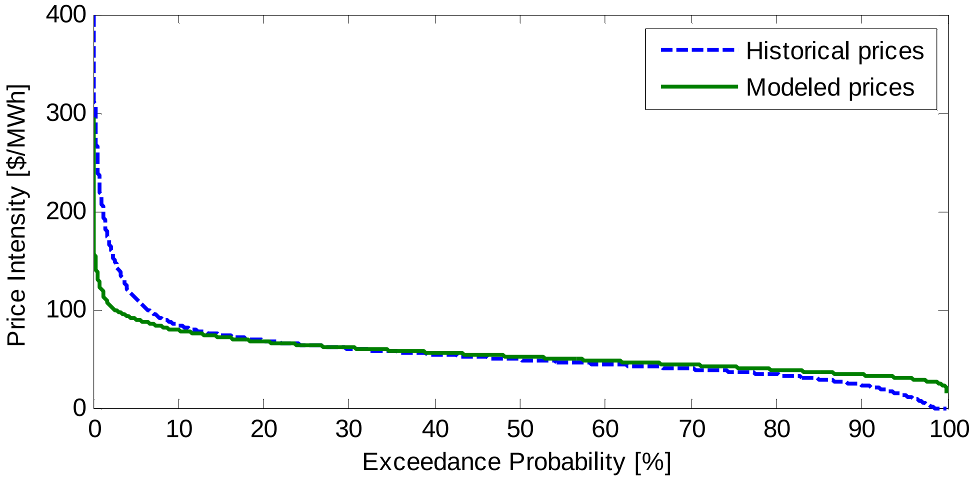

Figure 16 – Frequency of historical and modeled prices for an Annually-base ANN trained on all price ranges from 2005-2008

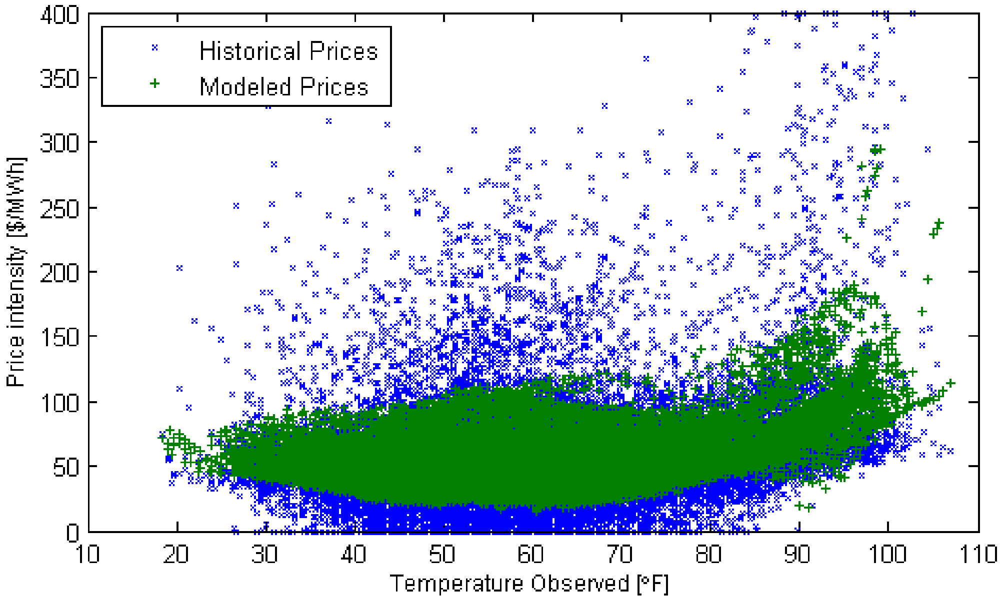

Figure 17 – Modeled prices for an Annually-based ANN trained on all price ranges (green +) and Historical prices (blue x) against temperature, 2005-2008

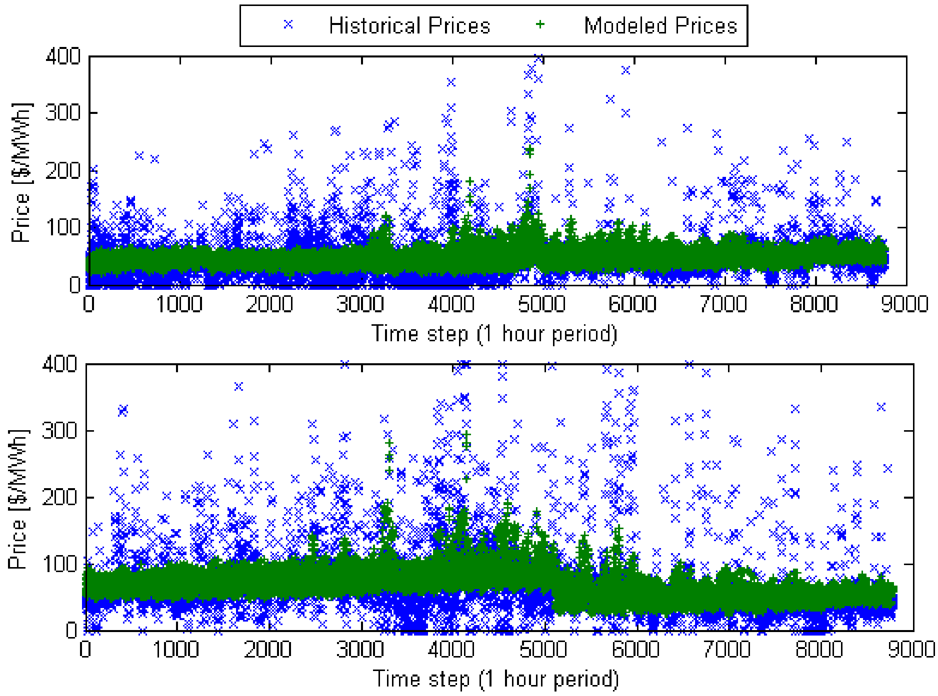

Figure 18 – Price time series for 2006 (top) and 2008 (bottom) for an Annually-based ANN model trained on all price ranges from 2005-2008 (green +), historical price (blue x)

6.4.2.2 Comparison of dataset breakdowns based on deterministic variables

Inspired by previous works, several dataset breakdowns have been considered during ANN calibration. For time-saving purposes, training was carried out only on parts of the dataset (e.g. for two hours of the day when an hourly-based data breakdown was considered). Based on the experimental results given in Table 8, further investigation was decided or not. The following data breakdowns were tried out and the range of R^2 and RMSE values obtained for the simulations are given in Table 7:

- Seasonally-based: Summer and Autumn
- Monthly-based: January, April and July
- Hourly-based: Hours 14 and 24
- Daily-based: Tuesday and Saturday
- Workdays- / Week-End-based
- Yearly-based: 2007

Table 7 - Range of R^2 and Root Mean Square Error (RMSE) values for different data breakdowns

Data breakdown	$R^2_{simulation}$	RMSE
Seasonally-based	0.22-0.43	0.126-0.145
Monthly-based	0.22-0.41	0.128-0.143
Hourly-based	0.25-0.26	0.125-0.150
Daily-based	0.24-0.36	0.116-0.142
Workdays- / Weekend-based	0.28-0.33	0.121-0.144
Yearly based	0.20	0.136

Table 8 - Summary of the results from ANN calibration for the data breakdowns experiments

Network architecture				Training algorithm			Results					
Price range - Dataset breakdown	**Inputs**	**Hidden layers**	**Hidden neurons**	**Activation function**	**Complex**	**Points per complex**	**Points per sub-complex**	R^2_{train}	R^2_{valid}	R^2_{test}	R^2_{sim}	**RMSE***
All	11	1	8	Tansig	8	51	50	0.30	0.24	0.27	0.28	0.140
January	9	1	8	Tansig	8	2*Npar+1	Npar+1	0.26	0.20	0.25	0.24	0.128
April	9	1	8	Tansig	8	2*Npar+1	Npar+1	0.42	0.33	0.39	0.39	0.143
July	9	1	8	Tansig	8	2*Npar+1	Npar+1	0,44	0,38	0,37	0,41	0,138
October	9	1	8	Tansig	8	2*Npar+1	Npar+1	0.25	0.20	0.18	0.22	0.132
Summer	10	1	8	Tansig	8	51	50	0.46	0.39	0.40	0.43	0.145
Autumn	10	1	8	Tansig	8	51	50	0.33	0.13	0.08	0.22	0.126
Hour 14	10	1	8	Tansig	8	2*Npar+1	Npar+1	0.30	0.24	0.20	0.25	0.150
Hour 24	10	1	8	Tansig	8	2*Npar+1	Npar+1	0.28	0.21	0.24	0.26	0.125
Tuesday	10	1	8	Tansig	8	2*Npar+1	Npar+1	0.28	0.24	0.17	0.24	0.142
Saturday	10	1	8	Tansig	8	2*Npar+1	Npar+1	0.41	0.24	0.33	0.36	0.116
WE-based	10	1	8	Tansig	8	51	50	0.38	0.27	0.30	0.33	0.121
Workdays-based	10	1	8	Tansig	8	51	50	0.29	0.25	0.28	0.28	0.144
Year 2007	11	1	8	Tansig	8	2*Npar+1	Npar+1	0.22	0.16	0.20	0.20	0.136
‘Normal prices’	11	1	8	Tansig	8	51	50	0.39	0.37	0.38	0.38	0.079
‘Medium prices’	11	1	8	Tansig	8	51	50	0.36	0.36	0.34	0.36	0.069
‘Low prices’	11	1	8	Tansig	8	51	50	0.10	0.09	0.04	0.08	0.035
‘High prices’	11	1	8	Tansig	8	51	50	0.17	0.15	0.15	0.16	0.249

*RMSE: Root Mean Square Error

The different data breakdowns are compared in the next paragraphs.

Hourly-based & Daily-based models

The hourly-based model was discarded from further analysis because it has a low $R^2_{\text{simulation}}$ range value and average RMSE value.

The correlation range for the daily-based model simulations is $R^2_{\text{simulation}} = 0.24 - 0.36$ and for the workdays-/ weekends- based model $R^2_{\text{simulation}} = 0.28 - 0.33$. The partition between workdays and weekends, requiring only two individual models, was preferred to a daily data breakdown and the daily-based models were abandoned. The division between weekends and workdays has already been used for short-term price forecasting (e.g. Gao et al., 2000) and will be assessed in detail later.

Hourly- and daily-based models have not been assessed based on other performance criteria (e.g. frequency distribution) because it would require building each individual models to extract monthly patterns and was considered too time consuming.

Yearly-based

The model developed for year 2007 has the lowest determination coefficient among all experiments with $R^2_{\text{simulation}} = 0.20$ and its RMSE value is not significantly reduced compared to the model built for all four years data. Figure 19 is a comparison of the revenue curves between this model and the model using the entire dataset for the months of June and December. Generally, monthly revenue curves developed for 2007's model are further away from the historical data (or do not have a significantly better fit) than the model using the four years of data. It was therefore decided to exclude the yearly-based model from further analysis.

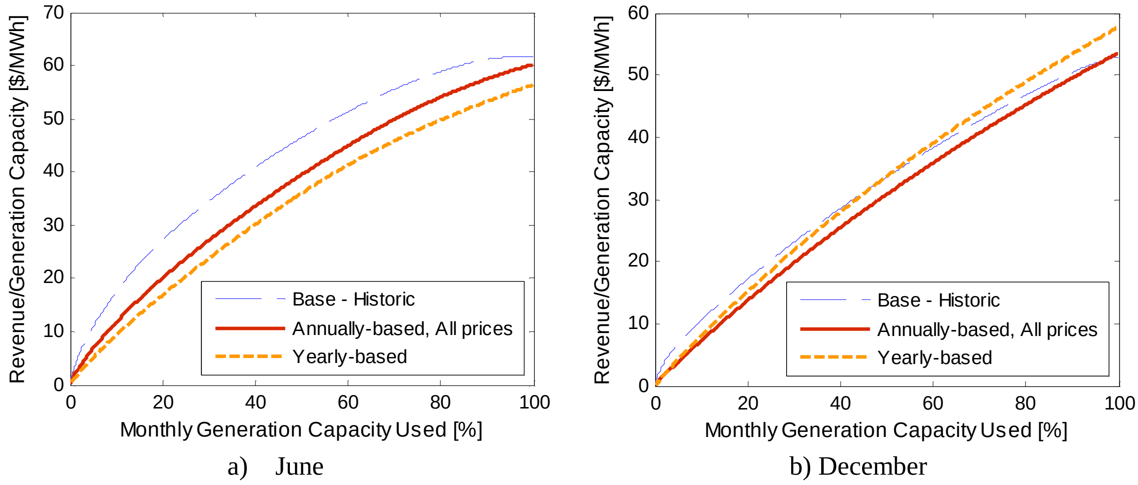

Figure 19 - Comparison of the revenue curves for Yearly-based ANN model calibrated on 2007's data and an Annually-based ANN calibrated on all data for June (a) and December (b)

Monthly-based, Seasonally-based, Workdays/WE- based

Figure 20 is a comparison of April's and July's revenue curves for four ANN models: seasonally-based, monthly-based, workday- and weekend-based models combined in parallel and Base model using all data. The best fit for the revenue curves can be observed for monthly-based models and summer model. The workdays/weekends-based model produced a better fit than the Base model for most months. It was decided to keep only one model for the next steps of this research and the monthly-based models were elected for the following reasons:

- Generally, those produced the best fit for the revenue curves and especially for the month of April where the other data partitions didn't fit so good;
- this partition seemed the most appropriate to capture the monthly variability of prices which is of interest in this research.
- $R^2_{\text{simulation}} = 0.22 - 0.41$ and RMSE=0.13-0.14 are among the best errors from the experiments together with the seasonal models;

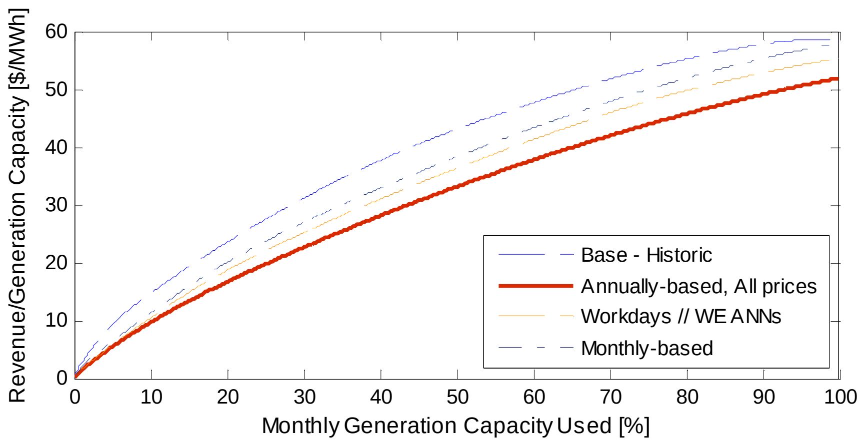

a) April

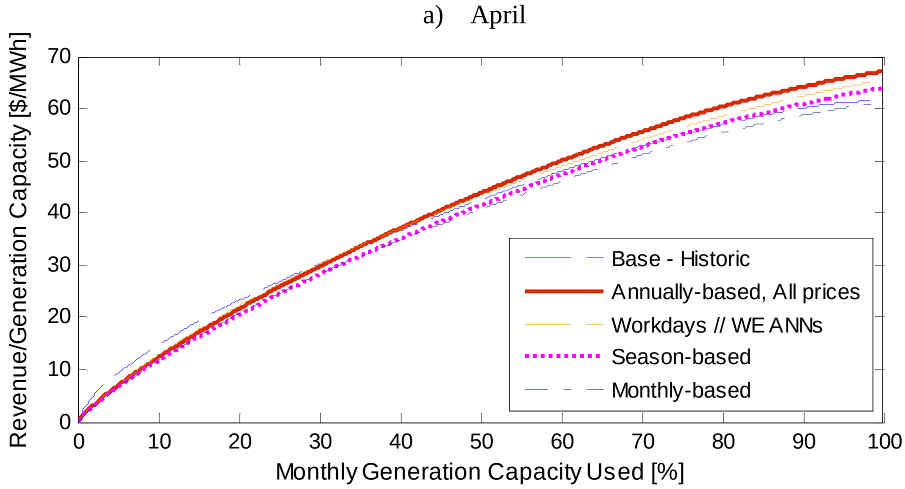

b) July

Figure 20 - Revenue curves for four ANN models: Base (calibrated on all data), workday and weekend-based models combined in parallel, Seasonally-based and Monthly-based models for April (a) and July (b)

6.4.2.3 Comparison of dataset breakdowns based on stochastic variables

Additional dataset breakdowns have been tried out. The motivations for the partitions considered are presented in this section and their implementation is detailed after.

The first partition was inspired by an experiment made by Olsson et al. (2004) for rainfall intensity classification. They have firstly divided their dataset in different categories based on rainfall intensity. Then they tried to use a stratified sample for ANN calibration, designed to contain an identical number of intensities in each category. This may improve the ANN training as the learning capacity of ANNs is commensurate with the quantity of data available (Olsson et al., 2004). This method was tried out in the present research as previous experiments haven't been able to capture low price intensities (below 25$/MWh) and high prices (above 125$/MWh). In light of these results, a non representative subsample designed to contain a similar number of price intensities in predefined price ranges was extracted.

The two following experiments were inspired by the work from Lu et al. (2005) and Zhao et al. (2007) who spotlighted the fact that ANNs were unable to model price spikes because of they are highly erratic, several orders of magnitude higher than the average price, often under-represented compared to normal prices and most likely not driven by the inputs selected in the present work. With respect to the use of ANN models, this is a delicate issue. ANNs are trained better on the range of intensities that is the most frequent in the calibration set (Olsson et al., 2004). Therefore, scattered outliers will be poorly modeled. According to Lu et al. (2005), almost all the existing techniques for short-term price forecasting require filtering out the price spike signals in order to forecast normal prices with rather high accuracy.

As defined by Lu et al. (2005) high price spikes are prices exceeding the threshold P_v:

$$P_v = \mu \pm 2\delta \qquad \textbf{(1)}$$

where μ is the mean of historical market price and δ is the standard deviation of the prices. In the present case study, price spikes correspond to prices exceeding 128$/MWh, including 3.7% of the price population (or 1191 data) and representing 12.9% of cumulated price intensities. Many high intensity prices happened in 2008 but probably aren't really price spikes as these resulted from a global increase in electricity prices. Their intensity is still 'abnormally' high so it was decided to make no distinction between those and other price spikes. Very few price spikes seemed to have occurred in 2005 but this is partly because four months of data were removed. Most spikes occurred in spring and summer.

Based on the previous comments, the following data partitions have been considered:

- Stratified dataset considering five price ranges.
- Division of the set between 'Normal prices' (below the threshold P_v) and price spikes.
- Division of the set between 'Low prices' (including the 10% lowest price intensities), 'Medium prices' (prices between Low prices and the threshold P_v) and Price spikes.

Stratified dataset breakdown

Five categories of prices p (given in [$/MWh]) were defined on the basis of the cumulative distribution of prices: $0 < p \leq 25$, $25 < p \leq 50$, $50 < p \leq 75$, $75 < p \leq 100$, $100 < p$. Each category contained 1000 data samples, giving a total of 5000 data samples, 15% of the original dataset. Then the set was divided into training, test and validation set as usual for calibration. The optimized ANN for 8 hidden neurons gave $R^2_{training} = 0.29$ and $R^2_{simulation} = 0.28$.

Figure 21 shows the prices plotted against temperature. Prices below 20$/MWh are still not captured and prices above 150$/MWh either. Visually, the agreement between historical and modeled prices is not improved for high temperatures compared to the earlier models, e.g. the Annually-based model calibrated on all prices. This ANN model calibrated on a stratified sample was abandoned as it did not capture the low and high prices as wished.

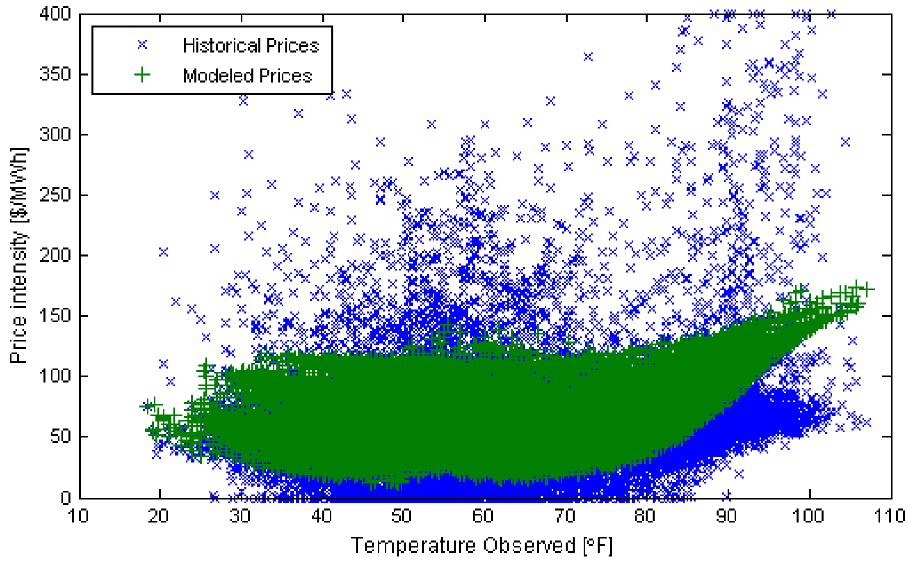

Figure 21 – Price obtained from the ANN trained over a stratified sample (2005-2008) against temperature

'Normal prices' model

The correlations obtained from the 'normal price' model are very much improved compared to the ANN developed for the entire dataset. The simulation for the optimal parameters gives $R^2_{simulation} = 0.38$ and RMSE = 0.08 (compared to $R^2_{simulation} = 0.28$ and RMSE = 0.14 for the Annually-based ANN trained over all prices). Figure 22 shows the prices plotted against temperature. Prices below 20$/MWh and above 90$/MWh are still not modeled properly. Too few data belong to these ranges compared to the quantity of data available in the interval 20-90$/MWh to be modeled adequately by the ANN. This observation conducted to the next experiment considering a division between Low, Medium and Price spikes.

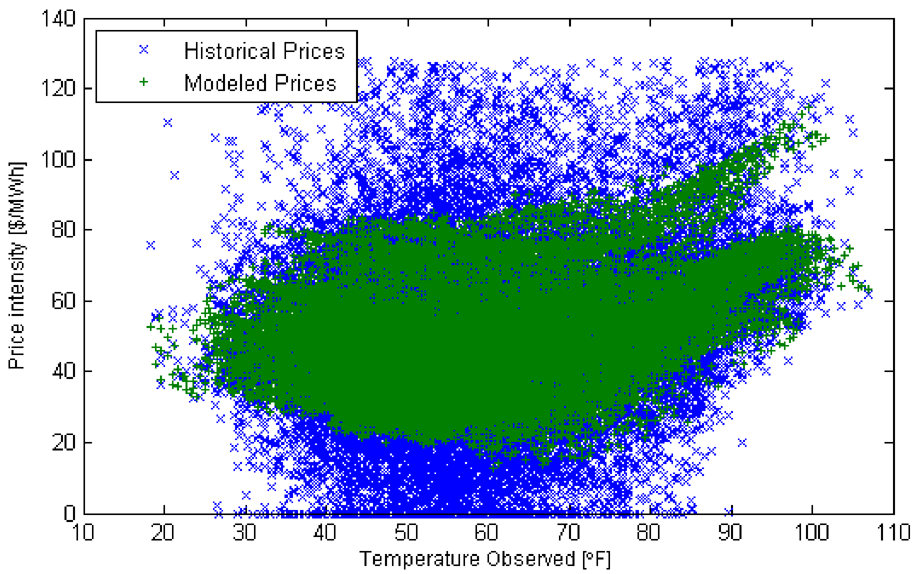

Figure 22 – Prices from an ANN model trained over 'normal' prices (below 128 $/MWh) against temperature (2005-2008)

A second ANN was developed for the set of price spikes. As expected these could not be modeled accurately because there are too few data (1191 data samples), the spikes are very volatile and they are probably not driven by the selected inputs. No further investigation to model price spikes was carried out as it is beyond the scope of this work. Further research could consider applying a 'damping scheme' as proposed by Yamin et al. (2004) or by a similar reasoning.

Price spikes represent only 3.7% of the price population but their summed intensities reach nearly 13% of the total. Two options were foreseeable to deal with price spikes: considering that a certain percentage of price spikes will occur in the future or that there won't be any more spikes. This depends on how the energy market is projected to evolve. Lu et al. (2005) spotlighted the fact that in an ideal competitive electricity market, price spikes should only occur when the demand exceeds the supply. However, most markets are not ideally competitive, and gaming behaviors probably influence the market (Lu et al., 2005). It has also been argued that suppliers take advantage of the vulnerability (difficulty of storing, generation capacity constraints and transmission congestion) of the electricity market by withholding their capacity so as to shift supply-demand curves and forcing price spikes (Zhao et al., 2007). Therefore, if the market operation is foreseen to stay as it is today – which is the assumption we make in the present work – then price spikes should be kept unimpaired as they will most likely continue to occur. If the market is envisaged to turn towards an 'ideal' competitive market or maybe towards a highly supervised market preventing spikes to occur, then spikes should be removed. The percentage of energy spikes in the future is assumed to be the same as in the base case. Unimpaired price spikes were added to the modeled price set and Figure 23 shows the revenue curves for the models calibrated on all prices or on normal prices for June and September. The model developed for 'normal prices' fits better historical data.

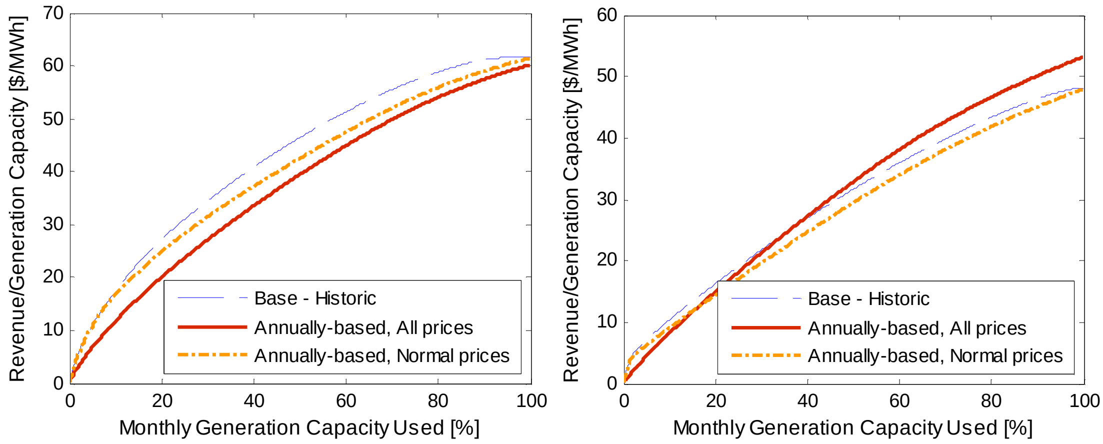

a) June b) September

Figure 23 - Comparison of the revenue curves for two Annually-based ANN models: one trained on all prices and on 'normal prices' (price spikes truncated) for June (a) and September (b). The historic proportion of price spikes in the market was assumed to remain constant for the second model.

<u>'Medium prices' and 'Low prices' models</u>

Figure 24 displays the plot of prices vs. temperature for the medium range prices which gives $R^2_{simulation}$ = 0.36 and RMSE = 0.07 (compared to $R^2_{simulation}$ = 0.38 and RMSE = 0.08 for the 'normal prices'). Surprisingly, these results are not far off from the results obtained for normal prices and the correlation in terms of R^2 value is even lower. The same price trend as for 'normal' prices is observed except that the lower bound of the modeled prices is now higher, around 35$/MWh. Truncating the 10% low prices did not help the ANN to reproduce the low range of the calibration set and increased the price set's average. ANNs usually return outputs where most data are available (Olsson et al., 2004); this may be at the origin of this phenomenon, otherwise no other explanation has been found out to explain this trend.

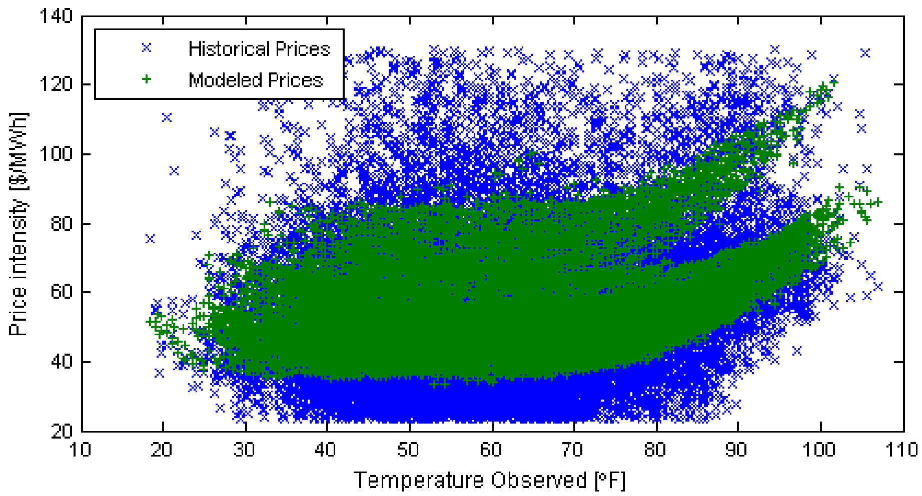

Figure 24 - Prices from an ANN model trained over 'medium' prices (between 22 and 128 $/MWh) against temperature (2005-2008)

The second model developed for the set of the 10% lowest values returned prices mostly around the average of the calibration set (cf. Figure 25) and the correlation is low, $R^2_{simulation} = 0.08$. It is hard to assess if the ANN returned the prices follow an underlying relationship; this dataset breakdown was abandoned.

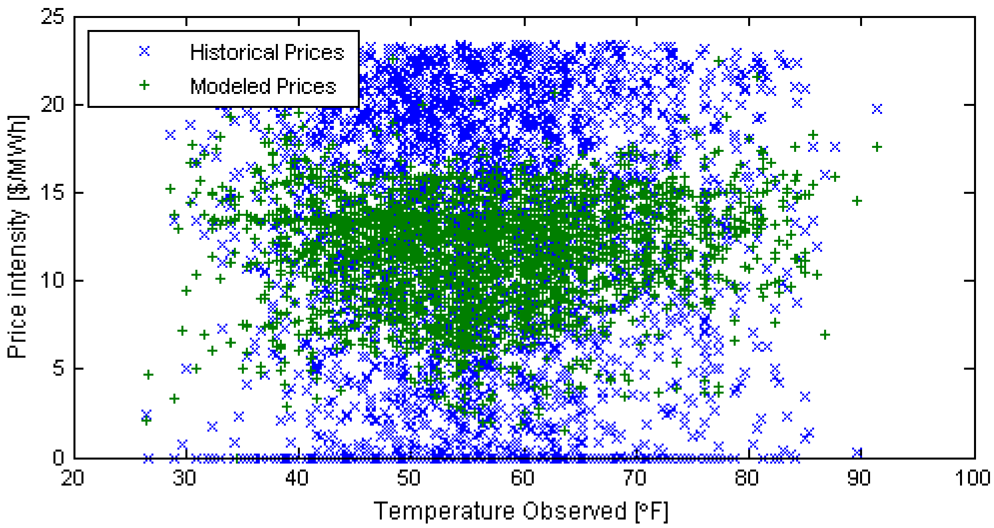

Figure 25 - Modeled and historical prices against temperature, low range, 2005-2008

6.4.3 Summary of the findings and choice of the optimum ANNs

Among all the dataset breakdowns tried out in this research, two divisions stand out:

- Monthly-based models (ANN1)
- Annually-based model calibrated on Normal price i.e. excluding price spikes (ANN2)

Monthly models were elected because they visually fit well historical patterns and seem appropriate to capture the monthly variability of energy prices. The annual model trained for normal prices improves the determination coefficient but requires filtering out the spikes, assuming that all prices over a certain range are non natural price spikes. The same proportion of spikes as for the period 2005-2008 was assumed to occur in the future.

The two models are compared hereafter in terms of monthly price frequency distribution using revenue curves. The visual agreement between the revenue curves for January, April and July (cf. Figure 26) is very similar between the two models and historical data; April is the only month of the year for which the curves have a significant different pattern.

Two models were kept because it is not possible to know which one is the most accurate.

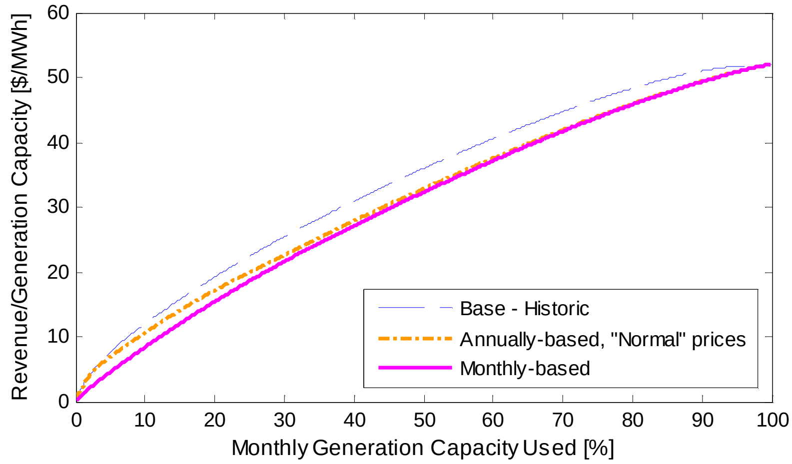

a) January

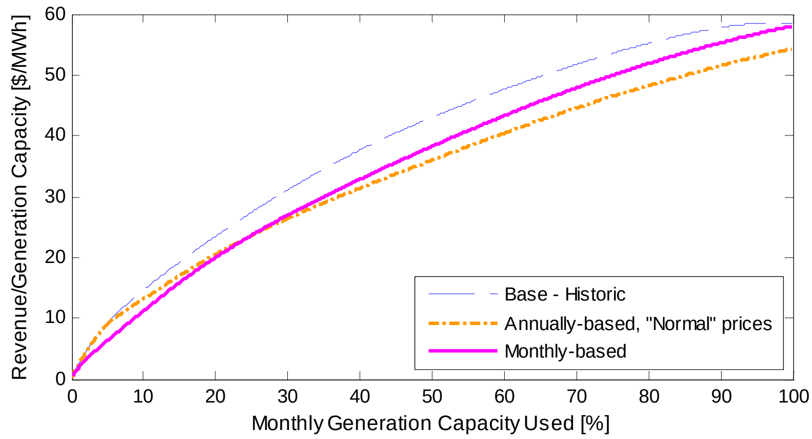

b) April

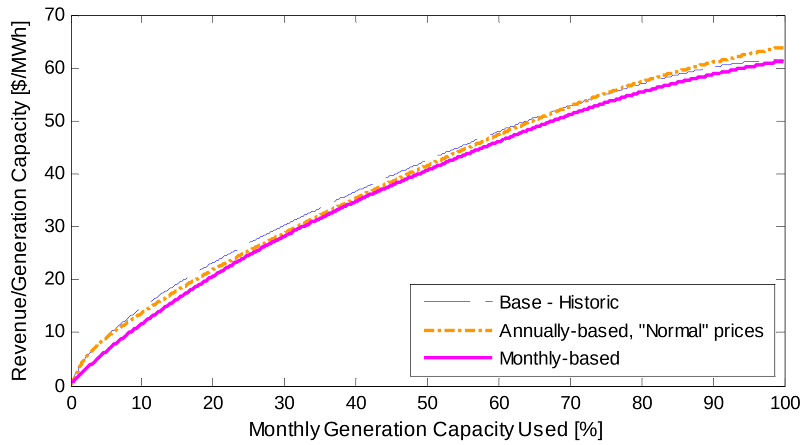

c) July

Figure 26 - Comparison of the revenue curves for the monthly based ANNs and the annually-based ANN calibrated on 'normal prices' (price spikes truncated) for January (a), April (b) and July (c)

6.5 Application of ANN to long-term price forecasting

6.5.1 Climate warming scenarios

The impacts of climate warming by 2100 on hourly electricity prices were estimated based on five scenarios given in Table 9 and adapted from the simulations of twenty-first century climates evaluated by Cayan et al. (2008). A strong assumption was made: the statewide temperature increase considered here is the average of the temperature increases for the two regions NOCAL and SOCAL estimated by Cayan et al. (2008); NOCAL corresponds to Sacramento region whereas SOCAL to the area around Riverside. This average value was considered to be representative of the highly electricity demanding areas, i.e. the highly-populated areas in California which are of interest in this work. Another assumption is that the increase estimated by Cayan et al. (2008) is based on mean values for the historical period (1961-1990) and that we consider the increase based on mean values for (2005-2008).

Four scenarios consider a constant temperature increase throughout the year and one high forcing scenario (GFDL-A2-Seasonal) considers a higher increase in summer and a lower increase in winter respectively, than in the rest of the year. As no more information was gathered about the temperature increases in spring and autumn, these values were assumed to be equal to the average annual temperature increase.

Table 9 - Climate Change Scenarios for California (adapted from Cayan et al. (2008))

			2070-2099 Temperature Change (°F) [1 2]		
Scenario Name	GCM	SRES	Winter (DJF)	Summer (JJA)	Spring (MAM) & Autumn (SON)
GFDL-A2-Annual	GFDL	A2	+8,0	+8,0	+8,0
PCM-A2-Annual	PCM	A2	+4,6	+4,6	+4,6
GFDL-B1-Annual	GFDL	B1	+4,9	+4,9	+4,9
PCM-B1-Annual	PCM	B1	+2,8	+2,8	+2,8
GFDL-A2-Seasonal	GFDL	A2	+6,0	+10,5	+8,0

[1] Values from two regions referred to as Nocal and Socal (North and South California) were averaged to produce an average considered to be representative for entire California.
[2] Temperature change in Spring and Autumn was assumed to be equal to the average annual temperature change

6.5.2 Results

Results for each climate warming scenarios and ANN model are presented in Table 10. The forecasted average price for all climate warming scenarios are always exceeding the base case average price (55 $/MWh). Monthly ANNs (ANN1) predict higher average price increases than the Annual ANN model trained on Normal prices for all scenarios; i.e. ANN1 estimates higher price increases than ANN2.

Table 10 – Price distribution statistics for each climate warming scenario & ANN model

Climate scenario	ANN model	Prices in $/MWh Average	Standard Deviation	Minimum	Maximum	Price Percentiles in $/MWh 10th	25th	50th	75th	90th
Base Case	-	54.87	36.54	0.00	399.99	23.88	36.88	49.13	64.14	84.28
GFDL-A2-Annual	ANN1	59.89	33.16	0.00	425.66	30.78	41.04	51.73	70.20	96.15
	ANN2	55.96	33.04	9.00	399.99	31.13	40.58	49.31	61.95	76.11
PCM-A2-Annual	ANN1	56.94	27.51	0.00	392.77	31.11	40.64	50.91	66.91	88.49
	ANN2	55.25	32.74	9.76	399.99	31.31	40.20	49.02	60.11	74.98
GFDL-A2-Seasonal	ANN1	61.55	35.28	0.00	425.66	31.20	41.69	52.38	71.93	99.75
	ANN2	56.67	33.07	9.00	399.99	31.64	41.15	49.87	63.24	76.89
PCM-B1-Annual	ANN1	55.82	25.09	0.00	384.30	31.42	40.55	50.64	65.44	85.00
	ANN2	55.03	32.57	10.73	399.99	31.67	40.24	48.98	48.98	74.42
GFDL-B1-Annual	ANN1	57.15	27.95	0.00	388.50	31.11	40.67	50.93	67.11	89.09
	ANN2	55.30	32.76	9.62	399.99	31.27	40.20	49.04	60.24	75.04

Figure 27 shows the forecasted price intensities against temperature for climate warming scenario PCM-A2-Annual for both ANN models chosen. Figure 28 is the same figure for scenario GFDL-A2-Annual. Prices increase for all scenarios for the highest temperatures relative to historical prices; high forcing scenarios lead to high price increases and low forcing scenarios to lower price increases.

Revenue curves for one month from each season (January, April, July, October) were plotted for climate scenarios GFDL-A2-Annual and PCM-A2-Annual in Figure 29 and Figure 30 for ANN1 and ANN2 respectively. For both ANN models, all climate warming scenarios lead to high increases in revenues in summer months, and more attenuated increases in spring and autumn. In winter, high forcing scenarios lead to higher price drops relative to Base case if compared to low forcing scenarios. These patterns correspond to what was expected, increased need for cooling in warm months and decreased need for heating in winter months. For all climate scenarios, the ANN2 returns similar revenue curves in April. April is the transition month between winter and spring seasons, so energy price patterns might be different between years and it is difficult for the ANN to learn the input-output relationship.

The lower increases in revenue using an Annually-based ANN compared to those using Monthly based ANNs probably result from the time scale of the ANN models. In the case of an Annual model, temperature data samples from all twelve months of the year are fed to the ANN during calibration and the trained ANN has knowledge of all historical temperature ranges. Most perturbed temperature samples for climate warming scenarios will not be out of range of the calibration temperature range, except for the extreme highest temperature. Monthly-based models use a monthly calibration set; they are independent from each other and have no knowledge of the price-temperature relationship mapped in other months. The highest perturbed temperatures accounting for CC of each monthly calibration set will be unknown by the corresponding ANN, but might be known by other monthly ANN models. Monthly models might overestimate future price intensities. For illustrative purposes, Figure 31 shows the price distribution against temperature from the Monthly- based and Annually-based ANN models under GFDL-A2-Annual scenario in March. The Monthly model estimates very high price increases for the highest temperatures experienced in that month (T>95ºF) whereas the Annual model estimates more moderate price increases, which seem more reasonable. Historically, this temperature range was experienced in other months of the year, in spring for example, and was not responsible for such high prices. Having no knowledge of the rest of the year, Monthly-based ANNs might misestimate the input-output relationship and an Annual model (or seasonal) may be more appropriate to deal with perturbed temperatures.

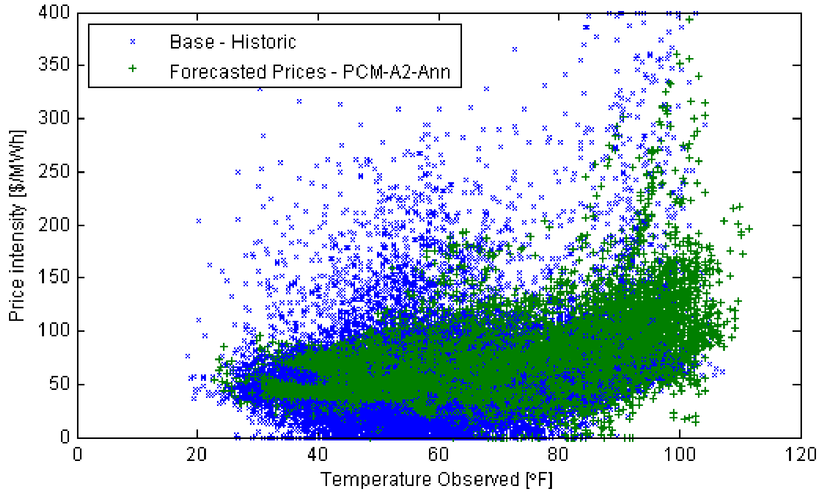

a) Monthly-based ANN (ANN1)

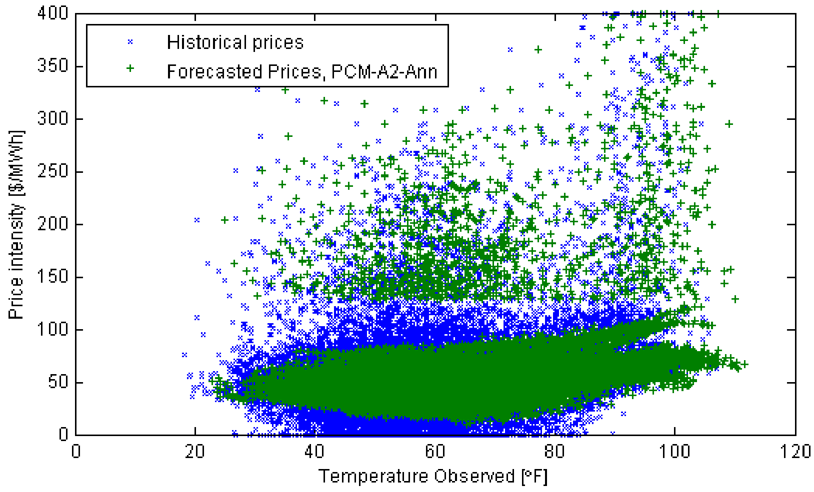

b) Annually-based ANN, Normal prices (ANN2)

Figure 27 - Simulated ANN prices and historical prices (2005-2008) for PCM-A2-Annual climate warming scenario for both ANN models: ANN1 (a) and ANN2 (b)

Another possible reason for the lower increases in revenue estimated by the Annual ANN model is also based on the fact that an ANN model learns from examples which are fed during the training procedure. Since this model was trained only for normal prices, it will not return prices much higher than the ones fed during training. In the first experiment (monthly models for all prices range), since price spikes were not removed, the ANN will more likely return high price intensities.

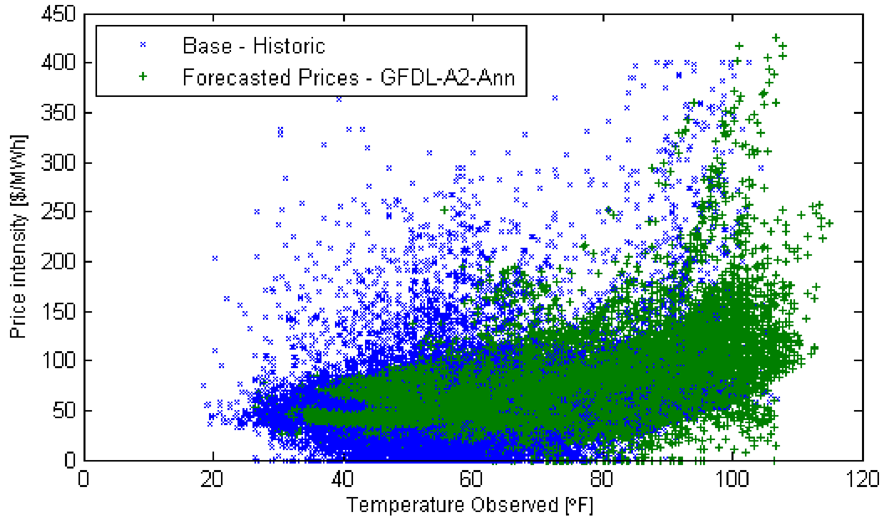

a) Monthly-based ANN (ANN1)

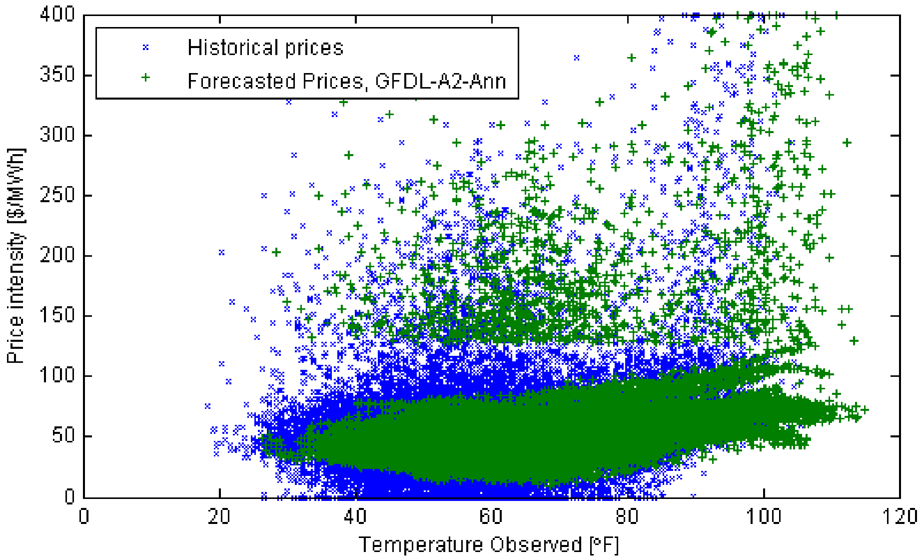

b) Annually-based ANN trained on Normal prices, i.e. price spikes removed from training dataset (ANN2)

Figure 28 - Simulated ANN prices and historical prices (2005-2008) for GFDL-A2-Annual climate warming scenario for both ANN models: ANN1 (a) and ANN2 (b)

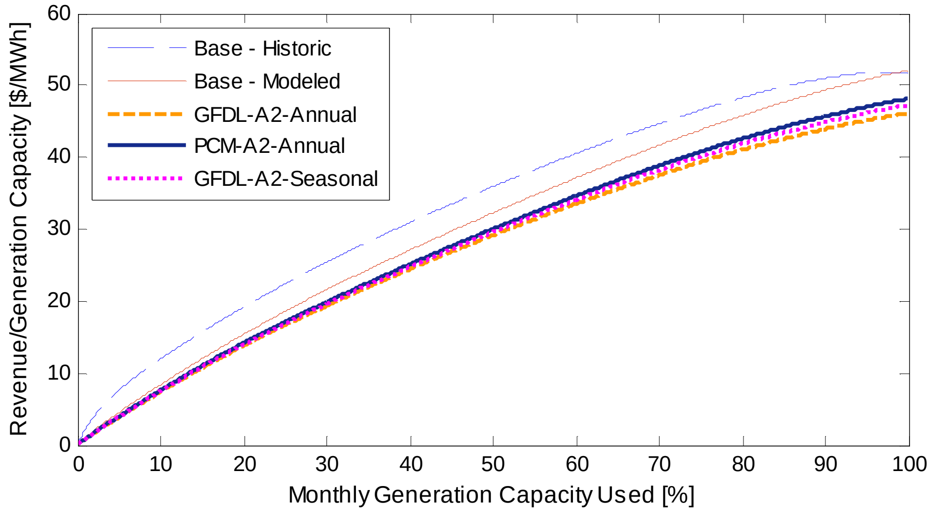

a) January

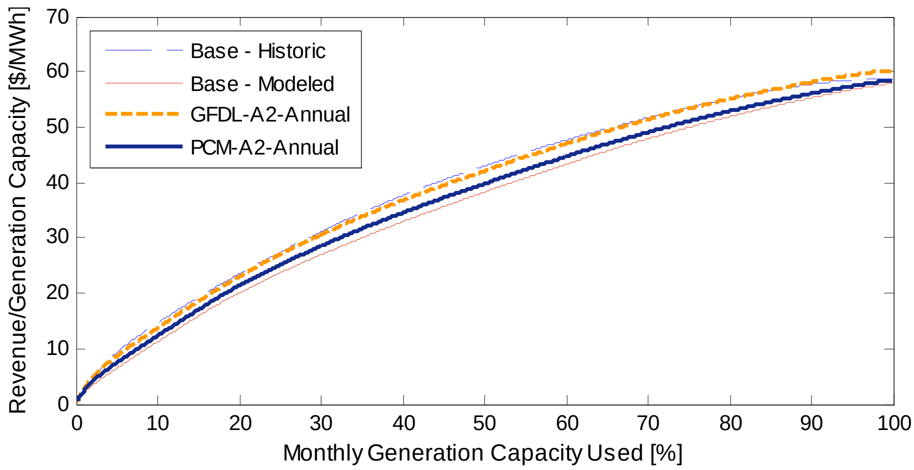

b) April

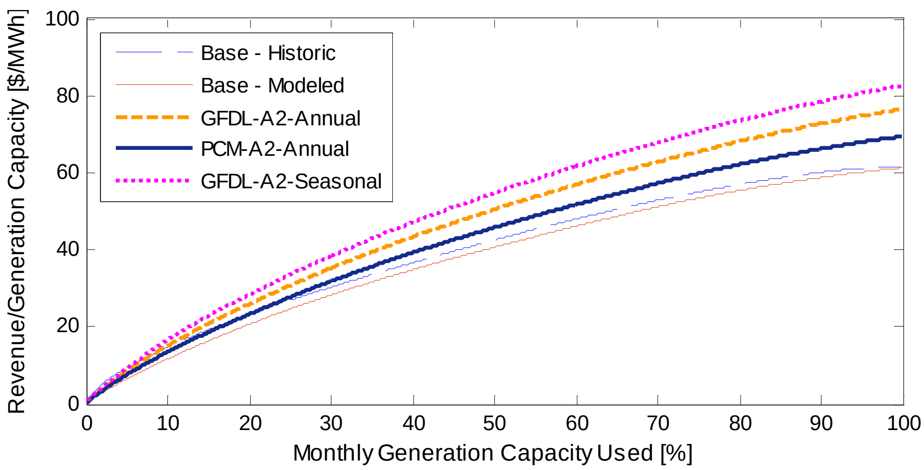

c) July

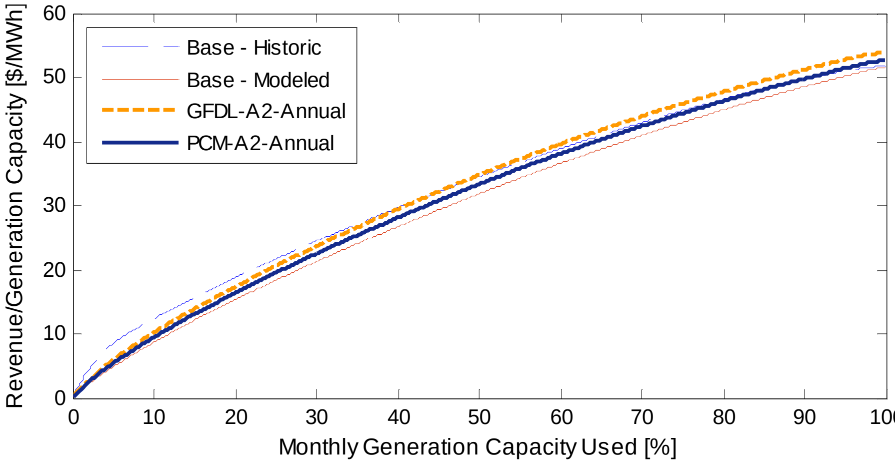

d) October

Figure 29 - Monthly Revenue Curves obtained from ANN1 model for January (a), April (b), July (c) and October (d) for different climate warming scenarios

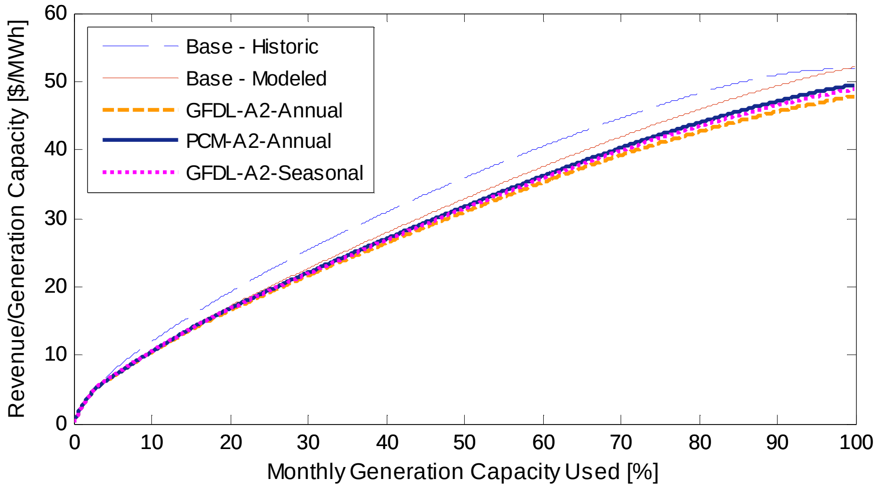

a) January

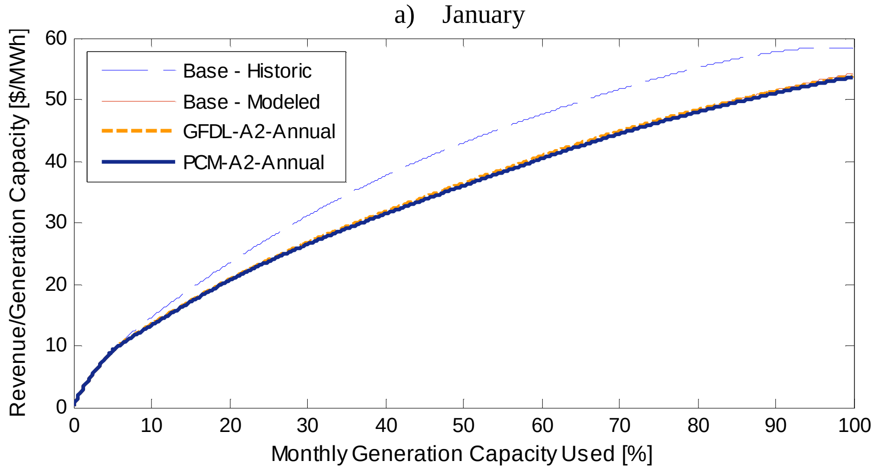

b) April

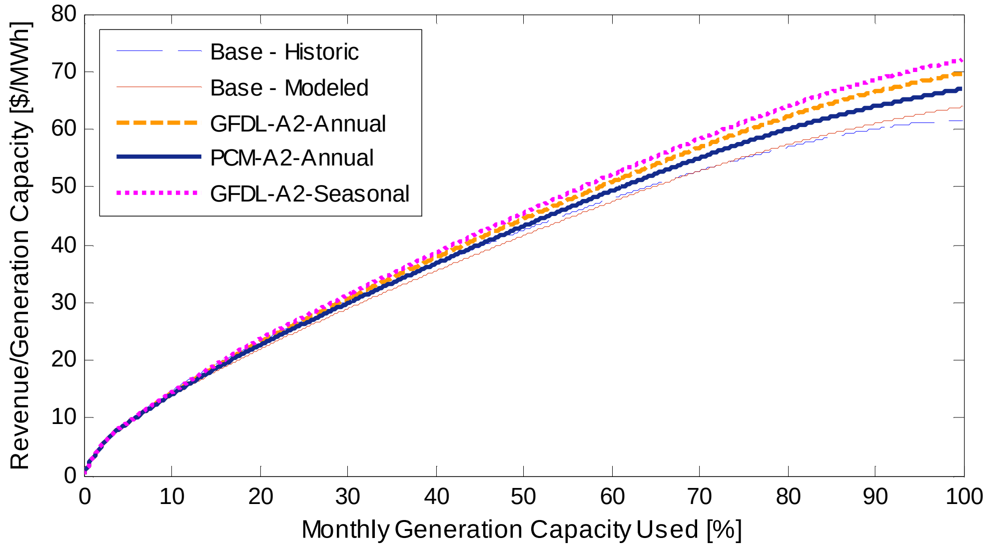

c) July

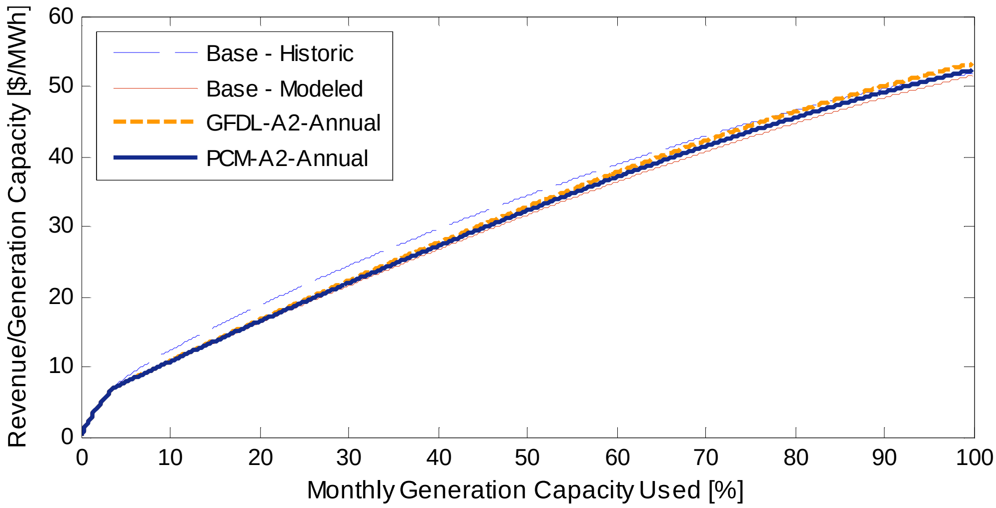

d) October

Figure 30 - Monthly Revenue Curves obtained from ANN2 model, for January (a), April (b), July (c) and October (d) for different climate warming scenarios (it is assumed that the same proportion of price spikes as in the 2005-2008 historical price set occur in the future under climate change scenarios)

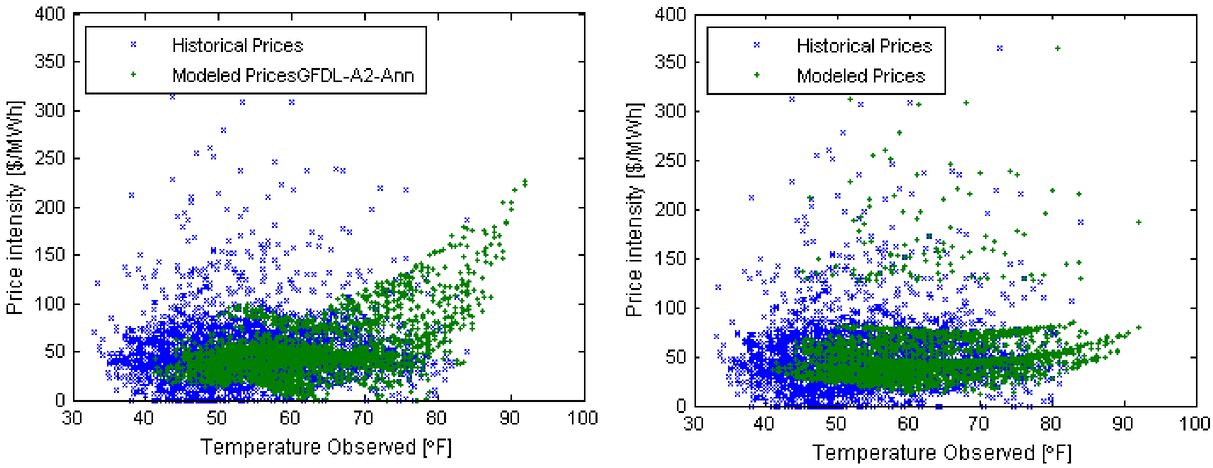

a) Monthly-based ANN (ANN1) b) Annually-based ANN, Normal prices (ANN2)

Figure 31 – Results from ANN1 (a) and ANN2 (b) for GFDL-A2-Annual climate warming scenario in March. Historical prices (blue x), Modeled prices (green +)

7 Energy-Based Hydropower Optimization Model

7.1 Model set up

This study investigates the effects of climate change on California's high-elevation hydropower plants using the Energy-Based Hydropower Optimization Model (EBHOM) developed by Madani and Lund (2009). EBHOM is a monthly step model which does all storage, release and flow calculations in energy units (Madani and Lund, 2009). It gives a big picture of the system and is an interesting alternative to conventional volume-based optimization models that usually require detailed information such as streamflows, turbine capacities, storage operating capacities and energy storage capacities at each individual plant of the system.

The flow chart of the EBHOM modeling process is given in Figure 32. The reader is referred to Madani and Lund (2009) for details on EBHOM's mathematical formulation. The input data required to run EBHOM are: runoff data, available storage capacity at each power plant, frequency of hourly electricity prices for each month of the year. Runoff data representative of three elevation ranges (1000-2000, 2000-3000 and >3000 feet) were gathered from several US Geological Survey (USGS) gauges as described in Madani and Lund (2009). Three elevation bands were chosen to take into account the different value of the snowpack and precipitation in each band. Monthly runoff distributions in each range were then perturbed using monthly runoff perturbation ratios of the adopted climate change scenarios as described by Vicuna et al. (2008). A perturbation ratio is "a simple ratio of average runoff predicted by a GCM for different eras for a given time period (eg. $Q_{2070–99}$/ $Q_{1960–90}$, where Q is average July streamflow)" (Vicuna et al., 2008). Madani and Lund (in press) finally adjusted these ratios at each elevation band as follow: dry and wet climate warming scenarios result in 20% less and 10% more annual runoff when going up one band, respectively.

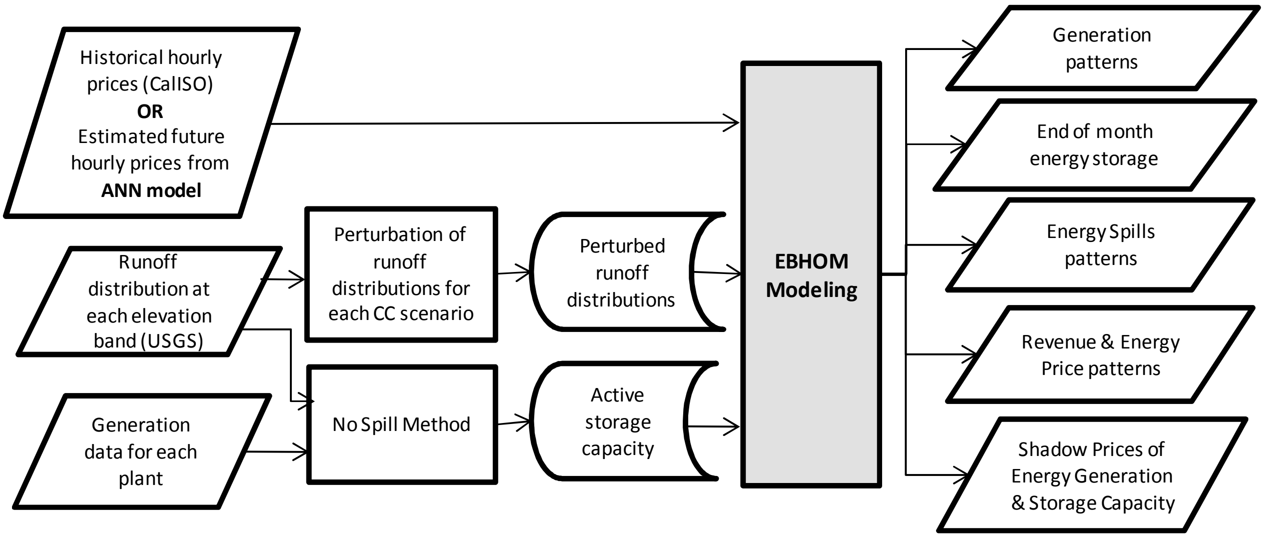

Figure 32 - Flow chart of EBHOM model

The available energy storage capacity at each power plant is determined using the No Spill Method (NSM) developed by Madani and Lund (2009), applicable when: plants are operated for net revenue maximization, storage volumes do not significantly affect the head and there is no over-year storage. These conditions are filled by California's high-elevation hydropower system (Madani and Lund, 2009).

The price representation used to run is either historical prices or forecasted prices from the earlier ANNs developed. Revenue curves were drawn by integration over the price frequency curves for each month and were then piecewise linearized into five segments to solve EBHOM through linear programming (Madani and Lund, 2009).

7.2 Climate warming and Price Increase Scenarios

The scenarios elected to run EBHOM are summarized in Table 11. A Dry warming GFDL-A2) and a Wet warming (PCM-A2) were chosen to be consistent with the previous research of Madani and Lund (in press). An additional Seasonal Dry warming scenario considering high temperature increases in summer and low temperature increases in winter was chosen. For each climate scenario, EBHOM was run under Historical price or price forecasts from either the Monthly-based ANN model (ANN1) or the Annually-based ANN model (ANN2). Running EBHOM based on price forecasts considers the changes in energy demand due to climate warming.

Two price increase scenarios (+30% or +100% by 2100) were defined. Inspired by the work from Aroonruengsawat and Auffhammer (2009), the first scenario assumes a discrete price increase of 30% by 2020 remaining to the same level until the end of the century. The second scenario is based on the historical trend of average retail prices in California described in section 3. A constant annual growth rate of 0.25 cents/KWh (calculated for the period 1960-2005, cf. Figure 4) results in retail prices increase by 100% by 2100. Each price increase scenarios is then coupled to each climate warming scenario, run under historical prices and the two ANN price models.

Table 11 – Scenarios defined to run EBHOM, including 4 climate scenarios and 3 price models. Additional scenarios were designed by coupling two pure price increase scenarios (+30%, +100%) to the scenarios in this Table.

<table>
<tr><th>Scenario Accronym</th><th>CC Scenario</th><th>Price Model</th><th>Price Increase</th></tr>
<tr><td>Base</td><td>Base Case</td><td rowspan="3">None: Historical prices</td><td rowspan="11">±0%</td></tr>
<tr><td>Dry</td><td>GFDL-A2-Annual</td></tr>
<tr><td>Wet</td><td>PCM-A2-Annual</td></tr>
<tr><td>Base ANN1</td><td>Base Case</td><td rowspan="4">ANN1: Monthly ANNs</td></tr>
<tr><td>Dry ANN1</td><td>GFDL-A2-Annual</td></tr>
<tr><td>Dry-Seas ANN1</td><td>GFDL-A2-Seasonal</td></tr>
<tr><td>Wet ANN1</td><td>PCM-A2-Annual</td></tr>
<tr><td>Base ANN2</td><td>Base Case</td><td rowspan="4">ANN2: Annual ANN for Normal Prices</td></tr>
<tr><td>Dry ANN2</td><td>GFDL-A2-Annual</td></tr>
<tr><td>Dry-Seas ANN2</td><td>GFDL-A2-Seasonal</td></tr>
<tr><td>Wet ANN2</td><td>PCM-A2-Annual</td></tr>
</table>

7.3 Results

7.3.1 Historical prices and climate change impact on hydrology only

EBHOM's results for 1985-1998 hydrologic conditions and 2005-2008 historical price dataset are presented here. Table 12 indicates how energy generation, energy spill and annual energy revenue change with Dry and Wet climate scenarios as well as the Base case scenario. In the present section, results are discussed and compared to those obtained by Madani and Lund (in press), who did the same study but with a different price dataset. Hourly electricity prices from 2005-2008 are also used here but prices from the period September-December 2005 was removed from the set as explained in Section 6.3.2.2. Other differences with the work of Madani and Lund (in press) are: a different piecewise linearization of the revenue curves was considered, and because the problem is relatively complex, the solver may not always come up with the globally optimal solution.

Energy generation, energy spills and revenues increase under Wet scenario but decrease under Dry scenario relative to the Base case. Energy spills increase drastically under Wet scenario with 8 times more spills than under Base case. Energy spills occur due to the limited storage capacity of the system and the abundant runoff available. These results are similar to those from Madani and Lund (in press). Even if average generation increases by nearly 6% under Wet scenario relative to Base case, average revenues only increase by 2%. Under Dry scenario, average generation decreases by 20% but revenues only decrease by 14% relative to Base case. The system adapts to the new climatic conditions to maximize profits. Revenues estimated in the present work are different from the ones obtained by Madani and Lund (in press).

Table 12 - EBHOM's results (average of results over 1985-1998 period) for different climate scenarios

	Base	Dry	Wet
Generation (1,000 GWh/year)	22.3	17.9	23.6
Generation change with respect to the base case (%)		*-19.8*	*+5.8*
Spill (GWh/year)	130	96	1112
Spill change with respect to the base case (%)		*-26*	*+756*
Revenue (million $/year)	1,726	1,482	1,762
Revenue change with respect to the base case (%)		*-14.1*	*+2.1*

7.3.1.1 Generation changes with climate warming

Figure 33 shows average monthly energy generation for 1985 to 1998 hydrologic conditions, modified for different climate changes. Results are summed from all 137 units modeled. On average, dry conditions lead to less generation than under Base case except in January and February. The monthly generation peaks occur in January and in June, when demand is high and energy is valuable. Generation between January and April is highest for the Wet scenario due to increased runoff. In the rest of the year, average monthly generation is slightly less than under Base case.

Figure 34 shows the frequency of optimized monthly generation for each month over the 14 year period (1985-1998) summed for all units, for the different climates. Over the entire study period, Dry climate leads to less generation than Base case and in contrast, Wet climate nearly always leads to more generation than Base case. If more storage capacity was available, the generation curve under Wet scenario would be closer to the Base case curve, with higher revenues.

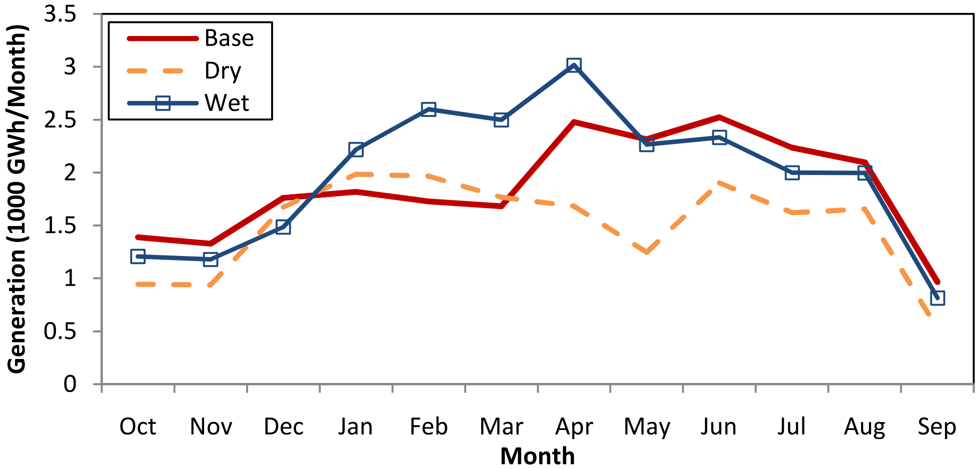

Figure 33 - Average Monthly Generation (1985-1998) under different climate scenarios and historical prices

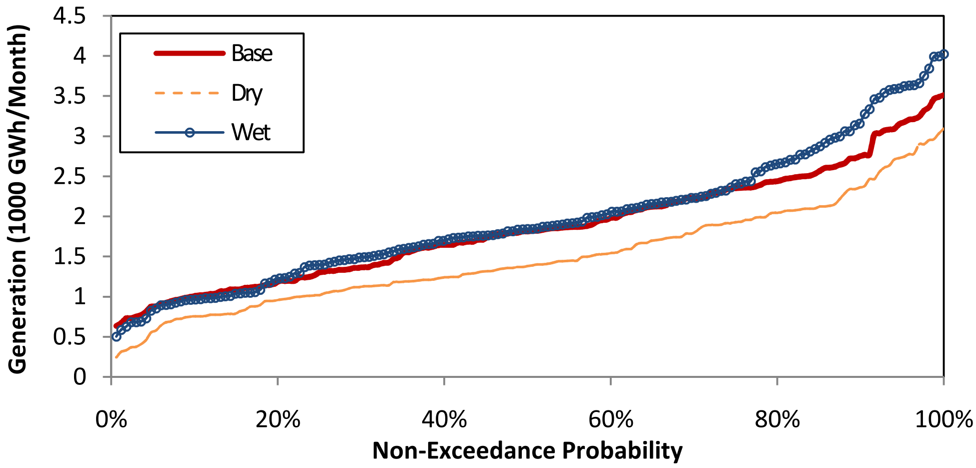

Figure 34 - Frequency of monthly optimized generation (1985-1998) under various climate scenarios (all months, all years, all units) and historical prices

7.3.1.2 Reservoir storage changes with climate warming

Figure 35 shows how average end-of-month energy storage in all reservoirs combined changes with climate when reservoirs are operated for energy revenues only. The starting month for reservoir refilling is January under Base and Wet scenarios and November under Dry climate. Under climate warming scenarios, reservoirs capture most of snowmelt water between January and May and release it progressively in months of high demand, maximizing profit. The timing of the patterns is similar to the monthly runoff distributions. The peak storage intensity is relative to the amount of water available, it is the largest under Wet scenario, then Base case and finally lowest under Dry scenario. The peak intensity is also lower under Base case than Wet scenario because some of the water is directly released and not stored for later. For instance, the end-of-month storage capacity in June is about the same for these two scenarios.

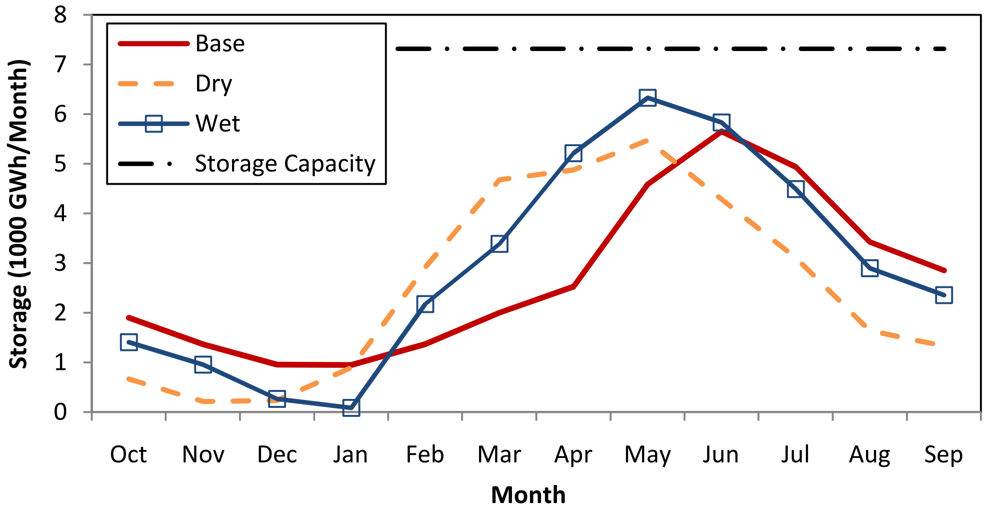

Figure 35 - Average total end-of-month energy storage (1985-1998) under different climate scenarios and historical prices. The black line is the system's storage capacity.

7.3.1.3 Energy spills with climate warming

Figure 36 shows the frequency of total monthly energy spills from the system for the study period (1985-1998) when the system is optimized for revenue maximization. Energy spill is the equivalent energy value of the water that cannot be stored nor sent through turbines because of limited capacities. Energy is spilled by the system in 35% of months under Wet climate, in 20% of months under Base case and in 10% of months under Dry climate. What is calculated as energy spill in this study is the increased energy spill with respect to the Base case, so zero spills under the Base case was expected. However, the results showed a minimal model error of 130GWh, corresponding to 0.6% of total generation on average, under the Base case.

Figure 37 shows the distribution of total average monthly energy spill for different climates. Spills occur only between January and May in all cases. Substantial energy spills (850 GWh in total) occur in February under Wet scenario even though the total storage capacity is not met. EBHOM has perfect foresight into the future and knows what will happen in the next months, so in this case it suggests spilling and emptying the reservoirs in advance.

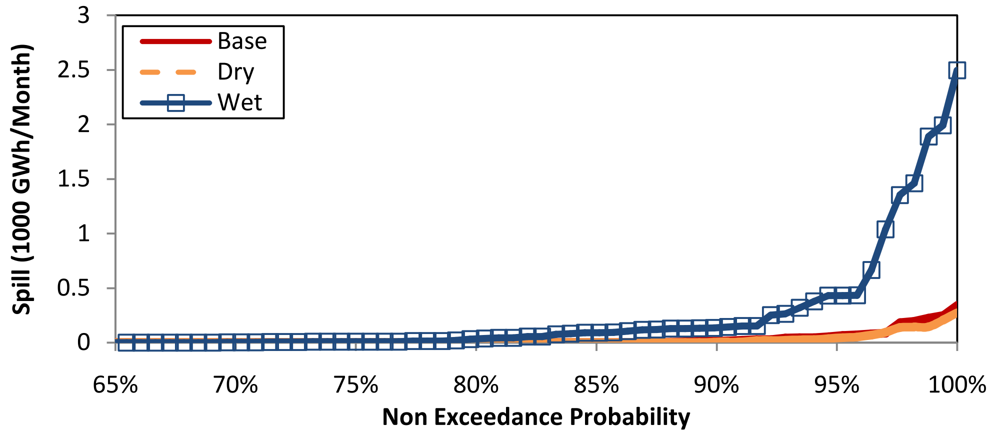

Figure 36 - Frequency of total monthly energy spill (1985-1998) under different climate scenarios (all months, all years, all units) and historical prices

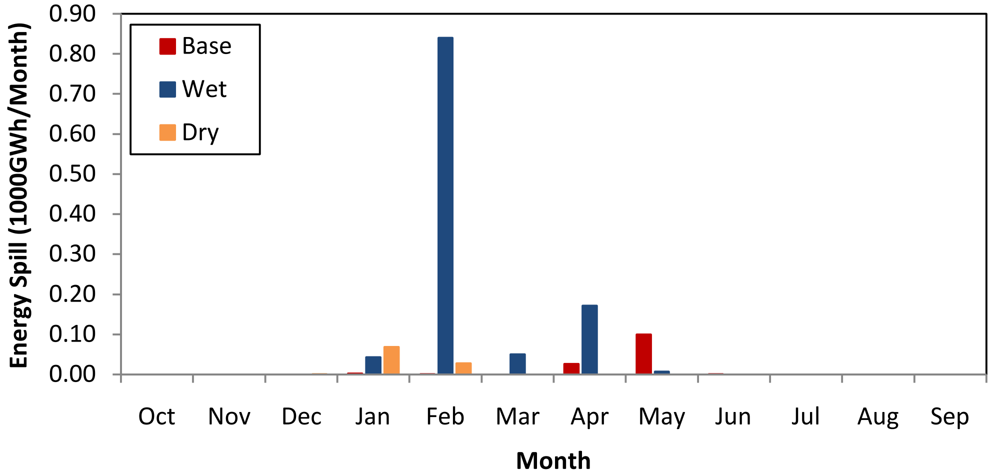

Figure 37 - Average Monthly Total Energy Spill (1985-1998) under different climate scenarios and historical prices

7.3.1.4 Revenue and energy price patterns under climate warming

Figure 38 shows climate warming effects on monthly average price received for generated energy in the period 1985-1998. Prices received under Dry scenario exceed the Base case prices 85% of the time, but monthly generation is less 100% of the time. This is what was expected given the non-linear relationship between electricity prices and generation. Prices received under Wet climate are similar to the ones under Base case, but never exceed those. Average prices received here reach 175 $/MWh under Dry climate, 150 $/MWh under Wet climate, and 135$/MWh under Base case whereas those did not exceed 135 $/MWh, 120 $/MWh and 120 $/MWh respectively in Madani and Lund (in press).

Figure 39 shows the effects of climate warming on the frequency of total annual revenues from the system for the 14 years period (1985-1998). Annual revenues are the highest 80% of the time under the Wet scenarios and the lowest 100% of the time under Dry scenario. Although monthly average prices received for generated energy were higher under the Dry scenario, the increase in average prices received does not compensate for the Dry scenario reduction in energy generation. On average, annual revenues are $210 million lower than the Base case for the Dry scenario.

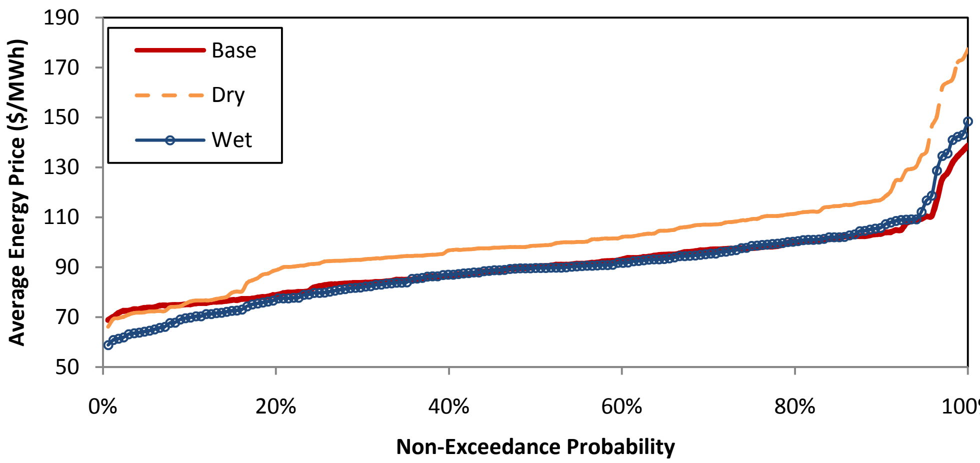

Figure 38 - Frequency of monthly energy price (1985-1998) under different climate scenarios (all months, all years, all units) and historical prices

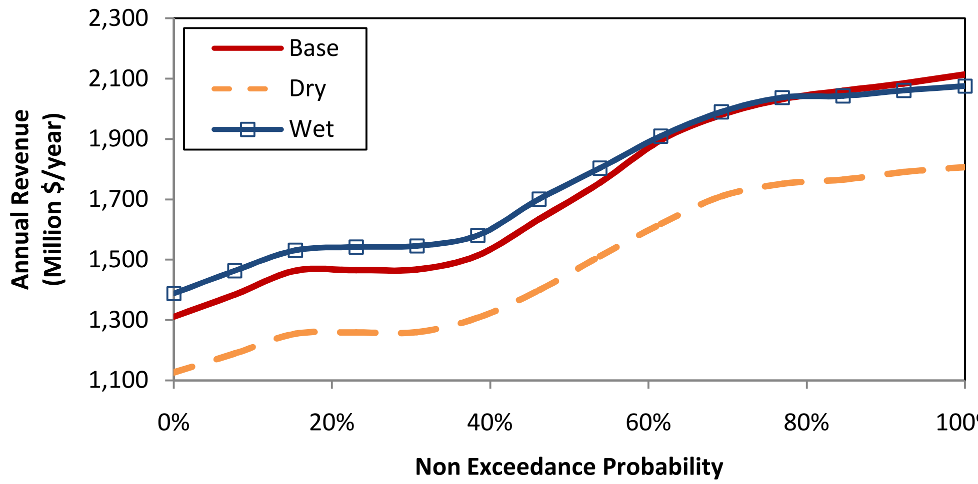

Figure 39 - Frequency of total annual revenue (1985-1998) under different climate scenarios and historical prices

7.3.1.5 Benefits of expanding energy storage and generation capacity

Figure 40 shows, on average, how energy storage capacity expansion changes hydropower generation revenues for different climate scenarios over the 14 years study period. This figure indicates the average shadow price of energy storage capacity (the increase in annual revenue per 1 MWh energy storage capacity expansion) for all 137 reservoirs. For instance, increase in annual revenue per 1MWh energy storage capacity expansion is less than \$29, \$48 and \$51 (compared to \$35, \$47 and \$54 in Madani and Lund (in press)) for the 137 studied plants under the Base, Dry and Wet scenarios. Storage capacity expansion reduces spills and allows for more release in summer when energy is the most valuable. Average annual revenues can be increased by expanding storage capacity in all plants (except for four plants under Base case), although such expansion might not be justified due to expansion costs. As expected, benefits of capacity expansion are greater for Wet scenario when the additional capacity can be more frequently used. Even with the historical hydrology, expanding storage capacity increases total annual revenues in all years.

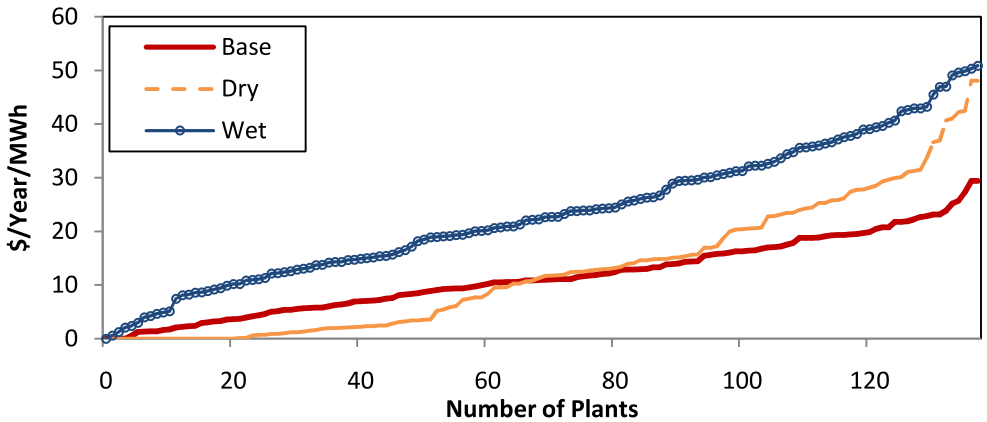

Figure 40 - Average Shadow Price of Energy Storage Capacity of 137 hydropower units in California for 1985-1998 period under different climate scenarios and historical prices

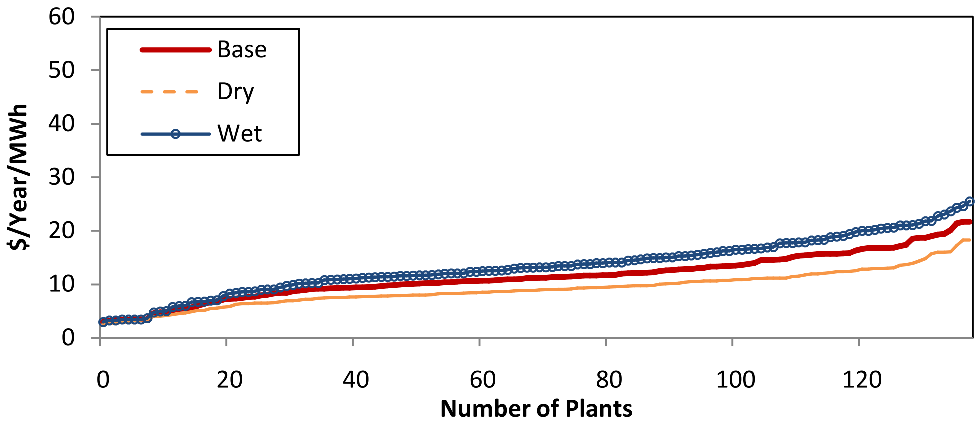

Figure 41 - Average Shadow Price of Energy Generation Capacity of 137 hydropower units in California for 1985-1998 period under different climate scenarios and historical prices

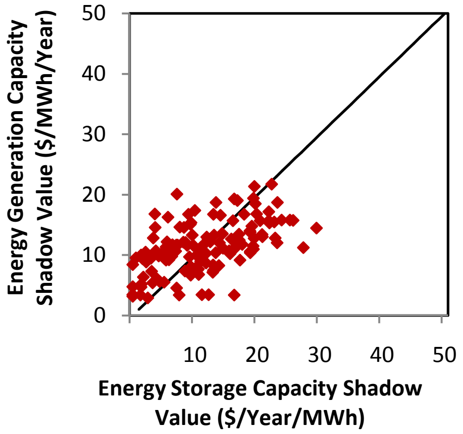

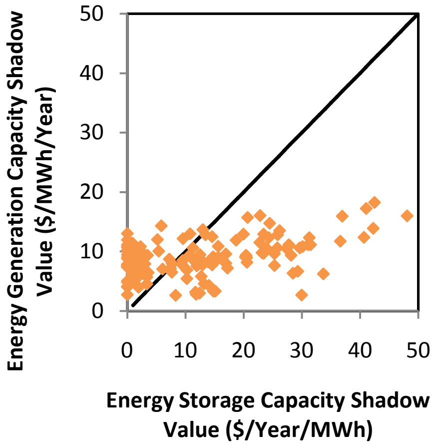

a) Base

b) Dry

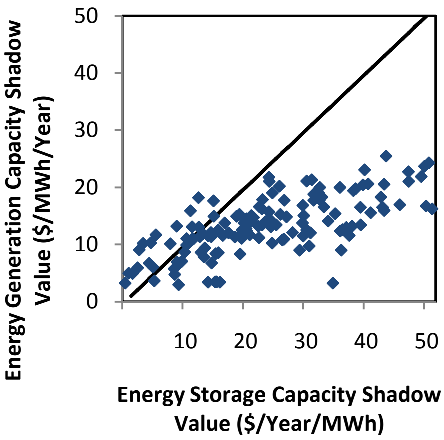

c) Wet

Figure 42 - Average shadow values of energy storage and generation capacity of 137 hydropower units in California in the 1985-1998 period under different climate scenarios and historical prices

Figure 41 indicates the average shadow price of energy generation (turbine) capacity (increase in annual revenue per 1 MWh of annual energy generation capacity expansion) for all 137 plants under different climate scenarios. All scenarios benefit from an increase in generation capacity, reducing spills and allowing more energy to be generated when prices are high. Increase in annual revenue per 1MWh energy storage capacity expansion is around $22, $18 and $25 for the 137 studied plants under the Base, Dry and Wet scenarios. Even though generation capacity expansion produces benefits, expansion costs might be prohibitive.

Figure 42 indicates how the marginal benefits of energy storage and generation capacity expansion of power plants vary with climate (each point in the figure is a plant). It clarifies the relative importance of extra energy generation and storage capacity for each unit for all climate scenarios. Under Base scenario, half of the power plants benefit more from energy storage capacity expansion than generation capacity expansion. However, storage capacity expansion is more beneficial in terms of revenue if the entire system is considered. Comparison of Figure 42a with Figure 42b–d shows how storage capacity becomes more valuable under climate warming as the scatter in the figures expands to the right, highlighting the higher benefit from energy storage capacity expansion than generation capacity expansion. Under Wet scenario, 86% of the units benefit more from storage capacity expansion. Finally for the Dry scenario, 55% of the power plants benefit more from energy storage capacity expansion than generation capacity expansion. However, nearly 40% of the plants increase their revenues by less than 5$ per MWh storage capacity expansion. The plants that do not spill are responsible for this low increase in average shadow prices.

Figure 43 shows the changes of marginal benefits of energy storage and generation (turbine) capacities relative to the base case (Figure 42a) with different climate warming scenarios. Under the Dry scenario, marginal benefits of energy generation capacity of all units are lower than the Base case, because water supply availability is the limiting factor. For about 50% of plants, the value of expanding energy storage under drier conditions is more than with the Base case, allowing more winter inflows to be shifted to high value summer power generation (the maximum difference can be as high as $28). For the Wet scenario, almost all units benefit from energy storage capacity expansion as well as from generation capacity expansion, reducing spills and shifting generation from low- to high-valued months. In this case, energy storage capacity expansion is more valuable than generation capacity expansion.

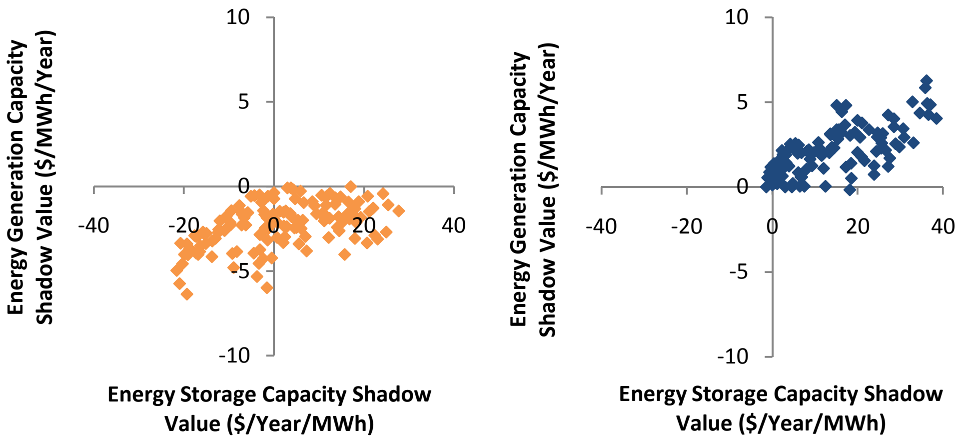

a) Dry b) Wet

Figure 43 - Average change of energy storage and generation capacity shadow values from the base case with different climate scenarios (for 137 hydropower units in California in the 1985-1998 period) based on historical prices

7.3.2 Climate change impact on energy demand, pricing and on hydrology

The previous section described climate warming effects on California's high-elevation hydropower system by focusing on the supply side (exploring the effects of hydrological changes on generation and revenues), ignoring the warming effects on hydropower demand and pricing. The present section extends the previous results by simultaneous consideration of climate change effects on high-elevation hydropower supply and demand in California. The ANNs developed in Section 6 are used as long-term price forecasting tools to estimate the impact of climate warming on energy prices. Two different ANN models were developed: 12 Monthly-based ANN models calibrated for all price ranges (ANN1), and a single Annually-based ANN model calibrated on Normal prices (ANN2). These models will be referred to as ANN1 and ANN2 respectively hereafter for simplification.

Table 13 indicates how energy generation, energy spill and annual energy revenue change relative to Base case for different climate scenarios and forecasted future energy pricing. For each climate warming scenario (Dry, Wet or Dry-Seasonal), the average annual generation and energy spills are the same no matter what the price representation is. Generally, when warming effects on demand are considered, annual revenues decrease relative to the Base case for both drier and wetter conditions. Depending on the ANN model used to forecast prices, there can be significant differences in average revenues received, especially under drier conditions. Under Dry climate, the difference in revenues between models using ANN1 or ANN2 is around 130 million $/year and under Dry-Seasonal climate it reaches 180 million $/year. Generally, ANN1 predicts higher annual average revenues than ANN2 under all climates. The Dry scenario estimates more important decreases in revenue than the Dry-Seasonal one.

Table 13 - EBHOM's results (average of results over 1985-1998 period) for different climate warming scenarios considering simultaneously the warming effects on hydropower supply and demand (ANN1: Monthly-based ANN model; ANN2: Annually-based ANN model calibrated on Normal prices)

Climate scenario	Base	Dry	Wet	Dry		Dry-Seas		Wet	
Price Model	Historical			ANN1	ANN2	ANN1	ANN2	ANN1	ANN2
Generation (1,000 GWh/year)	22.3	17.9	23.6	17.9		17.9		23.6	
Generation change with respect to the base case (%)		*-19.8*	*+5.8*	*-19.8*		*-19.8*		*+5.8*	
Spill (GWh/year)	130	96	1112	96		96		1112	
Spill change with respect to the base case (%)		*-26*	*+756*	*-26*		*-26*		*+756*	
Revenue (million $/year)	1,726	1,482	1,762	1,533	1,400	1,587	1,408	1,718	1,660
Revenue change with respect to the base case (%)		*-14.1*	*+2.1*	*-11.2*	*-18.9*	*-8.1*	*-18.4*	*-0.5*	*-3.8*

7.3.2.1 Generation changes with climate warming scenarios

Figure 44a-b shows average monthly energy generation for 1985 to 1998 for different climate warming scenarios, considering climate warming effects on high-elevation hydropower supply and demand simultaneously. Results are summed from all 137 units modeled.

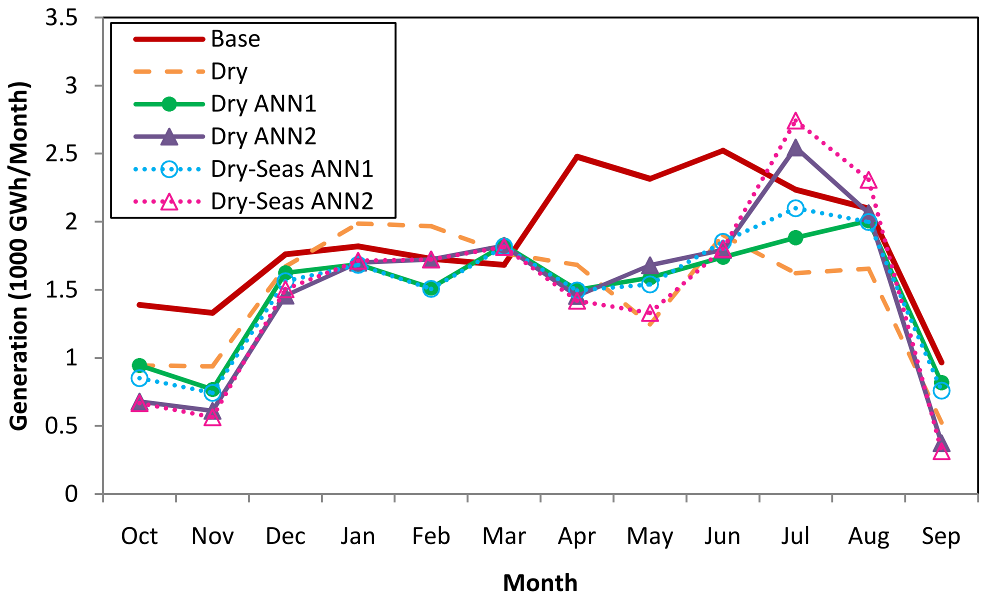

a) Dry scenarios

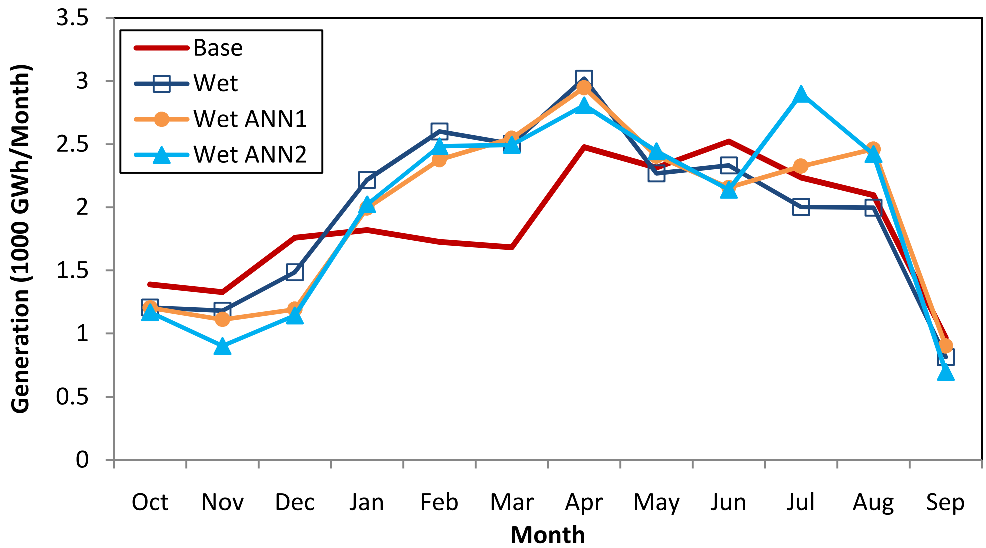

b) Wet Scenarios

Figure 44 - Average Monthly Generation (1985-1998) under dry (a) and wet (b) warming scenarios, considering the warming effects on hydropower supply and demand simultaneously (Future energy pricing is forecasted using ANNs – ANN1: Monthly-based model; ANN2: Annually-based model calibrated on Normal prices)

When climate warming effects on hydropower demand and pricing are considered, average monthly generation increases in June and July and decrease from November to February under all scenarios, compared to when those were ignored. Less generation in winter is necessary since there is less need for heating and increases in summer to satisfy the high demand for cooling. Generation is peaking in June or July depending on the ANN model considered, but both ANN models result in a peak in summer. The highest peaks occur in July for ANN2 and reaches 2,500GWh/Month for Dry ANN2, 2,700GWh/Month for Dry-Seasonal ANN2 and 2,900GWh/Month for Wet ANN2. Dry-Seasonal scenarios estimate more generation in July and August than Dry scenarios. Under the rest of the months, considering warming effects on energy demand results in similar behavior than ignoring them.

7.3.2.2 Reservoir storage changes with climate warming

Figure 45a-b shows how average end-of-month energy storage in all reservoirs combined changes with climate when reservoirs are operated for energy revenues only, for drier and wetter scenarios respectively, considering climate warming effects on high-elevation hydropower supply and demand simultaneously.

Reservoirs start refilling earlier in the Dry scenarios than in the Wet ones and Base case. In the dry scenarios, the system must take maximal advantage of the water available from late autumn to spring, to release it when prices are the highest, i.e. in summer. Between February and June, the system stores more water in its reservoirs when future changes in demand are considered than when they are ignored. This is true for both drier and wetter scenarios. Less energy is needed in cold months so more water is available to be stored until high-demanding months. The peak storage occurs in May under all climate change scenarios. In the rest of the months, less energy is stored when changes in demand are considered. On average, the system's total storage capacity is never met. The main difference between the two ANN models is that on average less energy is stored in summer for ANN2 compared to ANN1, because in that case generation peaked in July (by more than 500 GWh). There is no significant difference between the Dry and Dry-Seasonal scenarios, except slightly less storage in summer for the latter scenario.

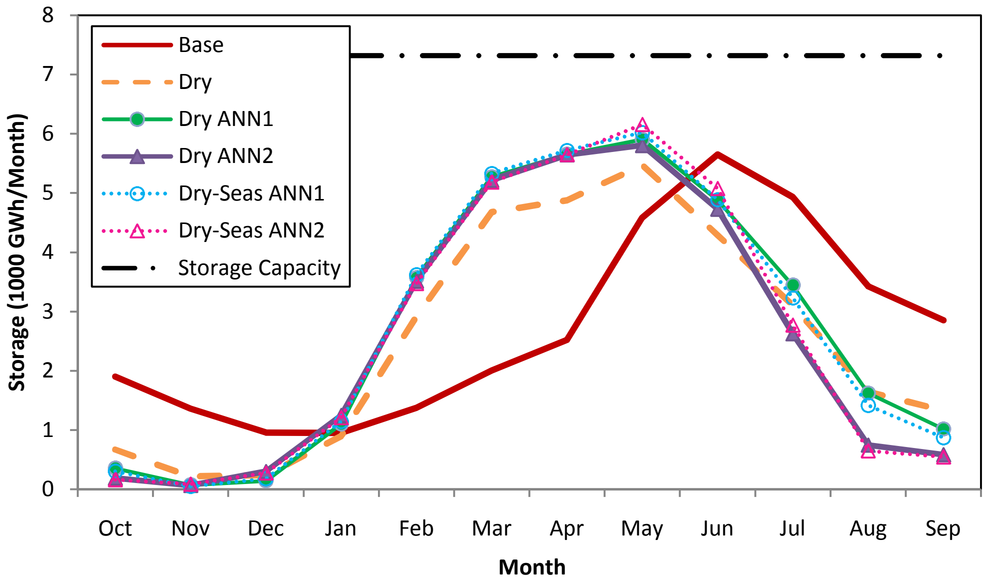

a) Dry scenarios

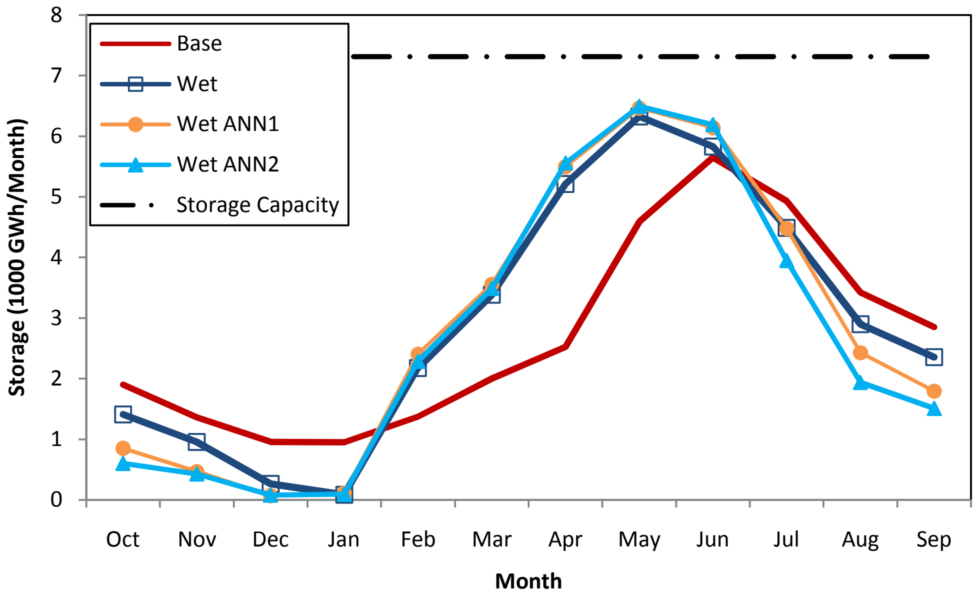

b) Wet scenarios

Figure 45 - Average total end-of-month energy storage (1985-1998) under dry (a) and wet (b) warming scenarios, considering the warming effects on hydropower supply and demand simultaneously (Future energy pricing is forecasted using ANNs – ANN1: Monthly-based model; ANN2: Annually-based model calibrated on Normal prices)

7.3.2.3 Energy spills with climate warming

Figure 46a-b shows the distribution of total average monthly energy spill for dry and wet climate scenarios considering changes in future demands. All spills occur in the refilling season (December to May) before release when demand and prices are high. The energy spill patterns are similar between all dry scenarios and between all wet scenarios. Considering warming effect on demand does not alter the average monthly spill pattern. Average energy spills of about 850GWh occur in February under Wet scenarios. EBHOM suggests emptying reservoirs in advance since it has perfect foresight into the future.

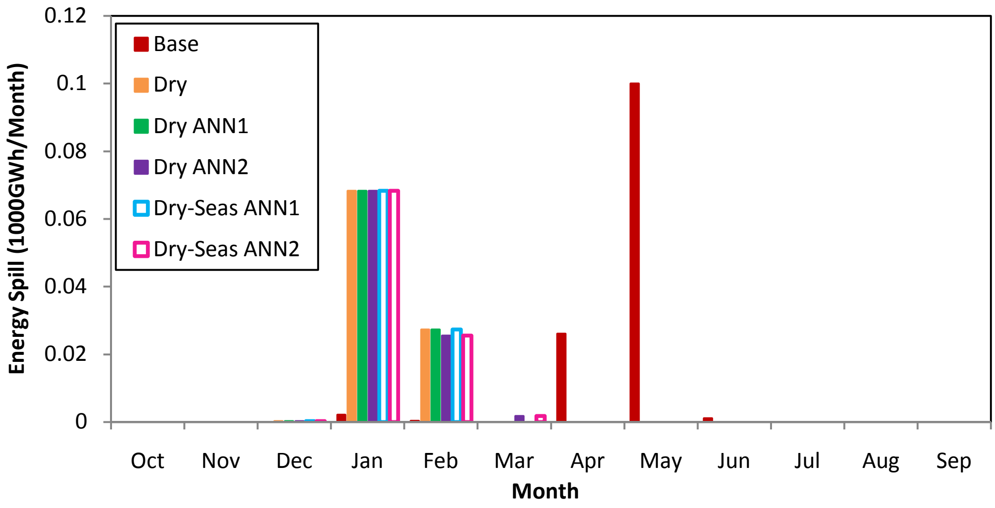

a) Dry scenarios

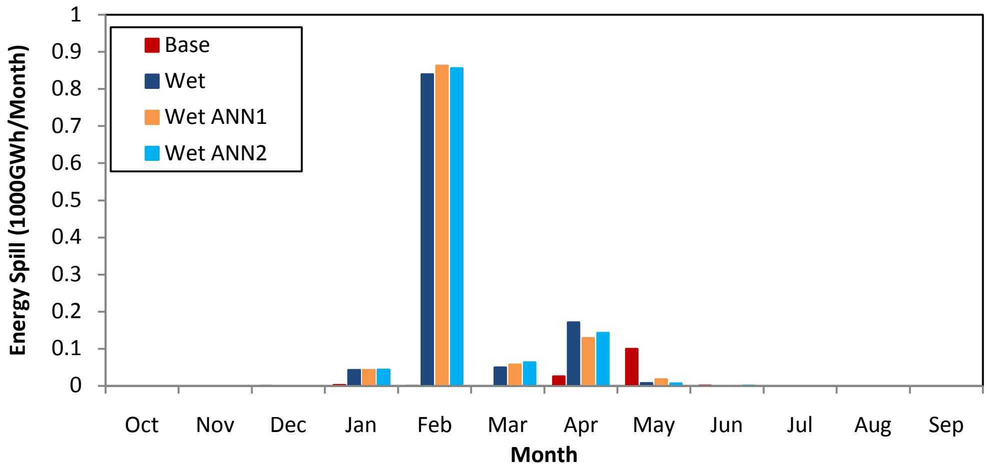

b) Wet scenarios

Figure 46 - Average Monthly Total Energy Spill (1985-1998) under different warming scenarios, considering the warming effects on hydropower supply and demand simultaneously (Future energy pricing is forecasted using ANNs – ANN1: Monthly-based model; ANN2: Annually-based model calibrated on Normal prices)

7.3.2.4 Revenue and energy price patterns under climate warming

Figure 47a-b shows climate warming effects on monthly average price received for generated energy, for drier (a) and wetter (b) scenarios respectively, considering climate warming effects on hydropower supply and demand simultaneously.

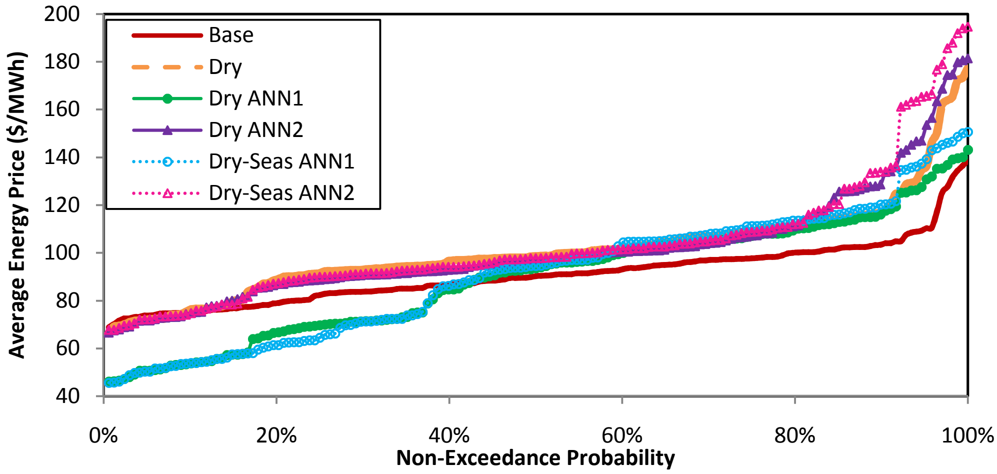

a) Dry scenarios

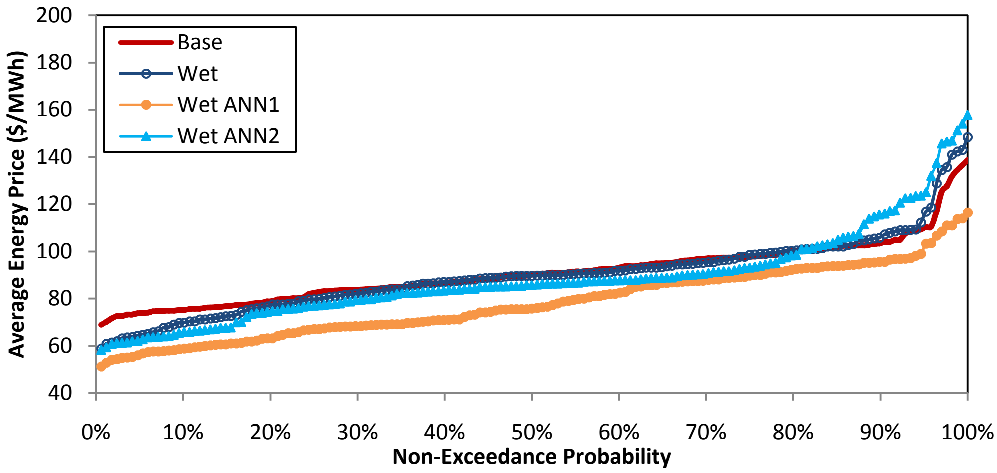

b) Wet Scenarios

Figure 47 - Frequency of monthly energy price (1985-1998) under dry (a) and wet (b) warming scenarios , considering the warming effects on hydropower supply and demand simultaneously (all months, all years, all units) (Future energy pricing is forecasted using ANNs – ANN1: Monthly-based model; ANN2: Annually-based model calibrated on Normal prices)

Energy prices received under Base case are exceeded 85% of time under Dry ANN2 and Dry-Seas ANN2 and 60% of time under Dry ANN1 and Dry-Seas ANN1. The aggregate monthly energy price received under both Dry-Seasonal scenarios exceeds those under their respective Dry scenario. Aggregate monthly energy prices for 1985-1998 is about 150-160 $/MWh when ANN1 is used whereas it is about 180-190

$/MWh when ANN2 is used under Dry scenarios. Generally, monthly energy prices received when the scenario is based on ANN2 exceed those when ANN1 is used. Monthly energy prices received under Wet ANN1 never exceed Base case neither other wet scenarios. Prices received under Wet ANN2 are lower than Base case and Wet scenario (based on historical prices) 85% of the time, but exceed both the rest of the times. Generally dry scenarios increase monthly energy prices relative to the Base case whereas wet scenarios decrease prices.

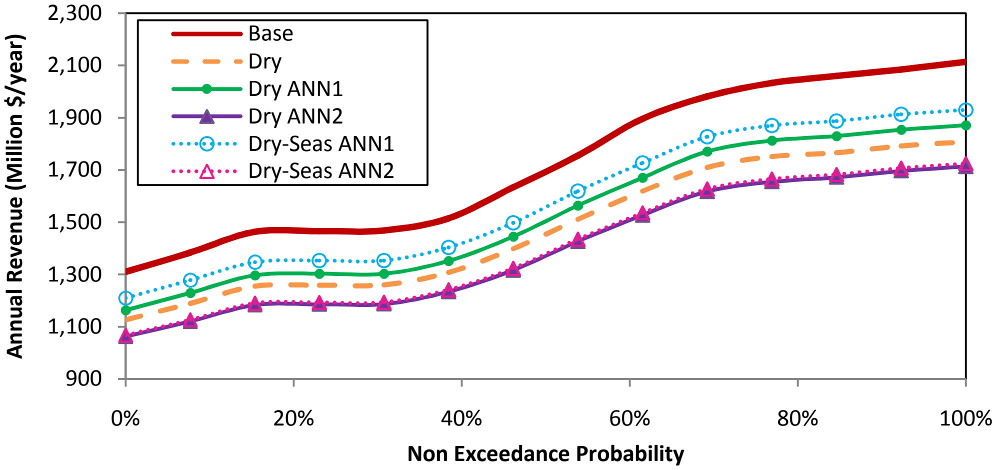

a) Dry scenarios

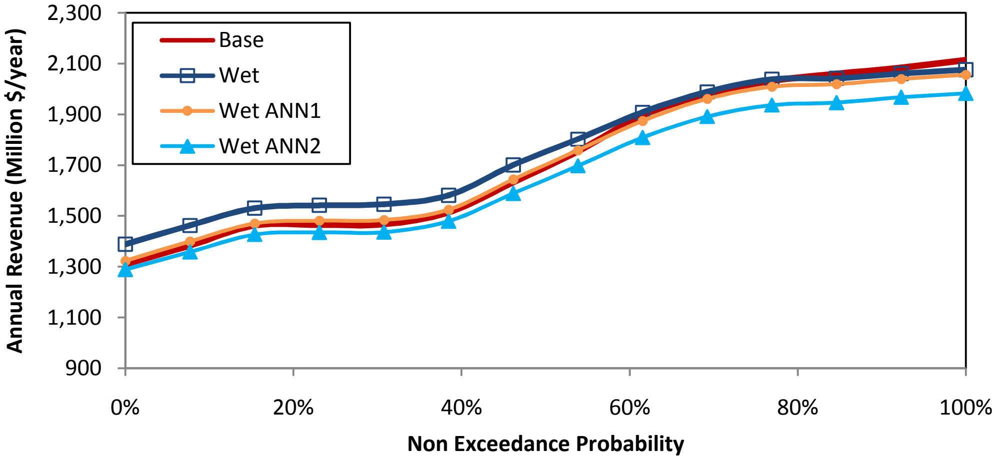

b) Wet Scenarios

Figure 48 - Frequency of total annual revenue (1985-1998) under dry (a) and wet (b) warming scenarios, considering the warming effects on hydropower supply and demand simultaneously (Future energy pricing is forecasted using ANNs – ANN1: Monthly-based model; ANN2: Annually-based model calibrated on Normal prices)

Figure 48a-b shows the effects of climate warming on the frequency of total annual revenues from the system for the 14 years period (1985-1998) for drier (a) and wetter conditions (b), considering climate warming effects on hydropower supply and demand simultaneously. Under Dry conditions, annual revenues received are always lower than those under Base case. Although monthly average prices received for generated energy were higher under the Dry scenarios, the increase in average prices received does not compensate for the Dry scenarios reduction in energy generation. For drier climate, considering the simultaneous effects of climate warming on hydropower supply and demand leads to an increase in annual revenues when the model is based on ANN1 and a decrease when the model is based on ANN2. For wetter conditions, considering the simultaneous effects of warming on hydropower supply and demand decreases revenues compared to when they were neglected. For all climate warming scenarios ANN1 increases revenues compared to ANN2; this has already been discussed in Section 6.5 dealing with to long-term price forecasting; Monthly-based models (ANN1) are likely to overestimate future prices.

7.3.2.5 Benefits of expanding energy storage and generation capacity

Figure 49a-b shows, on average, how energy storage capacity expansion changes hydropower generation revenues for drier (a) and wetter (b) climate scenarios over the 14 years study period. These figures indicate the average shadow price of energy storage capacity (the increase in annual revenue per 1 MWh energy storage capacity expansion) for all 137 reservoirs. Average annual revenues can be increased by expanding storage capacity in all plants (except for seven plants under Dry ANN1 and Dry ANN2), although such expansion might not be justified due to expansion costs. In summer, demand increases and energy is valuable, so the system benefits from storing more snowmelt water. Increase in annual revenue per 1MWh energy storage capacity expansion is between \$45 and \$81 for the 137 studied plants under drier scenarios considering changes in demand. It is hard to conclude on the benefits from expanding energy storage capacity under wetter scenarios. Expanding storage capacity can be more or less beneficial than when demand changes were ignored, depending on the ANN forecast model used. Under Dry ANN1, expanding energy storage capacity is more valuable for about 50 power than under wetter scenarios, which is surprising. Greater benefits of storage capacity expansion for Wet scenarios were expected since the additional capacity can be more frequently used. However the estimations from ANN2 seem more reasonable.

Figure 50a-b indicates the average shadow price of energy generation (turbine) capacity (increase in annual revenue per 1 MWh of annual energy generation capacity expansion) for the entire system, under drier (a) and wetter (b) climate warming scenarios. Considering climate warming effects on demand attenuates the benefits from expanding energy generation capacity under wetter scenarios relative to the Wet scenario based on historical pricing. The same comment is valid for drier conditions, except for Dry-Seasonal ANN1 scenario. Increase in annual revenue per 1MWh energy generation capacity expansion is \$22, \$15-17 and \$22-24 for the 137 studied plants under Base, drier and wetter scenarios respectively.

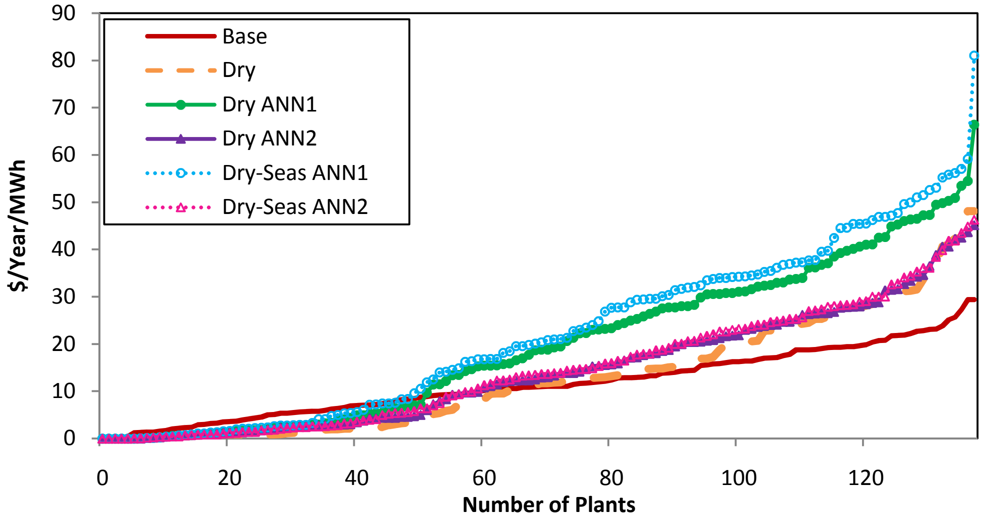

a) Dry

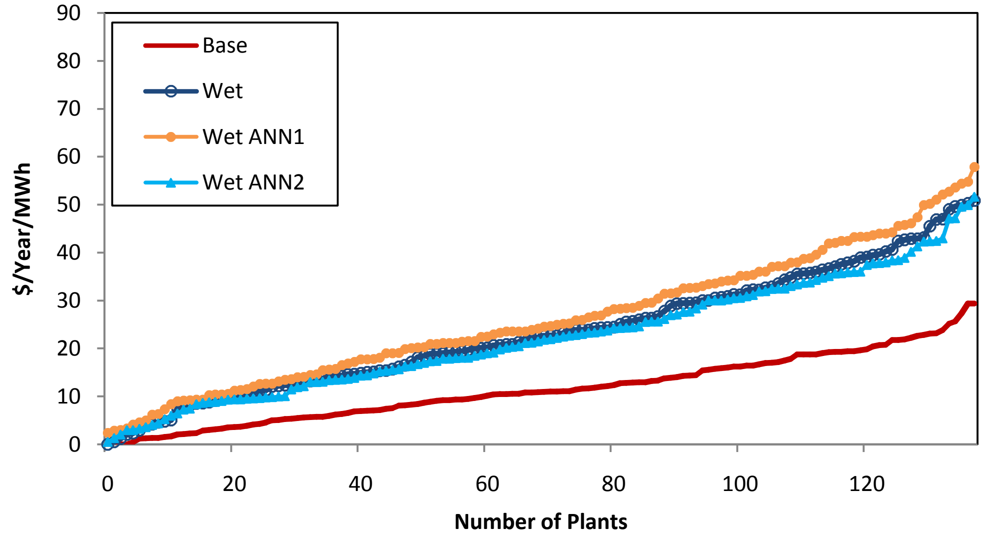

b) Wet

Figure 49 - Average Shadow Price of Energy Storage Capacity of 137 hydropower units in California in the 1985-1998 period under dry (a) and wet (b) warming scenarios, considering the warming effects on hydropower supply and demand simultaneously (Future energy pricing is forecasted using ANNs – ANN1: Monthly-based model; ANN2: Annually-based model calibrated on Normal prices)

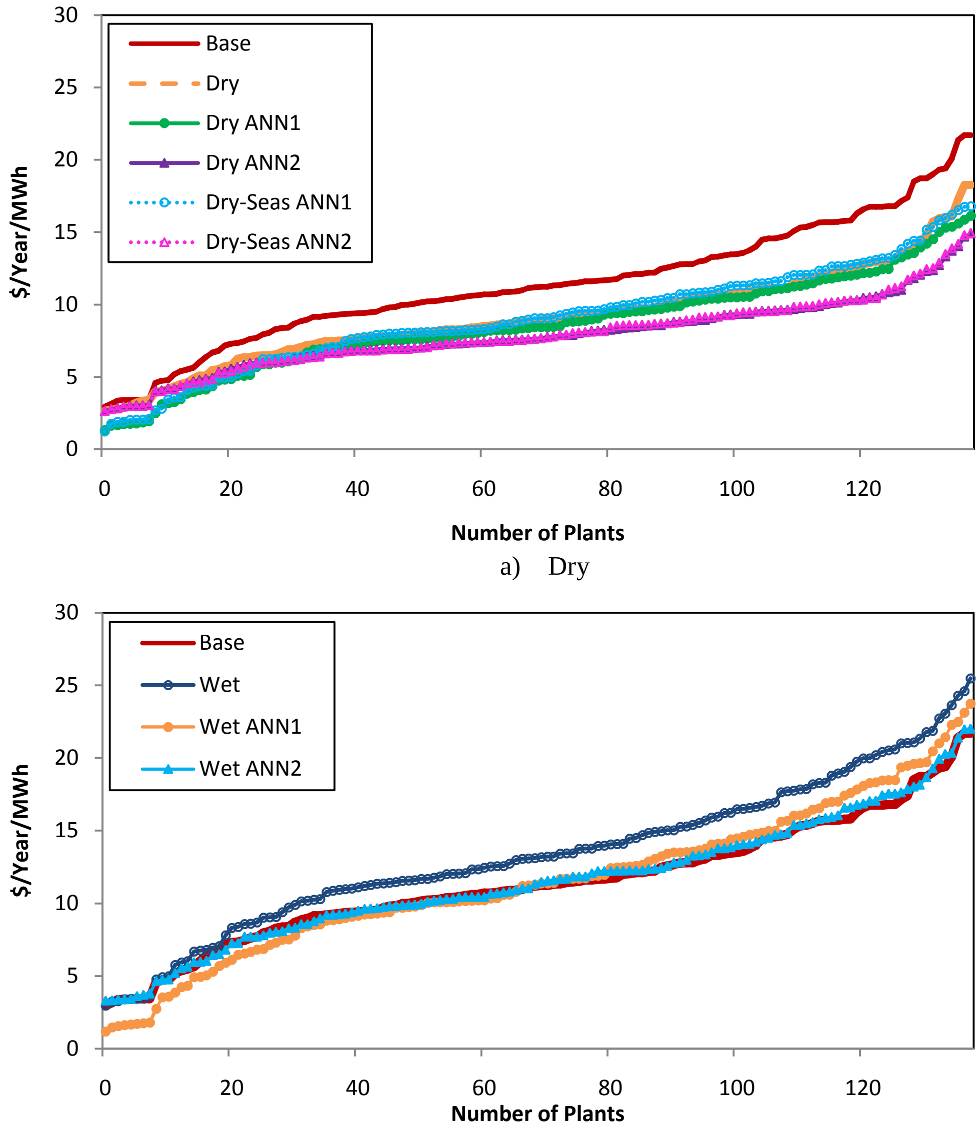

a) Dry

b) Wet

Figure 50 - Average Shadow Price of Energy Generation Capacity of 137 hydropower units in California in the 1985-1998 period under dry (a) and wet (b) warming scenarios, considering the warming effects on hydropower supply and demand simultaneously (Future energy pricing is forecasted using ANNs – ANN1: Monthly-based model; ANN2: Annually-based model calibrated on Normal prices)

Figure 51 indicates how the marginal benefits of energy storage and generation capacity expansion of power plants vary with the different scenarios (each point is a plant). It clarifies the relative importance of extra energy generation and storage capacity for each unit for all climate scenarios. Under all climate warming scenarios, expanding energy storage capacity is typically more beneficial than expanding generation capacity if the expansion costs are the same. Expanding energy storage capacity allows storing water in off-peak months and releasing it through turbines when prices are higher. Depending on the ANN forecast model, between 45 and 52 plants under drier scenarios, and only between 15 and 18 plants under wetter scenarios, benefit more from energy generation capacity expansion (out of 137 plants in total). Energy storage capacity shadow price is [1.81-2.32] and [1.93-2.27] times higher than the energy generation shadow price for all power plants under Dry and Wet scenarios considering warming effects on demand.

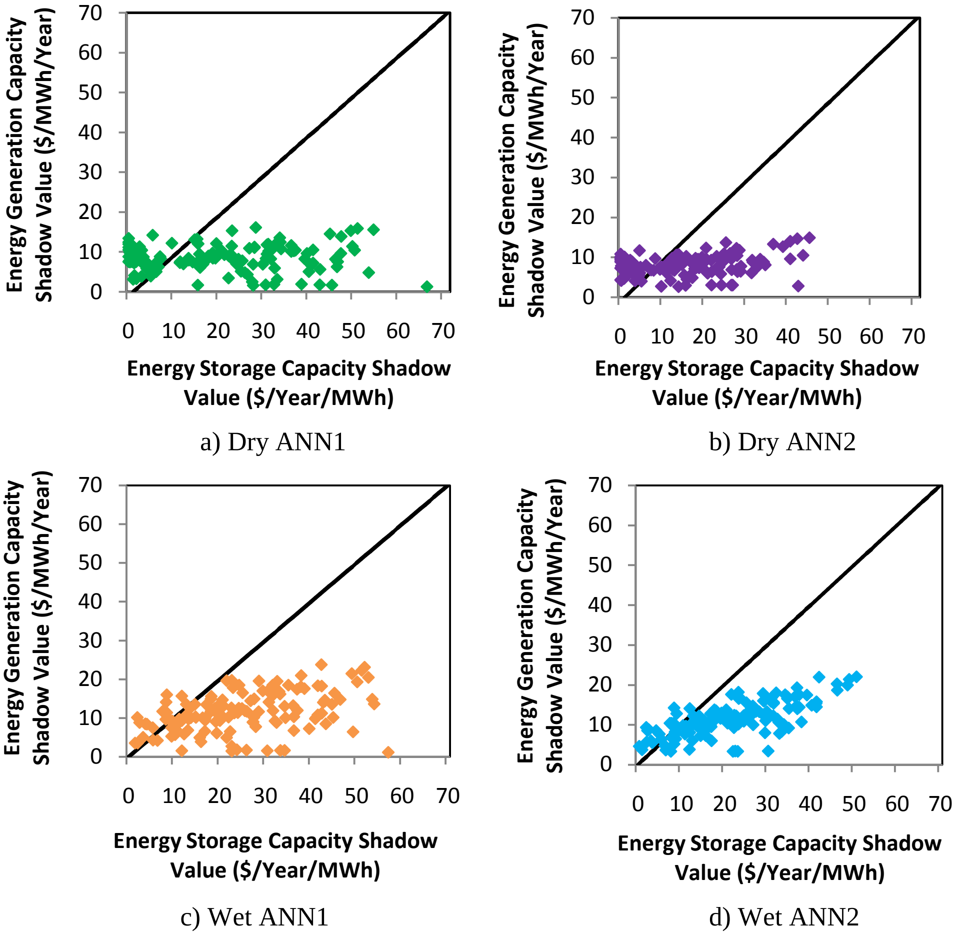

Figure 51 - Average shadow values of energy storage and generation capacity of 137 hydropower units in California in the 1985-1998 period under dry (a, b) and wet (c, d) warming scenarios, considering the warming effects on hydropower supply and demand simultaneously (Future energy pricing is forecasted using ANNs – ANN1: Monthly-based model; ANN2: Annually-based model calibrated on Normal prices)

Figure 52 shows the changes of marginal benefits of energy storage and generation (turbine) capacities relative to the Base case with drier and wetter warming scenarios. Patterns for Dry-Seasonal scenarios are similar to the Dry scenarios so they are not shown in the figure. Under Dry ANN1 and Dry ANN2, marginal benefits of expanding energy generation capacity for all units are lower than under Base case. There is less inflow, so the existing generation capacity is more often sufficient to avoid spills. For between 75 and 87 of plants (55-63%), the value of expanding energy storage capacity under drier conditions is more than under Base case. For Wet ANN1 and Wet ANN2 scenarios, most units (121 and 112 respectively) benefit more from energy storage capacity expansion than for Base case. Under the wetter scenarios about 50% of plants benefit from expanding both generation and storage capacities, but energy storage capacity expansion is more valuable, as the scatter in Figure 52c-d expands to the right.

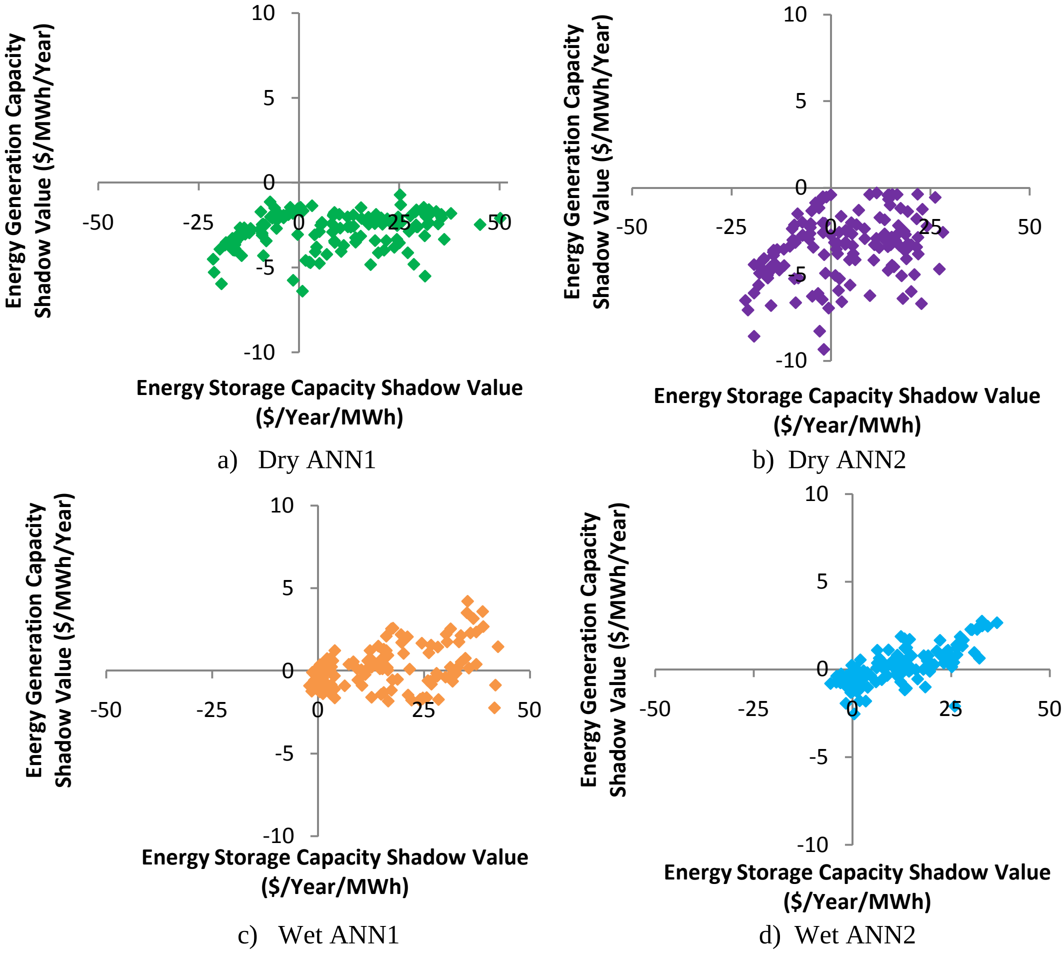

Figure 52 - Average change of energy storage and generation capacity shadow values from the base case from dry (a, b) and wet (c, d) warming scenarios (for 137 hydropower units in the 1985-1998 period), considering the warming effects on hydropower supply and demand simultaneously (Future energy pricing is forecasted using ANNs – ANN1: Monthly-based model; ANN2: Annually-based model calibrated on Normal prices)

7.3.3 Pure price increase scenarios coupled with climate warming scenarios

Average annual revenues for each price increase scenarios (±0%, +30% and +100% by year 2100) coupled to warming scenarios are shown on Figure 53. The inputs used to EBHOM are monthly revenue curves which are the integration over the price frequency distribution. Therefore, a linear price increase by K% increases annual revenues by K%. For instance, a price increase of 100% under a Dry scenario increases average annual revenue by 100% relative to the initial Dry scenario. Revenues are increased by K% (K=30 or 100) under each price increase scenario, so are average shadow prices of energy generation expansion and energy capacity expansion. Energy storage expansion and energy generation expansion become more valuable when price increase scenarios are considered.

Average annual energy generation and energy spills are identical whether or not a price distribution was increase by K% for each climate warming scenario. The same behavior is observed for average monthly generation, average end-of-month storage and energy spill patterns. The system optimized for revenue maximization responds in a similar manner to the price distribution increased by a constant percentage than to the initial price distribution.

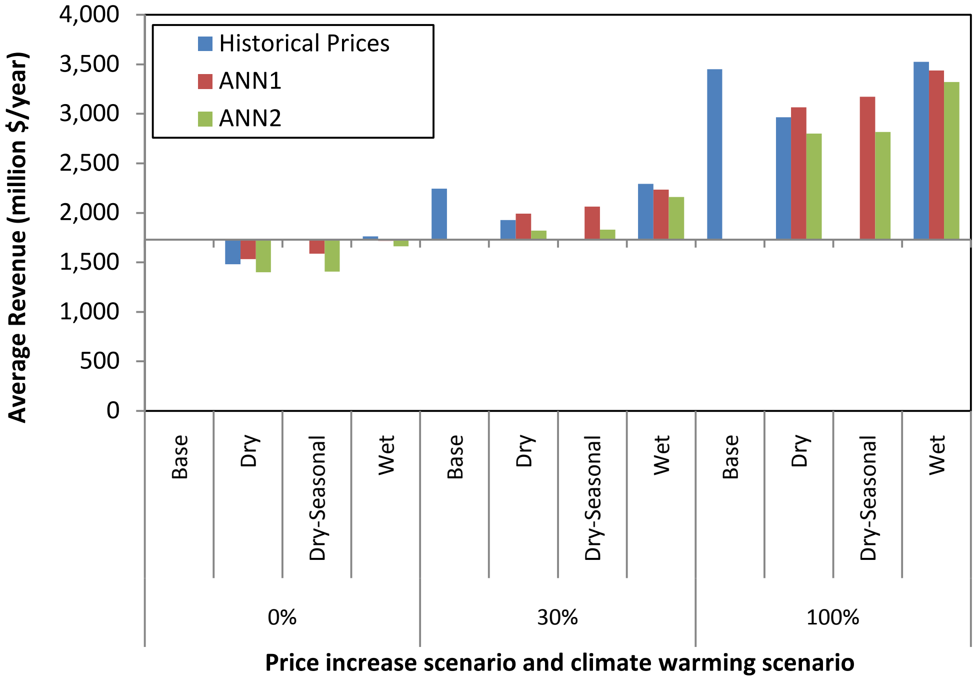

Figure 53 - EBHOM's annual revenue results (average of results over 1985-1998 period) for different climate warming scenarios coupled to price increase scenarios by 0%, 30% and 100%. Scenarios are based on historical prices, or forecasted future energy prices from Monthly ANN models (ANN1) or an Annual ANN model (ANN2). The horizontal axis crosses the vertical axis at the Base case (+0%) average revenue value.

8 Limitations and Future Direction

Climate warming might have impacts on California's high-elevation hydropower system in the next century. This work is aiming to estimate the effects from a change in both hydrological conditions and energy demand and pricing. What we are interested in is the 'big' picture; so many simplifying assumptions were necessary and should be considered in interpreting results. For instance, temperature data from several meteorological stations were averaged to define a temperature dataset for California, even if temperature varies consistently from area to area. Results from this work give however some insights on how the system works and how it might adapt to climate change.

Energy demand was included in ANN modeling as a third order polynomial function of temperature. This function was estimated by Franco and Sanstad (2006) to correlate the daily mean demand to the average daily temperature. Estimating hourly demands through this function implies that the hourly demand follows the same pattern as the mean daily demand. This seems to be a reasonable assumption knowing that we are interested in the big picture over California and that temperatures are also flattened. However this remains a limitation to map properly the hourly prices that contain many peaks which might result from periods of peak demand. Historically, peak loads have been increasing year after year and this is not considered in the present modeling. An interesting future development could be to improve the experiment tried out in this work, by considering the development of two ANNs in series: the first one to estimate a non linear response of demand from temperature and the second model, a nonlinear response of price from demand.

Processing time for ANN calibration is a limiting factor. Using a more powerful computer system or opting for a simpler ANN optimization method such as the Levenberg-Marquadt algorithm could allow enhancing the ANN architecture and accelerate the calibration process. Several independent calibration runs could then be performed to ensure finding the optimal set of weights (weights should converge to identical values). However, even if the SCE-UA optimization algorithm is complex, it should have a high probability of finding the global optimum (Duan et al., 1992).

In the present research two ANN models are developed; 12 parallel monthly models for all price ranges and one annual model for normal range prices (from which price spikes have been removed). Each approach presents advantages and drawbacks to map hourly prices accurately. Monthly models deal with all price ranges and there is no arbitrary elimination of price intensities that could be abnormal (or not). However, maybe the ANN does not learn anything from these high prices, which might bias the learning phase. One main drawback of monthly models appears when using ANNs as forecast tools and results from the inability of ANNs to extrapolate. The temperature data samples are perturbed to account for climate warming and then fed to the ANN. Some of these temperatures will be far off the range of the monthly calibrations datasets and the ANN will face new examples. This might lead to overestimation of the prices. An annual ANN model may be more appropriate to deal with increases in temperature because these temperatures might have occurred historically in other periods of the years, i.e. in other months. The Annual ANN model trained on normal prices should model those with rather high accuracy according to Lu et al. (2005), who mention that it is necessary to remove price spikes from calibration to improve accuracy. When using this Annual ANN model as a forecast tool, it is assumed that the future proportion of price spikes will remain the same as for 2005-2008. The future energy market was assumed to stay not ideally competitive, with operators giving priority to profit maximization, leading to possible manipulations of the market. However, it is worth mentioning that in an 'ideal' or highly-supervised energy market spikes should not occur except when demand exceeds supply. Further research should deepen price spikes modeling.

The two ANN models developed here do not distinguish workdays from week-ends or public holidays. This was seen in some works on short-term price forecasting (e.g. Gao et al., 2000; Amjady and Keynia, 2010b) and should be considered in further research. An idea could be to develop two parallel ANNs: one for workdays and one for both week-ends and holidays since those have similar price patterns.

Real-time energy prices for the period 2005-2008 were employed to calibrate the ANN models and to model the Base case of EBHOM. Application of longer-period price data sets might improve the ANN mapping accuracy as ANN models are reliant on the quantity and quality of data. The price set from 2005-2008 does not exactly match the energy prices from the runoff data period 1985-1998. This might cause some inaccuracies in EBHOM's estimation of revenues and energy prices but should not affect other results much (generation, spills and storage) as the energy price trends are similar between years (Madani and Lund, in press).

Calibration of EBHOM is likely to underestimate energy storage capacities (Madani and Lund, 2009) and therefore also underestimate the adaptability of the system to climate changes. Availability of spill or energy storage capacity data would reduce this source of error (Madani and Lund, in press).

Population growth rate is not considered here in the future scenarios. However, it was shown in the work from Aroonruengsawat and Auffhammer (2009) that it had significant impacts on projected demand. Even a low population growth rate of 0.18% per year predicts an increase of 65-70% in residential electricity demand by 2100, which completely outpaces the increase resulting from climate change (Aroonruengsawat and Auffhammer,2009). Additional scenarios including population increase scenarios could be developed in future research work.

Finally, price elasticity of demand is neglected in this work for problem simplification. If energy prices start rising substantially, it is very probable that consumers will save money by saving energy. The consequent demand decrease will affect energy prices and so on. A recurrent ANN could be more suitable for model such phenomenon if compared to a feed-forward ANN, but is more complex to implement and time-consuming to train. An econometric model could also be built to estimate this price elasticity of demand.

9 Conclusion

The main objectives of this research work were the followings: develop a tool to model the effects of climate warming on future energy demand and pricing and estimate the consequent impacts of climate change on California's high-elevation hydropower system. An ANN model was chosen to map the non-linear relationship between temperature, energy demand and prices. This model was then used to forecast energy prices for different climate warming scenarios. Two ANN models were developed, a Monthly-based model calibrated on all price ranges and an Annually- based ANN model calibrated on normal prices (price spikes removed). Price spikes in California ISO energy market were identified as prices exceeding 128$/MWh, based on real-time energy prices for the period 2005-2008. For the model calibrated on normal prices, the same proportion of price spikes (with the same intensities) was assumed to occur in future. In this work, the energy market was assumed to remain not ideally competitive with priority given to profit maximization.

The ANN price forecast model estimates higher energy revenues in warm months for high-forcing climate scenarios than for low-forcing scenarios, and vice-verse in cold months. This corresponds to the higher demand for cooling in summer and lower demand for heating in winter. The magnitude of changes in revenue is on average higher for the Monthly-based ANN models than for the Annually-based ANN model, but monthly models might overestimate prices.

EBHOM's results for Dry and Wet climate warming scenarios run under historical prices are the followings. Energy generation increases from January to April under Wet scenario; snowmelt water is plentiful and the system has limited capacity to store the shift in peak runoff. Average monthly generation increases also under Dry scenario from January to March relative to Base case, but decreases in the rest of the months since less inflow is available. For Dry warming scenarios, the reservoirs refilling month shift to earlier in the year to capture the shifted snowmelt. The peak end-of month storage is in May for both scenarios whereas it was in June under Base case. Under Wet scenario, energy spills increase by nearly 1,000 GWh between January and April compared to Base case. Energy spills occur when the system cannot store all the incoming runoff or send it through the turbines. Even if average generation increases by nearly 6% under Wet scenario relative to Base case, average revenues only increase by 2% because spills increase. Under Dry scenario, average generation decreases by 20% but revenues only decrease by 14% relative to Base case, showing that the system is able to adapt to a certain extent to changing hydrology. The system increases annual revenues if either energy storage or energy generation capacity is expanded under Wet and Dry scenarios relative to Base case. Energy storage capacity expansion is more beneficial than generation capacity expansion, although such expansion might not be justified due to expansion costs. As expected, benefits of capacity expansion are greater for Wet scenario when the additional capacity can be more frequently used.

EBHOM's results when climate change effects on high-elevation hydropower supply and demand in California are simultaneously considered are compared hereafter to those results when changes in demand were ignored. Energy generation increases in warm months when demand is high and energy is valuable, and decrease in winter when less heating is needed and prices are off-peak. This is true for both climate warming scenarios and both ANN models. Between February and June, the end-of-month storage increases under all scenarios relative to when changes in demand were ignored. Less energy is generated in the warmer winters and it is then available to be stored until the high-demanding season. Energy spills are not much different from EBHOM's results based on historical pricing. Under Wet scenarios, energy revenues decrease because average energy price received decrease and average energy revenues is lower than in Base case. Under Dry scenario, revenues are always lower than Base case and the Monthly-based ANN model suggests more revenues than the Annually-based ANN model. The system under Dry scenarios benefits more from energy storage capacity expansion than when historical prices were considered. Under wetter conditions is hard to conclude since it depends on the ANN model. Alongside, the marginal benefits from energy generation expansion under both Dry and Wet scenarios considering the effects of warming on demand are estimated to decrease relative to when they were neglected.

Finally, expanding energy storage capacity of California's high-elevation hydropower system seems to be the most beneficial option to adapt to climate change and maximize the increase in revenue, although such expansion might not be justified due to expansion costs. The benefits gained range from 29 to 81$/Year/MWh when changes in demand are considered, depending on the climate scenario. A case by case study of the benefits gained by each power plant should be performed to decide whether storage or generation capacities should be expanded at each unit.

Acronyms

ANN: Artificial Neural Network
ANN1: 12 monthly-based ANN model trained on all price ranges, 2005-2008
ANN2: 1 ANN model trained on Normal prices, excluding price spikes, 2005-2008
CAISO: see CalISO
CalISO: California Independent System Operator
CCCC: California Climate Change Center
CCE: Competitive Complex Evolution
CPI: Consumer Price Index
EBHOM: Energy-Based Hydropower Optimization Model
ECP: Electricity Consumption Per capita
GCM: Global Climate Model
GFDL: Geophysical Fluids Dynamics Laboratory
IPCC: Intergovernmental Panel on Climate Change
Logsig: Logistic sigmoid
MLP: Multi-Layer Perceptron
MSE: Mean-Squared Error
NCAR: National Center for Atmospheric Research
NN: Neural Network
NOAA: National Oceanic and Atmospheric Administration
NOCAL: Northern California Region referring to Sacramento area
NSM: No-Spill Method
OASIS: Open Access Same-time Information System
PCM: Parallel Climate Model
PG&E: Pacific Gas & Electric
RMSE: Root Mean-Squared Error
SCE: Southern California Edison
SCE-UA: Shuffle Complex Evolution – University of Arizona
SDG&E: San Diego Gas & Electric
SOCAL: Southern California region referring to the area around Riverside
SRES: Special Report on Emissions Scenarios
Tanh: see Tansig
Tansig: Hyperbolic tangent

Glossary

Nominal price: "The price paid for a product or service at the time of the transaction. Nominal prices are those that have not been adjusted to remove the effect of changes in the purchasing power of the dollar; they reflect buying power in the year in which the transaction occurred."
(Source: EIA, http://www.eia.doe.gov/glossary/index.cfm?id=N)

Normal prices: Prices that are not price spikes, i.e. positive price values below the threshold defining price spikes.

Predictor: neuron in the input layer of an artificial neural network

Predictand: neuron in the output layer of an artificial neural network

References

Amjady, N. & Hemmati, M., 2006. Energy price forecasting - problems and proposals for such predictions. *IEEE Power Energy Mag. 4 (2)*, pp. 20-29.

Amjady, N. & Keynia, F., 2010a. Electricity market price spike analysis by a hybrid data model and feature selection technique. *Electric Power Systems Research* 80, pp. 318-327.

Amjady, N. & Keynia, F., 2010b. Application of a new hybrid neuro-evolutionary system for day-ahead price forecasting of electricity markets. *Applied Soft Computing 10*, pp. 784-792.

Aroonruengsawat, A. & Auffhammer, M., 2009. *Impacts of climate change on residential electricity consumption: evidence from billing data*. California. California Climate Change Center, CEC-500-2009-018-D, [Online] March 2009. Available at: http://www.energy.ca.gov/2009publications/CEC-500-2009-018/CEC-500-2009-018-D.PDF

Azadeh, A. Ghaderi, S.F, Tarverdian, S. & Saberi, M., 2007. Integration of artificial neural networks and genetic algorithm to predict electrical energy consumption. *Applied Mathematics and Computation 186*, pp. 1731–1741.

ASCE, 2000. Artificial Neural Networks in Hydrology. I: Preliminary Concepts. *Journal of Hydrologic Engineering*, Vol. 5, No. 2.

Aspen Environmental Group & Cubed, M., 2005. *Potential changes in hydropower production from global climate change in California and the western United States*. California Climate Change Center, CEC-700-2005-010, [Online] June 2005. Available at: http://www.energy.ca.gov/2005publications/CEC-700-2005-010/CEC-700-2005-010.PDF

Bloom Energy, 2010. Understanding California's Electricity Prices. [Online] Available at: http://c0688662.cdn.cloudfiles.rackspacecloud.com/downloads_pdf_White_Paper_Calif_Elec_Prices.pdf [Accesses 10 April 2010]

California Energy Commission, 2009. Hydroelectric Power in California. [Online] (Updated 27th August 2008) Available at: http://www.energy.ca.gov/hydroelectric/index.html [Accessed 20 March 2010]

California Independent System Operator – Department of Market Monitoring, 2006. 2005 Annual Report on Market Issues and Performance. [Online] Available at: http://www.caiso.com/17d5/17d59ec745320.pdf [Accessed 24 March 2010]

California Independent System Operator – Department of Market Monitoring, 2009. 2008 Annual Report on Market Issues and Performance. [Online] Available at: http://www.caiso.com/2390/239087966e450.pdf [Accessed 24 March 2010]

Cayan, D. Maurer, E. Dettinger, M. Tyree, M. Hayhoe, K. Bonfils, C. Duffy, P. and Santer, B., 2006. *Climate scenarios for California*. California Climate Change Center, CEC-500-2005-203-SF, [Online] March 2006. Available at: http://www.energy.ca.gov/2005publications/CEC-500-2005-203/CEC-500-2005-203-SF.PDF

Cayan, D. R. Maurer, E. P., Dettinger, M. D., Tyree, M. Hayhoe, K., 2008. Climate change scenarios for the California region. *Climatic Change*, 87, 1, pp. 21-42.

California Climate Change Center, 2006. *Our Changing Climate – Assessing the Risks to California*. Ref: CEC-500-2006-077, [Online] Available at:

http://www.energy.ca.gov/2006publications/CEC-500-2006-077/CEC-500-2006-077.PDF

Congressional Budget Office (CBO), 2001. Causes and Lessons of the California Electricity Crisis. [Online] Available at: http://www.cbo.gov/ftpdocs/30xx/doc3062/ CaliforniaEnergy.pdf [Accessed 25 March 2010]

Dawson, C.W. and Wilby, R.L., 2001, Hydrological modelling using artificial neural networks. *Progress in Physical Geography* 25, 1, pp. 80–108.

Duan, Q. Sorooshian, S & Gupta V., 1992. Effective and Efficient Global Optimization for Conceptual Rainfall-Runoff Models. *Water Resources Research* Vol.28, No 4, pp. 1015-1031, Paper number 91WR02985.

Duan, Q. Sorooshian, S & Gupta V., 1994. Optimal use of the SCE-UA global optimization method for calibrating watershed models. *Journal of Hydrology* 158, pp. 265-284.

Franco, G. & Sanstad, A. H., 2006. *Climate change and electricity demand in California*. California Climate Change Center, CEC-500-2005-201-SF, [Online] February 2006. Available at: http://www.energy.ca.gov/2005publications/CEC-500-2005-201/CEC-500-2005-201-SF.PDF

Gao, F. Guan, X. Cao, X-R. & Papalexopoulos, A., 2000. Forecasting Power Market Clearing Price and Quantity Using a Neural Network Method. *IEEE Power Engineering Society Summer Meeting* 2000.

Hippert, H.S & Taylor, J.W, 2010. An evaluation of Bayesian techniques for controlling model complexity and selecting inputs in a neural network for short-term load forecasting. *Neural Networks 23*, pp. 386-395.

Hornik, K. Stinchcombe, M. White, H., 1989. Multilayer feedforward networks are universal approximators. *Neural Networks*, Vol. 2, No. 5, pp. 359-366.

Horowitz, M. J., 2007. Changes in Electricity Demand in the United States from the 1970s to 2003. *The Energy Journal*, Vol. 28, No. 3.

Hsieh, W. W. & Tang, B., 1998. Applying Neural Network Models to Prediction and Data Analysis in Meteorology and Oceanography. *Bulletin of American Meteorology Society*, Vol.79, No. 9.

Kandel, A. Sheridan, M. & Mcauliffe, P., 2008. *A comparison of per capita consumption in the United States and California*. Staff paper from California Climate Change Center, CEC-200-2009-015, [Online] Available at: http://www.energy.ca.gov/2009publications/CEC-200-2009-015/CEC-200-2009-015.PDF

Karunanithi, N. Grenney, W.J. Whitley, D. & Bovee, K., 1994. Neural network for river flow prediction. *Journal of Computing in Civil Engineering 8* (2), pp.201–220.

Kauffman, E., 2003. Climate and Topography. Atlas of the Biodiversity of California. [Online] Available at: http://www.dfg.ca.gov/biogeodata/atlas/pdf/Clim_12b_web.pdf [Accessed 31 March 2010]

Kingston, G. B. Maier, H. R. Lambert, M. F., 2005. Calibration and validation of neural networks to ensure physically plausible hydrological modeling. *Journal of Hydrology 314 (2005)*, pp. 158–176.

Lu, X. Dong Z.Y. & Li, X., 2005. Electricity market price spike forecast with data mining techniques. *Electric Power Systems Research* 73, pp. 19-29.

Madani K. & Lund, J. R, 2007. High-Elevation Hydropower and Climate Warming in California, *Proceeding of the 2007 World Environmental and Water Resources Congress, Tampa, Florida*, (Ed) Kabbes K. C., ASCE.

Madani, K. Vicuna. S. Lund, J. Dracup, J. & Dale, L., 2008. Different approaches to study the adaptability of high-elevation hydropower systems to climate change: the case of SMUD's upper American river project. In: Babcock RW,Walton R (eds) Proceeding of the 2008 world environmental and water resources congress, Honolulu, Hawaii. ASCE.

Madani, K. & Lund, J. R., 2009. Modeling California's high-elevation hydropower systems in energy units. *Water Resources Research* 45, W09413. doi:10.1029/2008WR007206.

Madani, K. & Lund, J. R., in press. Estimated impacts of climate warming on California's high-elevation hydropower. *Climatic Change*, doi:10.1007/s10584-009-9750-8

Maier, H. R. & Dandy G. C., 2000. Neural networks for the prediction and forecasting of water resources variables: a review of modelling issues and applications. *Environmental Modelling & Software* 15, pp. 101–124.

Medellín-Azuara, J. Harou, J.J. Olivares, M.A. Madani, K. Lund, J.R. Howitt, R.E. Tanaka, S. Jenkins, M.W. & Zhu, T., 2008. Adaptability and Adaptations of California's Water Supply System to Dry Climate Warming. Forthcoming in *Climatic Change*, **87** (Suppl 1):S75–S90.

Moser, S. Franco, G. Pittiglio, S. Chou, W. & Cayan D., 2009. The future is now: an update on climate change science impacts and response options for California. California Climate Change Center, CEC-500-2008-071, [Online] Available at: http://www.energy.ca.gov/2008publications/CEC-500-2008-071/CEC-500-2008-071.PDF

McKinney, J. et al., 2003. California Hydropower System: Energy and Environment. [Online] Available at: http://www.energy.ca.gov/reports/2003-10-30_100-03-018.PDF

National Oceanic and Atmospheric Administration (NOAA) – National Climatic Data Center, 2009. State of the Climate National Overview Annual 2008 [Online] (Updated 31st June 2009) Available at: http://www.ncdc.noaa.gov/sotc/?report=national&year=2008&month=13

Olsson, J. Uvo, C.B. Jinno, K. Kawamura, A. Nishiyama, K. Koreeda, N. Nakashima, T. & Morita, O., 2004. Neural Networks for Rainfall Forecasting by Atmospheric Downscaling. Journal for Hydrologic Engineering, ASCE.

Ortiz-Arroyo, D. Skov, M.K. & Huynh, Q., 2005. Accurate Electricity Load Forecasting with Artificial Neural Networks. In: International Conference on Computational Intelligence for Modelling, Control and Automation and International Conference on Intelligent Agents, Web Technologies and Internet Commerce (CIMCA-IAWTIC'06). IEEE 2005 (1), pp.94-99.

Pacific Gas and Electric Company (PG&E), 2008. News Release: Rising Natural Gas Prices and Lower Hydroelectric Power Supplies Expected to Increase Electricity Costs. [Online] Available at: http://www.pge.com/about/news/mediarelations/newsreleases/q2_2008/080610.shtml

Pew Center on Global Climate Change, 2009. Climate TechBook, chap: Hydropower. [Online] Available at: http://www.pewclimate.org/docUploads/Hydropower10%2009_FINAL_cleanPDF.pdf

Ranjbar, M. Soleymani, S. Sadati, N. & Ranjbar A. M., 2006. Electricity price forecasting using Artificial Neural Network. In: IEEE, *2006 International Conference on Power Electronic, Drives and Energy Systems*.

Rosenfeld, A., 2006. *Summing Up Energy Symposium: The 'Rosenfeld Effect'*. California Climate Change Center, CEC-999-2006-005, [Online] Available at: www.energy.ca.gov/2006publications/CEC-999-2006-005/CEC-999-2006-005.PDF

Tanaka, S.T. Zhu, T. Lund, J.R. Howitt, R.E. Jenkins, M.W. Pulido, .M.A. Tauber, M. Ritzema, R.S. & Ferreira I.C. (2006). Climate warming and water management adaptation for California. *Climatic Change 76(3–4)*, pp. 361–387.

Tanton, T., 2008. *California's Energy Policy – A Cautionary Tale for the Nation*. Competitive Energy Institute [Online] Available at: http://cei.org/cei_files/fm/active/0/Tanton_California Energy Policy.pdf

Union of Concerned Scientists, 2006. Global Warming and California's Electricity Supply - A fact sheet from the Union of Concerned Scientists. [Online] Available at: http://www.ucsusa.org/assets/documents/global_warming/ucs_electricity_final.pdf

Vicuna, S. Leonardson, R. Hanemann, M.W. Dale, L. L. & Dracup, J. A., 2008. Climate change impacts on high elevation hydropower generation in California's Sierra Nevada: A case study in the Upper American River. *Climatic Change*, 87 (Suppl 1), pp.123-137, doi: 10.1007/s10584-007-9365-x.

Vicuna, S. Dracup, J. A. & Dale, L., 2009. *Climate change impacts on the operation of two high-elevation hydropower systems in California.* California Climate Change Center, CEC-500-2009-019-D, [Online] Available at: http://www.energy.ca.gov/2009publications/CEC-500-2009-019/CEC-500-2009-019-D.PDF

Yamin, H.Y. Shahidehpour, S.M. Li, Z., 2004. Adaptive short-term electricity price forecasting using artificial neural networks in the restructured power markets. *Electrical Power and Energy Systems 26, (2004)*, pp. 571–581.

Zarezadeh, M. Naghavi, A. Ghaderi, S.F., 2008. Electricity price forecasting in Iranian electricity market applying Artificial Neural Networks. *IEEE Electrical Power & Energy Conference* 2008.

Zhang, G. Patuwo, B.E. & Hu, M.Y., 1998. Forecasting with artificial neural networks: the state of art. *International Journal of Forecasting, 14 (1)*, pp. 35-62.

Zhao, J.H. Dong, Z.Y. Li, X. & Wong K.P, 2005. A general method for electricity market price spike analysis. *Proc. IEEE Power Engineering Society General Meeting*, June 2005, pp. 563-570.

Zhao, J.H. Dong Z.Y. & Li, X., 2007. Electricity market price spike forecasting and decision making. *IET Gener. Transm. Distrib., 2007, 1, (4)*, pp. 647-654.

Zhu, T. Jenkins, M.W. & Lund, J.R., 2005. Estimated impacts of climate warming on California water availability under twelve future climate scenarios. Journal of the American Water Resources Association (JAWRA), 41(5): pp.1027-1038.